Dissolution Enhancement of Poorly Water Soluble Drugs

by

Sateesh Kumar Sathigari

A dissertation submitted to the Graduate Faculty of
Auburn University
in partial fulfillment of the
requirements for the Degree of
Doctor of Philosophy

Auburn, Alabama
May 9, 2011

Keywords: Dissolution Enhancement, Drug-Polymer Miscibility, Solid Dispersions, Hot-Melt Extrusion, Supercritical Antisolvent, Cyclodextrins

Approved by

Jayachandra Babu Ramapuram, Co-Chair, Assistant Professor of Pharmacal Sciences
Daniel L. Parsons, Co-Chair, Professor of Pharmacal Sciences
William R. Ravis, Professor of Pharmacal Sciences
Ram B. Gupta, Professor of Chemical Engineering
Muralikrishnan Dhanasekaran, Associate Professor of Pharmacal Sciences

Abstract

Aqueous solubility is a limiting factor in the oral bioavailability of a certain class of poorly water soluble drugs. A consequence of low aqueous solubility is a slow dissolution rate. For the drugs with low aqueous solubility and high permeability the dissolution rate will be the rate limiting step for absorption. The most successful techniques that are employed for dissolution enhancement are micronization, formulation of amorphous systems and cyclodextrins containing dosage forms. This dissertation focuses on these three approaches to improve the dissolution of some model poorly soluble drugs.

Micronization increases the dissolution rate of drugs through increased surface area. The high surface area of drug micro/nano particles renders them thermodynamically unstable, promoting agglomeration and crystal growth. Microparticles of the poorly water soluble drug, Itraconazole (ITZ) were produced by the supercritical antisolvent (SAS) method and simultaneously mixed with pharmaceutical excipients in a single step to prevent the drug agglomeration of drug particles. The drug microflakes were deposited on FFL by the SAS-DEM process and this method was successful in overcoming the agglomeration of drug microflakes. PLX produced crystalline drug microflakes in loose agglomerates with superior dissolution and flow properties even at higher drug loadings.

The amorphous form of the drug will have higher solubility than their crystalline form. However, the amorphous form is physically unstable due to a high energy state and

may recrystallize during storage. Binary physical mixtures of Efavirenz (EFV) and Eudragit EPO or Plasdone S- 630 were prepared and characterized for thermal and rheological properties to evaluate the miscibility and processibility for hot melt extrusion. Several equations were used to represent the glass transition (T_g) of blends with different drug loadings. The thermal and rheological studies revealed that the drug is miscible with both the polymers and plasticization of the polymers was observed with the drug. The amorphous systems were stable at ambient conditions for nine months and dissolution rate of EFV from these systems was significantly higher than its crystalline form and corresponding physical mixtures. Successful formation of amorphous solid dispersions of various drugs (carvedilol, itraconazole, nevirapine and nimodipine) in Plasdone S-630 was discussed in terms of thermo physical behavior and intermolecular interaction in drug-polymer systems.

In the third approach cyclodextrins (CDs) were used as pharmaceutical solubilizers. The inclusion complexes of EFV with β-CD and its derivatives were prepared and characterized both in liquid and solid states. Stability constants (Ks) for EFV-βCD, EFV - hydroxypropyl βCD and EFV - randomly methylated βCD systems were 288, 469 and 1073 M^{-1}, respectively. The dissolution of EFV was substantially higher with hydroxypropyl βCD and randomly methylated βCD inclusion complexes that were prepared by freeze drying method.

Acknowledgments

First and above all, I would like to praise and extend my thanks to Almighty God, Lord Jesus Christ for giving me the opportunity and granting me the strength, the patience, the knowledge and for guiding me through my struggles to help me accomplish this task with success. “All things were made through him and without him was not anything made that was made.” John 1:3

I would like to dedicate my work to my parents and family. It’s with their love, care and support, I have been able to quench my desire for higher studies. I express my deepest gratitude to Dr. Jayachandrababu Ramapuram for providing me this opportunity, for his guidance, support in and out of the lab and allowing me the room to work independently. My sincere thanks to Dr. Daniel Parsons for his guidance, support in research and throughout my stay in this department. I am grateful to Dr. William Ravis, Dr. Ram Gupta, Dr. Randall Clark and Dr. Muralikrishnan Dhanasekaran for extending timely help and guidance throughout my doctoral studies.

I am especially grateful to all my collaborators, Dr. Ram Gupta, Dr. Witold Brostow, Dr. Ioannis Kalogeras, Dr. Virginia Davis for their kind support in carrying out my work in their research labs and for their valuable inputs. I would like to thank Dr. Oladiran Fasina for allowing me to use his lab and for serving as an outside reader for my dissertation. I thank Dr. Vijay Rangari for providing the facilities for some DSC and XRD studies. I also thank Ganesh, Courtney, and Vinod for their valuable research

support and being co-authors in research articles. I also would like to thank Dr. Umang Shah, Dr. Ramana Malladi and Dr. Srikonda Sastry for their valuable suggestions and support.

My group members and friends Gurkishan, Julia and Kasturi need special appreciation for their assistance and creating a nice and joyful environment in the laboratory.

I would like to extend my appreciation and gratitude to all the faculty members, staff and fellow students at Dept. of Pharmacal Sciences. I would like to express my heartful gratitude to my colleagues and friends Dr. Karuppagounder, Dr. Uthayathas, Dr. Phyllis, Dr. Vanisree, Mr. Ravi, Mr. Kariharan, Mr. Ranjith, Mr. Manuj and Mr. Nataraju for their encouragement and personal friendship. Special thanks to Ranjit and Nataraju who made my stay very comfortable during writing my dissertation.

I would like to thank my dear friend Ramisetty and his soul mate Manasa for their unconditional love, emotional support and encouragement. My special thanks to my friends Ramisetty, Prashanth and Meher for their support and encouragement to come to United States. My friends Niranjan, Ravi, Kiran, Suneel, Prasad and my cousin Thomson deserve special mention for their continuous support.

Last but not least, a very special thank you to my wife Smitha Shalini for her love, support and encouragement and to my little son Sam, whose love and smile is worth it all.

Table of Contents

List of Figures

List of Tables

1. Introduction

Poor aqueous solubility of drugs is an industry wide issue for pharmaceutical scientists. Because of their low aqueous solubility, up to 40% of new chemical entities fail to reach market despite exhibiting potential pharmacodynamic activities.[1] In addition, up to 50% of orally administered drugs suffer from formulation problems related to their high lipophilicity.[2] Poorly aqueous soluble drugs are associated with slow drug absorption leading eventually to inadequate and variable bioavailability.[3,4] Oral absorption of a drug can be influenced by variety of factors, such as the physicochemical properties (e.g., pKa, solubility, stability, diffusivity, lipophilicity, polar-nonpolar surface area, presence of hydrogen bond functionalities, particle size and crystal form), physiological conditions (e.g., gastrointestinal pH, blood flow, gastric emptying, small intestinal transit time, colonic transit time and absorption mechanisms) and type of dosage form (e.g., tablet, capsule, solution, suspension and emulsionl).[5] Despite this complexity, the work of Amidon et al,[3] revealed that permeability of drug through the gastrointestinal (GI) membrane and solubility/dissolution of drug dose in the GI environment are the fundamental events in successful drug absorption. The Biopharmaceutics Classification system (BCS) proposed by Amidon et al., [6] classifies drugs into four categories (Table1.1) based on their solubility and permeability

characteristics. According to BCS, the oral bioavailability of class-II (poorly soluble and highly permeable) drugs is limited by their solubility and dissolution rate.[6] If the ratio of the drug dose to the lowest drug saturation solubility in the pH range of 1-8 is greater than 250 then the drug is called poorly soluble. So regardless of other factors, it is reasonable to conclude that a compound must be in solution form or solubilized in the GI tract to diffuse into and across the enterocytes lining the intestinal lumen for absorption.[7] The complete oral absorption of a drug depends on the events depicted in Figure 1.1, their importance relative to one another and the rate at which they occur.[8] Drug release (dissolution) and absorption must occur within the available transit time i.e., the time the drug spends in GI tract and at the site of absorption. The dissolution rate of the drug is given by the Noyes-Whitney equation.[9]

$$\text{Dissolution rate} = \frac{dX}{dt} = \frac{A.D}{h}\left(Cs - \frac{Xd}{V}\right) \qquad 1$$

Where A is the surface area of the drug; D is the diffusion coefficient of the drug; h is the effective boundary layer thickness; C_s is the saturation concentration of the drug under the local GI conditions; V is the volume of the fluid available to dissolve the drug, and X_d is the amount of drug already dissolved.

The diffusion coefficient (D) and diffusion layer thickness (h) are less suitable targets for dissolution rate enhancement/bioavailability optimization. D depends on the molecular weight of the drug and the viscosity of the gastro intestinal fluids, which varies in the fed and fasted state and is subject to large intra- and inter-subject variability. h also

largely depends on the hydrodynamics during GI transit.[4] Therefore, based on the equation 1, the possibilities for increasing the dissolution/bioavailability are to increase the effective surface area or to improve the apparent solubility of the drug. Different approaches to enhance the dissolution rate of poorly soluble drugs include, but are not limited to, particle size reduction,[10-13] inclusion complexation with cyclodextrins,[14-16] solid dispersion,[17-19] salt formation,[20,21] use of surfactants,[22,23] cosolvency,[24,25] and various particle engineering techniques.[26-28] Among, the different approaches, this research mainly focuses on micro/nano particle production by supercritical fluid technology, amorphous systems, and complexation with cyclodextrins for dissolution enhancement. We have focused our research on these three methods because they are the most successful technologies in terms of the number of commercial products which are on the market (Tables 1.2, 1.3 and 1.4).

1.1 Micro/Nano Particle Production

This is one of the most efficient and reliable methods used commercially to improve the bioavailability of poorly soluble drugs that is limited by poor dissolution rates.[29] Improvement in bioavailability after micronization of drugs has been well documented for numerous drugs.[11,12,29,30] Micronization increases the dissolution rate of drugs through increased surface area.[31] Reduction of the particle size to micron or nano size can be achieved by precipitation from a solution (built-up) or milling (sized–down). Milling is a well established technique which is relatively cheap, fast and is easy to scale-up, but it has several disadvantages.[32] This method has limited opportunity to control the final particle size, shape, morphology, surface properties and electrostatic charge and it is

difficult to reduce the particle size below 1 μm because of the cohesiveness of the particles. In addition, milling is a high energy process which causes disruptions in the drug's crystal lattice, resulting in the presence of disordered or amorphous regions in the final product.[33] Wet milling techniques (bead milling and high pressure homogenization) can produce submicron particles without any concern for particle cohesiveness. However, these techniques often require a long time, introduce impurities, can also cause disruptions in the drug crystal lattice, and limits flexibility in controlling particle morphology. These methods also require further pharmaceutical operations such as lyophilization or spray drying to produce solids for use in oral solid dosage forms. Spray drying is known to produce amorphous material due to rapid solvent evaporation.[13] Relative to mechanical micronization processes, precipitation from solution can offer greater flexibility for controlling the amorphous or crystalline form of the active ingredient as well as for achieving high drug loadings.[34] The use of super critical fluids for the precipitation of pharmaceuticals is of great interest in recent times. It has been used for the micronization of pharmaceuticals with low or no residual solvent, a narrow particle size distribution and, in the case of an oral drug, with increased dissolution rate profiles.[27,31,35-38]

A fluid behaves as a supercritical fluid when its temperature and pressure exceed the relevant critical temperature and pressure.[39] At the critical point, a single phase exists. Supercritical fluid has some properties that are similar to those of gases and liquids (Figure 1.2).[40] Similar to a gas, supercritical fluids have lower viscosity and higher diffusivity relative to that of liquid. These properties facilitate mass transfer and give good transport properties. Similar to a liquid, supercritical fluid have density values that

are high to exert solvent effects.[41] A supercritical fluid is dense, but highly compressible, thus any pressure change results in density alteration and consequently the solvent power. In the vicinity of the critical point, the compressibility is higher and a small pressure change causes larger changes in density.

Supercritical fluids are involved in numerous industrial processes and offer considerable advantages as solvents or anti solvents for crystallization and precipitation processes.[42] Among different methods using supercritical fluids, precipitation using supercritical carbon dioxide (CO_2) as an antisolvent is well known and has been used to micronize several kinds of compounds.[27,37,43] Carbon dioxide is an ideal supercritical fluid because of its low critical temperature (31.18^{o}C) and pressure (73.8 Pa), low cost, non-toxicity and inert nature. In addition, CO_2 is recyclable and environmentally safe.[36] The driving force for particle formation using supercritical fluids is super saturation which is same as that of traditional crystallization. In the supercritical anti-solvent (SAS) process the solubilization power of a solvent is decreased by addition of a supercritical fluid as an antisolvent in which the solute is insoluble. The nucleation and consequent growth of the crystals from the solute-organic solvent-antisolvent are governed by the diffusion of the antisolvent into the organic phase and the evaporation of the organic solvent into the antisolvent phase.[37] The rapid diffusion of antisolvent into the organic solvent produces the supersaturation of the solute that leads to nucleation and particle formation. In our current research we investigated the effect of pharmaceutical excipients on particle formation and de-aggregation in the supercritical fluid environment. To the best of our knowledge, these parameters have not been explored nor reported in literature.

1.2 Amorphous Systems

Amorphization is one of the techniques to enhance the dissolution rate and bioavailability of poorly water soluble drugs.[44] Delivering the pharmaceutical active ingredient in the amorphous form is very attractive due to the potentially large increases in drug solubility, dissolution rate, and bioavailability.[45,46] The amorphous form of drugs can have as much as a 10-1600 fold higher solubility than their crystalline forms.[47] The improvement in dissolution of amorphous systems can be attributed to improved wetting of the drug, deagglomeration and micellization of the drug with hydrophilic polymers and the high energy amorphous state of the drug.[48]

However, the amorphous forms of drugs are physically unstable due to their higher energy state and may recrystallize over pharmaceutically relevant time scales, negating any solubility advantage.[49] The most typically used approach to stabilize an amorphous system is to combine it with pharmaceutically acceptable polymers, such as polyvinylprrolidone, polyvinylpyrrolidone vinyl acetate, polyethylene glycol and various hydroxypropylmethyl cellulose and polyacrylic acid derivatives.[4,49-51] Thermodynamically the drug has a lower chemical potential when mixed with a polymer, resulting in a change of crystallization driving force.[52] The long polymeric chains can sterically hinder the association between drug molecules and, thereby, inhibit the recrystallization of drug. In addition, the interaction between the drug and polymer provides an increased energy barrier for nucleation and, consequently, enhances the physical stability.[53] Amorphous drug-polymer systems are commonly characterized in terms of physical properties such as the glass transition temperature (*Tg*), heat capacity and miscibility. Although it is still not completely clear as to how the polymer stabilizes

the amorphous drug in the mixture, drug polymer miscibility is generally considered as one of the critical attributes that affect the stability of the amorphous systems, which in turn is dictated by the thermodynamics of mixing.[54] The entropy of mixing is always favorable (an increase on mixing) providing one driving force facilitating mixing. The enthalpic component of the Gibbs function of mixing is controlled by the relative strength of the cohesive drug - drug, polymer - polymer and the drug - intercomponent interactions. Understanding of these relationships is necessary for optimization of amorphous systems. An immiscible drug – polymer system could lead to unexpected destabilization during storage. We have studied various drug – polymer miscibility interactions in order to stabilize the amorphous drug - polymer systems for long term storage so that these systems can be utilized in the formulation of solid dosage forms.

Amorphous systems are predominantly produced by solvent evaporation and melt extrusion methods.[55,56] In the solvent method, both drug and the polymer are dissolved in a common organic solvent and a secondary drying step is used to remove the solvent. Usually in amorphous systems, in order to have fast drug release, the hydrophobic drug is combined with hydrophilic polymers and it is difficult to find a common solvent for both. The handling of organic solvents in the manufacturing facilities of pharmaceutical dosage forms also poses occupational safety and environmental concerns.[57] A small amount of the solvent can plasticize the solid dispersions and lead to physical instability. On the other hand, melt extrusion offers numerous advantages over other pharmaceutical processing techniques. Solvents, including water, are not necessary, reducing the number of processing steps and eliminating time consuming drying steps. There are environmental advantages due to elimination of solvents in the processing and intense

mixing and agitation imposed by rotating screws cause deaggregation of suspended particles in the molten polymer resulting in a more uniform dispersion. The process is also continuous and efficient.[58-60]

For the successful development of amorphous systems by melt extrusion, it is necessary to evaluate the miscibility and processibility of the blends and to also establish processing conditions for melt extrusion. The drug – polymer blends were characterized in the molten and solid states in order to understand their molecular interactions and various hot melt extrusion process parameters were established to produce stable solid dispersions of the drug efavirenz and polymer.

1.3 Complexation with Cyclodextrins

Cyclodextrins (CDs) have been used extensively in pharmaceutical research and development, and there are currently over 30 marketed cyclodextrins containing pharmaceutical products world wide.[61,62] Some of the cyclodextrins based marketed products world wide are given in Table 1.4.[63] Most commonly, CDs are used in drug formulations as solubility enhancers because of their ability to form water soluble inclusion complexes with poorly soluble drugs.[64] The complexation with CDs enhances the solubility, dissolution rate, and bioavailability of poorly soluble drugs.[64,65] In addition, CDs are used to enhance stability, to mask drug taste, to aid pharmaceutical processes by serving as filler, binder and channeling agents, etc., and as an osmogen in controlled release osmotic pump dosage forms.[66-70]

CDs are cyclic (α-1,4)-linked oligosaccharides of α-D-glucopyranose containing a relatively hydrophobic central cavity and hydrophilic outer surface. The central cavity

provides a lipophillic microenvironment into which suitably sized lipophilic drug molecules can be accommodated due to hydrophobic interactions. No covalent bonds are formed in the drug/cyclodextrin (CD) complexation and the complexes are readily dissociated. The three natural CDs are α-CD, β-CD, and γ-CD which are made up of 6, 7 or 8 glucopyranose units respectively.[71] Several chemically modified CD derivatives have been reported in the literature to enhance the aqueous solubility, physical and microbiological stability and to reduce toxicity of the parent CDs.[61,63,72] The most widely used approach to study inclusion complexation is the phase solubility method described by Higuchi and Connors.[73] The majority of drugs form apparent 1:1 complexes with CDs although the formation of higher order complexes is not uncommon.[64] The fundamental property that describes the strength of the interaction between a drug and CD is the binding constant (or stability constant). The value of the stability constant is used to compare the affinity of drugs for different CDs or their derivatives. Binding constant values of 0 to approximately 100,000 have been reported with 0 corresponding to the absence of binding.[72] Very weak binding is roughly characterized by a binding constant less than 500 M^{-1}, while weak, moderate, strong and very strong binding are characterized by binding constants in the ranges of 500-1000 M^{-1}, 1000-5000 M^{-1}, 5000-20,000 M^{-1}, and greater than 20,000 M^{-1}, respectively.[62] In fact, Szejtli suggested that a binding constant value of > 10,000 M^{-1} significantly reduces bioavailability due to the inability of the complex to dissociate and release the free drug.[66] We utilized two different CD derivatives, hydroxypropyl β-CD and randomly methylated β-CD as drug solubilizers in our research.

The main objective of this dissertation research was to enhance the dissolution rate of poorly water soluble drugs that eventually leads to improvement in bioavailability for better therapeutic effect. The research has been divided into three major sections:

The aim of section I (chapter 2) was to utilize supercritical fluid technology for the production of micro and nanoparticles for dissolution enhancement. However, the micron and nano sized particles have a tendency to agglomerate due to high surface free energy, van der Waals attraction and hydrophobic interactions leading to a decrease in effective surface area. A novel method of simultaneous production of micro/nano particles and co-mixing with pharmaceutical excipients for dissolution enhancement has been developed to address the drug agglomeration issues. The aim of section II (chapter 3-5) was to develop and characterize a physically stable amorphous system of a poorly soluble drug by melt extrusion. The drug polymer blends were studied for their miscibility and compatibility by measuring their glass transition temperature *(T_g)*. The T_g – composition diagrams were represented by several mathematical equations to identify the one that yields the most reliable results for the present work. Stabilization of amorphous systems in terms of thermophysical behavior (suppression of crystallization, negative excess volumes of mixing) and intermolecular interactions (concentrations of proton donating/accepting groups) in drug + polymer systems were investigated and results presented in chapters 3-5. The aim of section III (chapter-6) was to utilize β-CD and its derivatives for the dissolution improvement of an insoluble drug. The inclusion complexes were prepared and characterized in the solid and liquid states and dissolution properties of these complexes are presented.

1.4 References

1. Lipinski CA. 2002. Poor aqueous solubility- An industry wide problem in drug discovery. Am Pharm Rev 5(3):82-85.
2. Gursoy RN, Benita S 2004. Self-emulsifying drug delivery systems (SEDDS) for improved oral delivery of lipophilic drugs. Biomed Pharmacother 58(3):173-182.
3. Amidon GL, Lennernas H, Shah VP, Crison JR 1995. A theoretical basis for a biopharmaceutic drug classification: the correlation of in vitro drug product dissolution and in vivo bioavailability. Pharm Res 12(3):413-420.
4. Leuner C, Dressman J 2000. Improving drug solubility for oral delivery using solid dispersions. Eur J Pharm Biopharm 50(1):47-60.
5. Dahan A, Miller JM, Amidon GL 2009. Prediction of solubility and permeability class membership: provisional BCS classification of the world's top oral drugs. AAPS J 11(4):740-746.
6. Yu LX, Amidon GL, Polli JE, Zhao H, Mehta MU, Conner DP, Shah VP, Lesko LJ, Chen ML, Lee VH, Hussain AS 2002. Biopharmaceutics classification system: the scientific basis for biowaiver extensions. Pharm Res 19(7):921-925.
7. Gullapalli RP Soft gelatin capsules (softgels). J Pharm Sci 99(10):4107-4148.
8. Dressman JB, Reppas C 2000. In vitro-in vivo correlations for lipophilic, poorly water-soluble drugs. Eur J Pharm Sci 11 Suppl 2:S73-80.
9. Noyes AA, Whitney WR. 1897. The rate of solution of solid substances in their own solutions. J Am Chem Soc 19:930-934.
10. Rasenack N, Mueller BW. 2002. Dissolution Rate Enhancement by in Situ Micronization of Poorly Water-Soluble Drugs. Pharm Res 19(12):1894-1900.

11. Jounela AJ, Pentikainen PJ, Sothmann A. 1975. Effect of particle size on the bioavailability of digoxin. Eur J Clin Pharmaco 8(5):365-370.
12. Liversidge GG, Cundy KC. 1995. Particle size reduction for improvement of oral bioavailability of hydrophobic drugs: I. Absolute oral bioavailability of nanocrystalline danazol in beagle dogs. Int J Pharm 125(1):91-97.
13. Vogt M, Kunath K, Dressman JB. 2008. Dissolution enhancement of fenofibrate by micronization, cogrinding and spray-drying: Comparison with commercial preparations. Eur J Pharm Biopharm 68(2):283-288.
14. Brewster ME, Loftsson T, Estes KS, Lin JL, Fridriksdottir H, Bodor N. 1992. Effect of various cyclodextrins on solution stability and dissolution rate of doxorubicin hydrochloride. Int J Pharm 79(2-3):289-299.
15. Badr-Eldin SM, Elkheshen SA, Ghorab MM. 2008. Inclusion complexes of tadalafil with natural and chemically modified beta-cyclodextrins. I: Preparation and *in-vitro* evaluation. Eur J Pharm Biopharm 70(3):819-827.
16. Sathigari S, Chadha G, Phillip LYH, Wright N, Parsons DL, Rangari VK, Fasina O, Babu RJ. 2009. Physicochemical characterization of efavirenz-cyclodextrin inclusion complexes. AAPS PharmSciTech 10(1):81-87.
17. Joshi HN, Tejwani RW, Davidovich M, Sahasrabudhe VP, Jemal M, Bathala MS, Varia SA, Serajuddin ATM. 2004. Bioavailability enhancement of a poorly water-soluble drug by solid dispersion in polyethylene glycol-polysorbate 80 mixture. Int J Pharm 269(1):251-258.
18. Dannenfelser RM, He H, Joshi Y, Bateman S, Serajuddin ATM. 2004. Development of clinical dosage forms for a poorly water soluble drug I:

application of polyethylene glycol-polysorbate 80 solid dispersion carrier system. J Pharm Sci 93(5):1165-1175.

19. Kennedy M, Hu J, Gao P, Li L, Ali-Reynolds A, Chal B, Gupta V, Ma C, Mahajan N, Akrami A, Surapaneni S. 2008. Enhanced Bioavailability of a Poorly Soluble VR1 Antagonist Using an Amorphous Solid Dispersion Approach: A Case Study. Mol Pharm 5(6):981-993.
20. Han HK, Choi HK. 2007. Improved absorption of meloxicam via salt formation with ethanolamines. Eur J Pharm Biopharm 65(1):99-103.
21. O'Connor KM, Corrigan OI. 2001. Comparison of the physicochemical properties of the N-(2-hydroxyethyl)pyrrolidine, diethylamine and sodium salt forms of diclofenac. Int J Pharm 222(2):281-293.
22. Balakrishnan A, Rege BD, Amidon GL, Polli JE. 2004. Surfactant-mediated dissolution: Contributions of solubility enhancement and relatively low micelle diffusivity. J Pharm Sci 93(8):2064-2075.
23. Chiou WL, Chen SJ, Athanikar N. 1976. Enhancement of dissolution rates of poorly water-soluble drugs by crystallization in aqueous surfactant solutions. I: sulfathiazole, prednisone, and chloramphenicol. J Pharm Sci 65(11):1702-1704.
24. Kawakami K, Miyoshi K, Ida Y. 2004. Solubilization behavior of poorly soluble drugs with combined use of Gelucire 44/14 and cosolvent. J Pharm Sci 93(6):1471-1479.
25. Viernstein H, Weiss-Greiler P, Wolschann P. 2003. Solubility enhancement of low soluble biologically active compounds-temperature and cosolvent dependent inclusion complexation. Int J Pharm 256(1-2):85-94.

26. Blagden N, de Matas M, Gavan PT, York P. 2007. Crystal engineering of active pharmaceutical ingredients to improve solubility and dissolution rates. Adv Drug Deliv Rev 59(7):617-630.

27. Jung J, Perrut M. 2001. Particle design using supercritical fluids: Literature and patent survey. J Supercrit Fluids 20(3):179-219.

28. Loth H, Hemgesberg E. 1986. Properties and dissolution of drugs micronized by crystallization from supercritical gases. Int J Pharm 32(2-3):265-267.

29. Jonghwi L. 2003. Drug nano and microparticles processed into solid dosage forms: physical properties. J Pharm Sci 92(10):2057-2068.

30. Farinha A, Bica A, Tavares P. 2000. Improved bioavailability of a micronized megestrol acetate tablet formulation in humans. Drug Dev Ind Pharm 26(5):567-570.

31. Barrett AM, Dehghani F, Foster NR. 2008. Increasing the Dissolution Rate of Itraconazole Processed by Gas Antisolvent Techniques using Polyethylene Glycol as a Carrier. Pharm Res 25(6):1274-1289.

32. Wong SM, Kellaway IW, Murdan S. 2006. Enhancement of the dissolution rate and oral absorption of a poorly water soluble drug by formation of surfactant-containing microparticles. Int J Pharm 317(1):61-68.

33. Saleki-Gerhardt A, Ahlneck C, Zografi G. 1994. Assessment of disorder in crystalline solids. Int J Pharm 101(3):237-247.

34. Matteucci ME, Hotze MA, Johnston KP, Williams RO, 3rd. 2006. Drug nanoparticles by antisolvent precipitation: mixing energy versus surfactant stabilization. Langmuir 22(21):8951-8959.

35. Rogers TL, Gillespie IB, Hitt JE, Fransen KL, Crowl CA, Tucker CJ, Kupperblatt GB, Becker JN, Wilson DL, Todd C, Broomall CF, Evans JC, Elder EJ. 2004. Development and Characterization of a Scalable Controlled Precipitation Process to Enhance the Dissolution of Poorly Water-Soluble Drugs. Pharm Research 21(11):2048-2057.

36. Reverchon E, Della PG. 2001. Supercritical fluids-assisted micronization techniques: Low-impact routes for particle production. Pure Appl Chem 73(8):1293-1297.

37. Pasquali I, Bettini R, Giordano F. 2008. Supercritical fluid technologies: An innovative approach for manipulating the solid-state of pharmaceuticals. Adv Drug Deliv Rev 60(3):399-410.

38. Lengsfeld CS, Delplanque JP, Barocas VH, Randolph TW. 2000. Mechanism Governing Microparticle Morphology during Precipitation by a Compressed Antisolvent: Atomization vs Nucleation and Growth. J Phys Chem B 104(12):2725-2735.

39. Pasquali I, Bettini R, Giordano F. 2006. Solid-state chemistry and particle engineering with supercritical fluids in pharmaceutics. Eur J Pharm Sci 27(4):299-310.

40. Gupta RB, Shim JJ. 2007. Solubility in Supercritical Carbon Dioxide. New York; Taylor and Francis Group.

41. Pasquali I, Bettini R. 2008. Are pharmaceutics really going supercritical? Int J Pharm 364(2):176-187.

42. Baldyga J, Czarnocki R, Shekunov BY, Smith KB. 2010. Particle Formation in Supercritical Fluids – Scale-up Problem. Chem Eng Res Des 88:331-341.

43. Yasuji T, Takeuchi H, Kawashima Y. 2008. Particle design of poorly water-soluble drug substances using supercritical fluid technologies. Adv Drug Deliv Rev 60(3):388-398.

44. Ito A, Watanabe T, Yada S, Hamaura T, Nakagami H, Higashi K, Moribe K, Yamamoto K. Prediction of recrystallization behavior of troglitazone/polyvinylpyrrolidone solid dispersion by solid-state NMR. Int J Pharm 383(1-2):18-23.

45. Hancock BC, Zografi G. 1997. Characteristics and significance of the amorphous state in pharmaceutical systems. J Pharm Sci 86(1):1-12.

46. Yu L. 2001. Amorphous pharmaceutical solids: preparation, characterization and stabilization. Adv Drug Deliv Rev 48(1):27-42.

47. Hancock BC, Parks M. 2000. What is the true solubility advantage for amorphous pharmaceuticals? Pharm Res 17(4):397-404.

48. Chokshi RJ, Zia H, Sandhu HK, Shah NH, Malick WA. 2007. Improving the dissolution rate of poorly water soluble drug by solid dispersion and solid solution: pros and cons. Drug Deliv 14(1):33-45.

49. Konno H, Taylor LS. 2006. Influence of different polymers on the crystallization tendency of molecularly dispersed amorphous felodipine. J Pharm Sci 95(12):2692-2705.

50. Serajuddin AT. 1999. Solid dispersion of poorly water-soluble drugs: early promises, subsequent problems, and recent breakthroughs. J Pharm Sci 88(10):1058-1066.

51. Ivanisevic I. Physical stability studies of miscible amorphous solid dispersions. J Pharm Sci 99(9):4005-4012.

52. Qian F, Huang J, Hussain MA. Drug-polymer solubility and miscibility: Stability consideration and practical challenges in amorphous solid dispersion development. J Pharm Sci 99(7):2941-2947.

53. Yang J, Grey K, Doney J. 2010. An improved kinetics approach to describe the physical stability of amorphous solid dispersions. Int J Pharm 384(1-2):24-31.

54. Marsac PJ, Rumondor AC, Nivens DE, Kestur US, Stanciu L, Taylor LS. Effect of temperature and moisture on the miscibility of amorphous dispersions of felodipine and poly(vinyl pyrrolidone). J Pharm Sci 99(1):169-185.

55. Vasanthavada M, Tong WQ, Serajuddin ATM. 2008. Development of Solid Dispersions for Poorly Water-Soluble Drug. In Water-Insoluble Drug Formulations; Liu R, Ed.; Informa Health-care: New York; pp:149-184.

56. Karanth H, Shenoy VS, Murthy RR. 2006. Industrially feasible alternative approaches in the manufacture of solid dispersions: a technical report. AAPS PharmSciTech 7(4):87.

57. Lakshman JP, Cao Y, Kowalski J, Serajuddin AT. 2008. Application of melt extrusion in the development of a physically and chemically stable high-energy amorphous solid dispersion of a poorly water-soluble drug. Mol Pharm 5(6):994-1002.

58. Chokshi RJ, Sandhu HK, Iyer RM, Shah NH, Malick AW, Zia H. 2005. Characterization of physico-mechanical properties of indomethacin and polymers to assess their suitability for hot-melt extrusion processs as a means to manufacture solid dispersion/solution. J Pharm Sci 94(11):2463-2474.

59. Crowley MM, Zhang F, Repka MA, Thumma S, Upadhye SB, Battu SK, McGinity JW, Martin C. 2007. Pharmaceutical applications of hot-melt extrusion: part I. Drug Dev Ind Pharm 33(9):909-926.

60. Dong Z, Chatterji A, Sandhu H, Choi DS, Chokshi H, Shah N. 2008. Evaluation of solid state properties of solid dispersions prepared by hot-melt extrusion and solvent co-precipitation. Int J Pharm 355(1-2):141-149.

61. Davis ME, Brewster ME. 2004. Cyclodextrin-based pharmaceutics: past, present and future. Nat Rev Drug Discov 3(12):1023-1035.

62. Carrier RL, Miller LA, Ahmed I. 2007. The utility of cyclodextrins for enhancing oral bioavailability. J Control Release 123(2):78-99.

63. Loftsson T, Brewster ME. Pharmaceutical applications of cyclodextrins: basic science and product development. J Pharm Pharmacol 62(11):1607-1621.

64. Rao VM, Stella VJ. 2003. When can cyclodextrins be considered for solubilization purposes? J Pharm Sci 92(5):927-932.

65. Brewster ME, Loftsson T. 2007. Cyclodextrins as pharmaceutical solubilizers. Adv Drug Deliv Rev 59(7):645-666.

66. Szejtli J. 1994. Medical applications of cyclodextrins. Med Res Rev 14:353-386.

67. Okimoto K, Rajewski RA, Stella VJ. 1999. Release of testosterone from an osmotic pump tablet utilizing (SBE)7m-beta-cyclodextrin as both a solubilizing and an osmotic pump agent. J Control Release 58(1):29-38.

68. Okimoto K, Miyake M, Ohnishi N, Rajewski RA, Stella VJ, Irie T, Uekama K. 1998. Design and evaluation of an osmotic pump tablet (OPT) for prednisolone, a poorly water soluble drug, using (SBE)7m-beta-CD. Pharm Res 15(10):1562-1568.

69. Zannou EA, Streng WH, Stella VJ. 2001. Osmotic properties of sulfobutylether and hydroxypropyl cyclodextrins. Pharm Res 18(8):1226-1231.

70. Miller LA, Carrier RL, Ahmed I. 2007. Practical considerations in development of solid dosage forms that contain cyclodextrin. J Pharm Sci 96(7):1691-1707.

71. Challa R, Ahuja A, Ali J, Khar RK. 2005. Cyclodextrins in drug delivery: an updated review. AAPS PharmSciTech 6(2):E329-357.

72. Rajewski RA, Stella VJ. 1996. Pharmaceutical applications of cyclodextrins. 2. In vivo drug delivery. J Pharm Sci 85(11):1142-1169.

73. Higuchi T, Connors KA. 1965. Phase solubility techniques. Adva Anal Chem Instr 4:212-217.

Table 1.1 Biopharmaceutics Classification System[3]

Class-I High Solubility, High Permeability	**Class-II** Low Solubility, High Permeability
Class-III High Solubility, Low Permeability	**Class-IV** Low Solubility, Low Permeability

Table 1.2 List of nano/microparticle based drugs that are commercialized or under development[43]

Description	Drug	Technology	Brand name	Company
Down-Sizing				
1.Milling	Aprepitant	NanoCrystal (Elan)	Emend®	Merck
	Sirolimus	NanoCrystal (Elan)	Rapamune®	Pfizer
	Fenofibrate	NanoCrystal (Elan)	Tricor®	Abbott
	Paliperidone Palmitate	NanoCrystal (Elan)	Invega Sustenna®	Janssen
	Megestrol Acetate	NanoCrystal (Elan)	Megace ES®	Par Pharmaceuticals
2.Homogenization	Fenofibrate	IDD™	Triglide®	SkyePharma
Built-Up				
1. Supercritical fluid technology	-	SCF Milling	Under development	DuPont
	-	SFEE	Under Development	Ferro Corp.
	-	SAS-EM™	Under Development	Thar Tech.

Table 1.3 Commercially available solid dispersions[74]

Drug	Brand name	Company
Griseofulvin	Gris-PEG®	Pedinol Pharmacal Inc.
Nabilone	Cesamet®	Valeant Pharmaceuticals
Lopinavir, Ritonavir	Kaletra®	Abbott
Itraconazole	Sporanox®	Janssen Pharmaceutica
Etravirin	Intelence®	Tibotec
Everolimus	Certican®	Novartis
Verapamil	Isoptin SR-E®	Abbott
Nivaldipine	Nivadil®	Fujisawa Pharmaceutical Co.Ltd.
Tacrolimus	Prograf®	Fujisawa Pharmaceutical Co.Ltd.
Troglitazone	Rezulin®	Developed by Sankyo, manufactured by Parke-Davis division of Warner-Lambert

Table 1.4 List of marketed pharmaceutical products containing cyclodextrins[63]

Drug	Brand name	Company	Formulation
α-cyclodextrin (αCD)			
Cefotiam –hexetil HCl	Pansporin T	Takeda	Tablet
OP-1206	Opalmon	Ono	Tablet
β-*cyclodextrin (βCD)*			
Benexate Hcl	Ulget	Teikoku	Capsule
	Lonmiel	Shionogi	Capsule
Cephalosporin	Meiact	Meiji Seika	Tablet
Nicotine	Nicorette	Pfizer	Tablet
Nimesulide	Nimedex	Novartis	Tablet
2-Hydroxy propyl- β-cyclodextrin (HPβCD)			
Itraonazole	Sporanox	Janssen	Oral and IV solution
Sulfabutyl ether-β-cyclodextrin sodium salt			
Voriconazole	Vfend	Pfizer	IV Solution
Ziprasidone Mesylate	Geodon Zeldox	Pfizer	IM solution
Aripiprazole	Abilify	BMS	IM Solution
2-Hydroxy propyl-γ-cyclodextrin (HPγCD)			
Tc-99 Teoboroxime	Cardio Tec	Braco	IV Solution

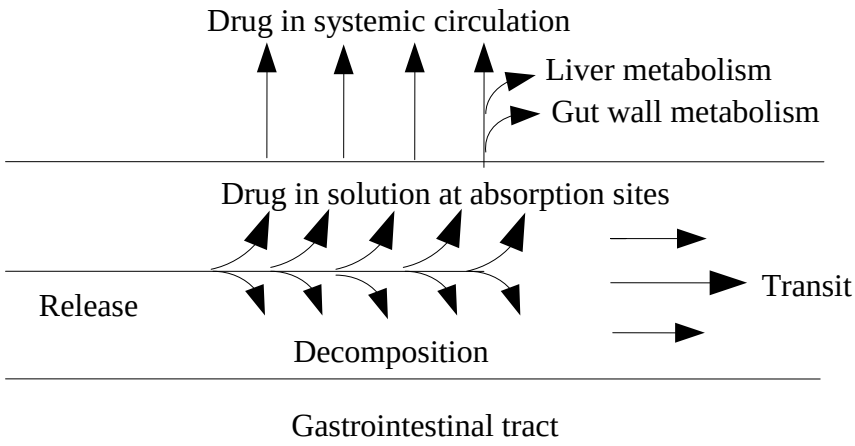

Figure 1.1 Events in the GI tract following administration of an oral dosage form.[8]

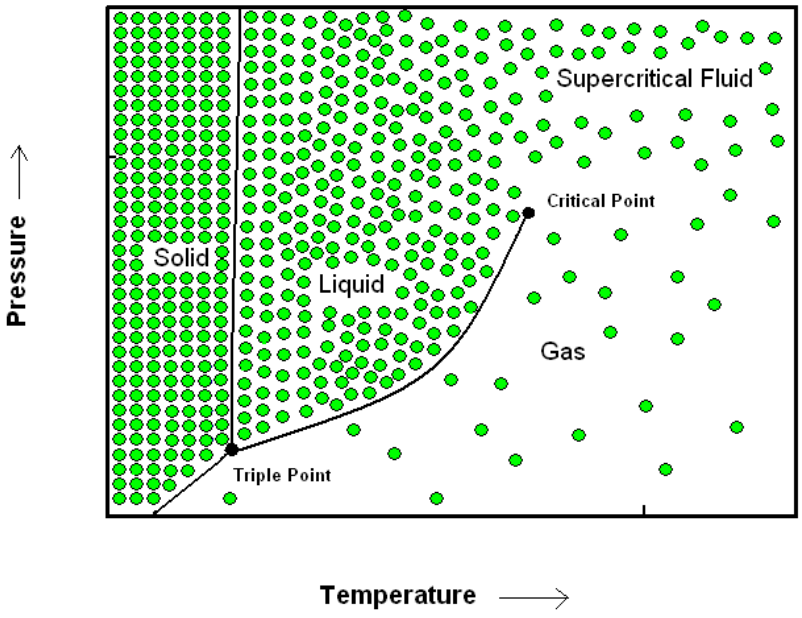

Figure 1.2 Phase diagram showing supercritical fluid region.[40]

2. Single-Step Preparation and Deagglomeration of Itraconazole Microflakes by Supercritical Antisolvent Method for Dissolution Enhancement

2.1 Abstract

Itraconazole (ITZ) microflakes were produced by supercritical antisolvent (SAS) method and simultaneously mixed with pharmaceutical excipients in a single step to prevent drug agglomeration. Simultaneous ITZ particle formation and mixing with fast-flo lactose (FFL) was performed in a high pressure stirred vessel at 116 bar and 40^{o}C by the supercritical antisolvent - drug excipient mixing (SAS-DEM) method. The effect of stabilizers, such as sodium dodecyl sulfate (SDS) and poloxamer 407 (PLX), on particle formation and drug dissolution were studied. Drug/excipient formulations were characterized for surface morphology, crystallinity, drug–excipient interactions, drug content uniformity, and drug dissolution rate. Mixture of drug microflakes and FFL formed by the SAS-DEM process show that the process was successful in overcoming drug-drug agglomeration. PLX produced crystalline drug flakes in loose agglomerates with superior dissolution and flow properties even at higher drug loadings. Characterization studies confirmed the crystallinity of the drug and absence of chemical interactions during the SAS process. The dissolution of itraconazole was substantially higher due to SAS and SAS-DEM processes; this improvement can be attributed to the

microflake particle structures, effective deagglomeration, and wetting of the drug flakes with the excipients.

2.2 Introduction

Poor aqueous solubility of the drugs is an industry wide issue for pharmaceutical scientists. For example aqueous solubility of drugs is the most critical property affecting the oral bioavailability of class-II (poorly soluble and highly permeable) drugs according to the biopharmaceutical classification system (BCS).[1] If dissolution rate of these compounds can be enhanced, bioavailability following oral administration may be significantly improved.[2] Different approaches to enhance the dissolution rate of poorly soluble drugs include, but are not limited to, particle size reduction,[3-6] inclusion complexation with cyclodextrins,[7-10] solid dispersion,[11-14] salt formation,[15-17] use of surfactants,[18-22] cosolvency,[23-24] and various particle engineering techniques.[25-28] Particle size reduction of the active pharmaceutical ingredient is an efficient and reliable method to improve the bioavailability of poorly soluble drugs.[29]

Improvement in bioavailability after micronization has been well documented for many drugs.[4,5,30,31] Micronization increases the dissolution rate of the drugs through increased surface area.[32] The use of supercritical fluids for the production of micro/nanoparticles is of great interest in recent years due to advantages such as low or no residual solvent in the process, a narrow particle size distribution, effective deagglomeration of the cohesive drug particles, and increased dissolution rate profiles.[2,14,25-28,32] Among different methods using supercritical fluids, precipitation using supercritical carbondioxide (CO_2) as an antisolvent (SAS) is well known and has been

used to micronize several kind of compounds. Carbon dioxide is an ideal supercritical fluid because of its low critical temperature (31.18^{o}C) and pressure (73.8 Pa), low cost, non-toxicity, and inert nature. In addition, CO_2 is recyclable and environmentally safe.[33] The driving force for particle formation using supercritical fluids is supersaturation which is the same as that of traditional crystallization. In the supercritical antisolvent (SAS) process, the solubilization power of a solvent is decreased by addition of a supercritical fluid as an antisolvent in which the solute is insoluble. The nucleation and consequent growth of the crystals from the solute-organic solvent-antisolvent are governed by the diffusion of the antisolvent in to the organic phase and the evaporation of the organic solvent into the antisolvent phase.[34] The rapid diffusion of antisolvent in to the organic solvent produces the supersaturation of the solute that leads to nucleation and particle formation. The fundamental mechanisms of SAS precipitation process that control the generation of various particles with different morphologies and the critical process parameters that affect the paricle size and shape of the micronized particles are seldom reported in the literature.[35-40] Jet atomization and gas plume formation are the two competitive mechanisms that determine the size of the particles formed when operated above mixture critical point.[35-36]

The high surface area of drug micro/nano particles renders them thermodynamically unstable, promoting agglomeration and crystal growth. The individual micron or nano size particles can form agglomerates ranging from loose flocculates to completely fused particles due to high surface free energy, vander Waals attraction, and hydrophobic interactions.[41-44] Currently available mixers are not effective in deagglomeration of highly cohesive drug particles or they require very high shear or

impaction acting as particle size reduction devices rather than conventional mixers. The use of high energy mixers may affect the crystal lattice of the particles, influencing the physicochemical stability of the drug. The tumbler mixer, most commonly used in pharmaceutical industry, is not effective for deagglomeration of micron/nano-sized particles.[45] In an earlier paper, we reported supercritical anti-solvent (SAS) process by which nevirapine microparticles were prepared and simultaneously deposited on excipients in a single step.[46] This method utilized environmentally benign antisolvent (CO_2) to produce highly homogenous blend of drug and excipient particles and these blends demonstrated enhanced drug dissolution when compared to the microparticle (drug) / excipient mixture obtained by conventional physical mixing.[46]

Itraconazole is a highly water insoluble drug (solubility ~ 1 ng/ml) and categorized as a BCS class II compound.[32] Different methods such as complexation with cyclodextrins,[47] solid dispersions,[48] eutectic mixtures[49] and nanoporous silica[50] were utilized to improve the solubility and dissolution of this drug. Recently, it has been demonstrated that itraconazole in its supersaturated state provokes formation of nanofibers leading to reduction of trans-epithelial transport across $Caco_2$ cell monolayers. However, nanofiber growth can be prevented if the drug is presented in the form of micelles with a surfactant.[51] In the current study we find that itraconazole (ITZ) forms microflakes by supercritical antisolvent–drug excipient mixing (SAS-DEM) process and these flakes further undergo particle aggregation. It has been reported that polymers such as polyvinyl pyrrolidone and hydroxypropyl methyl cellulose at a low concentration can affect the surface morphology of ITZ spray dried microparticles.[52] We presume that co-mixing of surfactants during SAS process can minimize the flake formation or alter their

structure and the surface morphology. Surfactants during SAS process also may minimize particle aggregation. Therefore we studied the effect of two surfactants [sodium dodecyl sulfate (SDS) and polaxamer 407 (PLX)] on particle formation, deagglomeration, and dissolution of ITZ at different drug loadings with spray dried lactose.

2.3 Materials and Methods

2.3.1 *Materials*

Micronized itraconazole was purchased from Hawkins Pharmaceutical Group (Minneapolis, MN). Spray dried lactose NF (FastFlo 316, average size ~ 100 μm) was obtained as a gift sample from Foremost, Inc (Baraboo, WI). Poloxamer 407 (Lutrol F127) was obtained as a gift sample from BASF Corp. (Parsippany, NJ). Sodium dodecyl sulfate was purchased from Spectrum Chemical Manufacturing Corp. (Gardena, CA). Dichloromethane (HPLC grade) was purchased from Mallinckrodt Baker, Inc. (Phillipsburg, NJ). Bone-dry CO_2 was purchased from Air Gas (Opelika, AL). All reagents were used as received.

2.3.2 *Production and co-mixing of drug microflakes with pharmaceutical carriers*

Micronized drug - fast-flo lactose (FFL) mixtures were produced in the SAS-DEM apparatus previously described.[46] A schematic diagram of the apparatus is shown in Figure 2.1. It consists of a compressed carbon dioxide (CO_2) gas cylinder, chiller, piston pump for pumping CO_2, heater, high pressure stirred vessel, high pressure liquid pump, and back pressure regulator. For SAS-DEM experiments, a desired amount of the excipient, lactose, was placed inside the high pressure vessel. The vessel (450 ml) was

subjected to a desired pressure (116 bar) using CO_2. A high pressure was preferred due to ease in suspending excipient particles. Stirrer speed was maintained at 400 rpm during operation. The temperature of the vessel was maintained at 40^{o}C using heating tape. ITZ solutions (10mg/ml) were prepared by dissolving the drug in dichloromethane. The flow rate of the drug solution was kept at 1 ml/min while the flow rate of antisolvent (supercritical CO_2) was kept at 20 gm/min. A capillary nozzle (PEEKsil, Upchurch Scientific, Oak Harbor, WA) of 75 μm in diameter and 15cm in length was used for the delivery of drug solution inside the vessel. After injection was complete, the high pressure vessel was flushed with supercritical CO_2 to remove any residual solvent. The flush time was around 2hr at a CO_2 flow rate of 20 gm/min. The drug or drug/excipient mixture was collected by slow depressurization of the vessel.

Itraconazole mixtures which included stabilizers were produced using SDS and PLX in 1% and 10% w/w ratios to the drug. Since SDS is insoluble in dichloromethane, it was dissolved in methanol and added to the drug solution. The PLX was dissolved along with the drug in dichloromethane. In both cases, the drug solution was sprayed into high pressure vessel following the procedure detailed above. At the end of each supercritical anti-solvent (SAS) operation, the vessel has a deposit of a thin layer of powder on its surface. This served as a pre-coat and this was left on the vessel to avoid absorptive loss of SAS drug at each run.

2.3.3 *Preparation of physical mixtures*

Itraconazole flakes produced by SAS and FFL were spatula mixed for approximately 2 minutes at 25 wt% drug loading and stored in an air-tight glass vial prior to analysis.

2.3.4 *Scanning electron microscopy (SEM)*

Surface morphologies were studied using a scanning electron microscope (Zeiss EVO 50, UK). The samples were spread onto double-sided adhesive carbon tape on an aluminum stub. A thin coating (~ 15 nm) of gold was applied on to the sample using a sputter coater (Electron Microscopy services, EMS 550X) prior to microscopy.

2.3.5 *Particle size measurements*

Particle size was determined by measuring light obscuration with an Accusizer 780 AD particle size analyzer (Particle Sizing Systems, Santa Barbara, CA). The samples were dispersed in a saturated solution of the drug (0.2 wt% SDS in deionized water), gently hand-shaken, and then introduced 0.5 ml of the dispersion to the flow cell for the measurement. In the case of ITZ-FFL mixtures, care was taken to ensure that lactose was completely dissolved before performing analysis. The PSD is expressed as a number weighted diameter, and the results are expressed as d_{50} and d_{90}, denoting the diameter of the 50^{th} and 90^{th} percentile of the distribution, respectively. To verify the accuracy of the particle size measurements made by light obscuration method, latex standards of 0.8 µm, 2 µm and 5 µm were tested. Average diameters were measured as 0.8 µm, 2.02 µm and 4.96 µm, respectively.

2.3.6 *X-ray diffraction studies (XRD)*

Drug crystallinity was evaluated using a Rigaku X-ray diffractometer (Rigaku Americas, The Woodlands, TX) equipped with a Cu $K\alpha_1$ radiation source at 40 kV, 40 mA, and a miniflex gonoiometer. Diffraction patterns were obtained in 2θ range of 5–50° using a step size of 0.05° and scan speed of 5°/min.

2.3.7 *Differential Scanning Calorimetry (DSC)*

DSC was performed using a Q200 differential scanning calorimeter (TA Instruments, New Castle, DE). About 5 mg of each sample was weighed in aluminum pan and the thermographs were recorded using a heating rate of 10^{o}C/min over the temperature range of 25-200^{o}C.

2.3.8 *Fourier transform infrared (FTIR) spectroscopy*

Infrared spectra of the samples were obtained on a Nicolet IR 100 spectrometer (Thermo Scientific, USA) in the 400 to 4000 cm^{-1} range using 64 scans and a resolution of 2 cm^{-1}. Samples were mixed with 100 fold KBr for preparing the pellets.

2.3.9 *Brunauer, Emmett and Teller (BET) Surface area*

The specific surface area of the supplier ITZ and SAS-produced ITZ flakes were determined using a Nova 3000 surface area analyzer (Quantachrome Corporation, Boynton Beach, FL) to measure nitrogen sorption. The surface area per unit powder mass was calculated by fitting the BET equation.

2.3.10 *Drug loading and content uniformity*

The drug loading of the ITZ/FFL and ITZ/PLX/FFL mixtures was determined using UV/Vis spectrophotometer (Jasco Inc., Tokyo, Japan) at λ = 261 nm. A known amount of sample was dissolved in acetonitrile to obtain the amount of ITZ in each mixture. The effect of PLX and FFL concentration on ITZ absorbance was negligible. As a measure of drug content uniformity, the relative standard deviation (RSD) of the drug was calculated using:

$$RSD = \frac{\sigma}{\overline{C}}$$

$$\sigma^2 = \sum_{i=1}^{n} \frac{(\overline{C} - C_i)^2}{n-1}$$

Where n is the total number of samples, σ is the variance, σ^2 is the standard deviation, $\overline{C}$ is the mean concentration, and C_i is the sample concentration. A lower RSD value signifies better homogeneity.

2.3.11 *Saturation solubility measurements*

Saturation solubility studies were carried out according to Higuchi and Connors.[53] A formulation equivalent to 10 mg of drug was added to 5 ml of water in a 20 ml scintillation vial and sonicated for 30 mins, five times a day for two days. After equilibrium for 24 hrs, aliquots were withdrawn, filtered (0.22 μm pore size nylon filters from Whatman International, England) and spectrophotometrically assayed for the drug content at 261 nm.

2.3.12 *Dissolution studies*

Dissolution studies were carried out in 900 ml of 0.1N HCl with 0.3% SDS dissolution medium using a USP-II dissolution apparatus (Hansen Research, Chatsworth, CA) operated at 37 °C and 50 rpm. A formulation equivalent to 10 mg of the drug was sprinkled on to the top of the dissolution medium. Liquid samples were withdrawn at time intervals of 5, 10, 15, 20, 30, 45, 60, 75, 90 and 120 minutes, filtered (0.45 μm pore size nylon filters from Whatman International, England) and assayed for drug content by UV spectrophotometry at 261 nm.

2.3.13 *Data Analysis*

Amount of ITZ dissolution of various samples was plotted as a function of time. The data were presented as mean ± standard deviation of 6 formulations. The mean cumulative amount ITZ dissolved in 30 or 60 minutes is expressed as D_{30} or D_{60}, respectively. Analysis of variance of D_{60} data was performed using GraphPad Prism. The mean data with $P < 0.05$ were considered to be significantly different.

2.4 Results and Discussion

2.4.1 *Characterization by SEM and particle size analysis*

Figure 2.2a shows SEM image of micron-sized drug particles as obtained from the supplier. The drug particles have a rectangular shape with a wide PSD, as shown in Table 2.1 (d_{50} = 1.55 ± 0.49 μm; d_{90} = 10.31 ± 2.30 μm). The drug produced by SAS is shown in Figure 2.2b, where flaky particles formed loose agglomerates (Figure 2.2b1). The sizes of the primary particles, as observed under SEM, were between < 1 μm and 14

μm, whereas the thickness of the flakes is in the submicron range (Figure 2.3). The PSD of the SAS flakes was found to be narrow as determined by light obscuration method (d_{50} = 0.94 ± 0.05 μm; d_{90} = 5.09 ± 0.39 μm). The particle size is expressed in number weighted distribution, which is useful for determining the size of the primary particles in agglomerated systems. The closer the number weighted and volume weighted PSDs, the narrower the distribution.[54] The shape and size of the drug particles produced by SAS can be affected by the supersaturation and nucleation rate of the drug particles in the supercritical fluid, and with the change of solvent strength. Kim et al reported that different size and shape particles can be produced by change in the organic solvent.[55] Due to higher diffusivity of supercritical fluid, faster super-saturation of the solute is achieved leading to precipitation of smaller particles during SAS re-crystallization process.[39] The diameter of the capillary injector also has an effect on particle formation. Studies have shown the effect of jet break up and droplet formation on the size of the particles.[35-36] The gas plume formation (single-phase mixing) and jet break-up are the two competitive mechanisms that determine the size of the particles formed when operated above mixture critical point (MCP). At conditions below the MCP, the interfacial tension persists, and a multiphase mixing system results after jet break-up into droplets. When operated above MCP conditions, due to nucleation mechanisms, nanoparticles are formed if the interfacial tension is completely disappeared before the jet break-up, whereas microparticles are formed if jet break up dominates. The operating conditions employed in the process are above the critical point of the solvent - CO_2 mixture; however the effect of solute on the MCP was not taken into account. The formation of microparticles in our process suggests that the jet break up may be the dominant phenomenon.

In addition to the processing parameters such as solution flow rate, type of solvent, drug concentration, pressure, temperature and antisolvent (CO_2) flow rate that can affect supersaturation, the PSD of the particles produced by SAS process also depends on the drug properties such as melting point, log octanol-water-partition coefficient (log P).[56]

The de-agglomeration of flaky drug particles by simple mixing with pharmaceutical excipients is difficult due to their shape.[57] We presume that the SAS-DEM process is suitable for de-agglomerating flaky particles of micron or nano size thicknesses than simple blending. SAS-DEM process employs pharmaceutical carriers on which the micro- or nanoparticles are deposited while they are produced by the SAS process. The drug-excipient mixtures thus obtained will have pharmaceutical advantages such as enhanced dissolution rate of insoluble drugs because of increased surface area and wettability by depositing on to hydrophilic or porous excipients, enhanced flow properties of the micronized drug particles due to deposition of micronized particles on to the freely flowable excipients. SAS-DEM process also reduces the toxicity during handling of highly potent nano/micro size drug due to the dilution of the drug with excipients and reduction in various handling steps**.**

Figure 2.4 shows the SEM images of SAS-DEM processed drug and lactose at various drug loadings. The lactose particles are mostly spherical in shape (Figure 2.4a). In SAS-DEM processed drug and lactose at 6 wt% drug loading as shown in Figure 2.4b, the flaky drug particles are deposited on the lactose surface and there are no free drug agglomerates seen in the sample. The magnified image presented in Figure 2.4b1 clearly shows the deposition of tiny flaky structures on lactose. As the drug loading is increased

to 23 wt%, the entire surface of the lactose is covered by the flaky drug particles (Figure 2.4c). This image also shows the presence of a few loose drug agglomerates. These agglomerates are the result of fusion of several primary drug particles due to van der Waals attraction and hydrophobic interactions.[43-45] As the drug loading was further increased, a large number of free drug agglomerates were observed in the sample (Figure 4d) and the surface of the lactose was fully covered with drug particles (Figure 2.4d1). To determine whether free drug particles not associated with lactose formed loose agglomerates, the samples were suspended in saturated drug solution and sonicated for 2 min. The particles were examined by SEM imaging after drying on the stub, as described earlier. The SEM image indicates that there is still presence of few smaller agglomerates in the sample at higher drug loadings (> 23 wt%, data not shown).

The PSD of the drug in the drug/FFL SAS-DEM products are shown in Table 2.1. These results represent the size distribution of the drug particles after eliminating lactose in the samples by dissolving out in water. The particles are significantly smaller in SAS-DEM products at lower drug loading (6 wt%) as compared to SAS drug; this is due to the deposition on lactose which reduced particle growth and/or agglomeration of drug particles. As the drug loading was increased to 23 wt%, the particle size was significantly increased because the lactose surface was completely covered and the excess drug formed agglomerates. As seen in the SEM images, due to the flaky nature of the SAS drug, the deposition of the drug on the lactose surface did not result in ordered drug-excipient mixture. These results are in contrast to our earlier study on SAS-DEM produced nevirapine particles, where nevirapine was recrystallized to tiny rectangular particles, due

to which even at higher drug loading in the mixture the particles are able to deposit on the surface of the lactose and form ordered drug excipient mixtures.[46]

We presumed that the addition of stabilizers such as surfactants or polymers would help in deagglomerating the flaky drug particles. The SAS-DEM process was carried out in the presence of SDS and PLX as stabilizers. In order to observe the effect of stabilizer, experiments were conducted initially without FFL. SDS did not serve as an effective de-agglomeration agent at 1% w/w concentration as shown in Figure 2.5a. Large number of drug-drug agglomerates are observed under SEM, similar to drug produced from SAS process. As the SDS concentration was increased to 10 wt% there was a decrease in drug agglomeration (Figure 2.5b), but it was observed that the size of individual flaky drug particles was more than the SAS drug. We assume this may be due to the changes in supersaturation levels by addition of methanol to the drug solution. As SDS is not soluble in dichloromethane, it was initially dissolved in 10 ml of methanol and added to drug in dichloromethane. Figure 2.6 shows the SEM image of the drug along with the PLX stabilizer in two proportions. The individual drug flakes were inter-connected with PLX and formed loose agglomerates of the drug at both 1 and 10 wt% PLX. Similar type of observation was reported when danazol and naproxen drug particles were precipitated in the presence of PLX from an organic solvent.[2] To confirm the drug particles that are associated with PLX are loose agglomerates, the samples were suspended in an 0.3% SDS solution (previously saturated with the drug) so that PLX is dissolved leaving the free drug particles. These solutions were analyzed for the PSD by light obscuration method as explained earlier. The PSD of the drug produced from the SAS method along with PLX at 10% w/w was found to be smaller than the drug

produced from SAS alone (d_{50}: 0.82 ± 0.06 µm; d_{90}: 3.45 ± 0.19 µm). The agglomerates as observed under SEM are around 20 to 40 µm and composed of primary particles, but when suspended in aqueous medium (saturated with the drug), these agglomerates are easily broken into primary particles of micro/nanometer size as shown in Table 2.1. These particles appear to have better flow properties than the particles produced without PLX, where the drug formed large irregular agglomerates due to the flaky nature of the drug. Further experiments are needed to evaluate the flow properties of these mixtures. Current experimentation was designed to produce smaller batches which are insufficient to measure flow properties of the powders**.** Figure 2.7 shows the SEM images of SAS-DEM product of drug/PLX/FFL at two different drug loadings. As shown in Figure 2.7a, the flaky drug particles are deposited on the surface of lactose and at higher drug loadings, loose agglomerates of the free excess drug in association with the PLX were formed in the mixture. In absence of PLX the excess free drug formed large irregular agglomerates, whereas in the presence of PLX at a higher drug loading on lactose (> 23 wt%), the surface of lactose totally covered with drug particles and the excess free drug formed agglomerates. The flow of these powders is much better than the SAS-DEM processed drug/lactose products at the similar drug loading (Figure 2.4c).

2.4.2 *Characterization by XRD*

XRD patterns for the bulk ITZ (as purchased from supplier), the drug produced by SAS process, the drug produced by SAS along with the stabilizers (PLX and SLS) in 10 wt% are shown in Figure 2.8. ITZ exhibited intense characteristic crystalline peaks at 2-theta values of 14.35, 17.46, 20.31, and 23.41 degrees. The XRD pattern for the drug

produced from the SAS and drug produced from SAS along with SDS were superimposable to the spectra of drug from supplier, indicating the drug has maintained the crystallinity in the SAS process. The XRD pattern for drug produced from the SAS along with PLX showed characteristic crystalline peaks, indicating crystalline nature. The decrease in the intensity of the peak at 17.46 may be due to association of PLX on the specific crystal surface. It was reported in the literature that ITZ with PLX in dichloromethane, when precipitated by evaporative precipitation into an aqueous solution the drug maintained its crystallinity.[58] Drug also has maintained its crystallinity during SAS-DEM process with lactose (data not shown). It was reported in our previous study that the SAS-DEM process with lactose did not alter the crystallinity of nevirapine.[46]

2.4.3 *Characterization by DSC*

Figure 2.9 shows DSC thermographs for the bulk ITZ, SAS drug, and SAS drug with 10 wt% stabilizers (SDS or PLX). ITZ showed a typical behavior of anhydrous crystalline drug with a well defined melting peak at 167°C (ΔH = 825.5 J/g). The SAS treated drug also showed a distinct endothermic peak with no change in heat flow at (ΔH =784.7 J/g), confirming there is no change in the crystallinity by the process. The thermographs of the drug produced by SAS along with the stabilizers also show a distinct characteristic endothermic peak, indicating the crystalline nature of the drug was not affected by the addition of stabilizers either. The mixtures produced by the SAS-DEM process also show the melting endotherm of the drug, confirming the crystalline nature.

2.4.4 *Characterization by FTIR*

FTIR spectra of bulk drug, SAS drug, and various SAS-DEM mixtures are shown in Figure 2.10. The spectra of the SAS drug and SAS drug stabilized with PLX or SDS are similar to that of the bulk drug from supplier, with no shift of peaks due to SAS process with or without the excipients. These results indicate that there are no significant changes in the physicochemical properties of ITZ and there is no chemical interaction between the drug and the excipients or stabilizers with the SAS-DEM process.

2.4.5 *Surface area*

The surface area of the bulk drug (from the commercial supplier) was 2.008 m^2/g whereas that of SAS drug was 2.105 m^2/g. SAS drug even though produced flaky particles in nanometer thicknesses, the formed agglomerates leading to reduction in the surface area of the discrete particles (microflakes). These agglomerates are composed of smaller primary particles in the micron-sized range as can be seen from the SEM results in Figure 2.3. Even though the specific area of SAS drug is similar to micron sized drug from supplier, the SAS drug demonstrated a narrow particle size distribution. The small size and the morphology of the SAS produced primary drug particles should lead to a high dissolution compared to the bulk powder.

2.4.6 *Drug content homogeneity*

The drug content uniformity data of SAS-DEM processed drug/FFL and drug/Stabilizer/FFL mixtures of different drug loadings are given in Table 2.2. The RSDs

for all the mixtures are less than 5%, indicating the drug is uniformly dispersed in the mixture(s) by this process at various drug loadings.

2.4.7 *Dissolution studies*

The dissolution profiles for bulk drug (from supplier), SAS drug, and for SAS-DEM products of various drug loadings are given in Figure 2.11. The dissolution rate of SAS drug was found to be about 2.5 fold higher (D_{60} = 65%) than the dissolution rate of the micronized drug from the supplier (D_{60} =24%). The increased dissolution of the SAS drug is due to the decrease in the particle size as shown in Table 2.1. According to Noyes-Whitney equation, particle size reduction leads to increased surface area and that leads to enhancement in the dissolution rate.[59] In addition, the solubility of SAS drug (0.247 gm/ml) is higher than that of the bulk drug (0.187 mg/ml). In contrast to our particle size observation, the surface area of the SAS drug is similar to the surface area of bulk drug (supplier) and this was found to be due to formation of agglomerates of primary particles of the SAS drug in the dry state. During particle size measurement, when the SAS drug is suspended in aqueous medium with 0.2 wt % SDS (presaturated with drug), the agglomerates were broken into primary drug particles of submicron size (Table 2.1). In the similar manner, the loose agglomerates of the SAS drug should produce primary drug particles in the dissolution media leading to larger surface area and enhanced dissolution. The bulk drug (unprocessed) demonstrated poor dissolution than the SAS processed drug mixtures.

In the case of SAS-DEM drug/FFL mixtures significantly higher dissolution rate was observed for 6 and 23 wt% drug loadings on lactose (D_{60} = 91% and 86%,

respectively) than the physical mixture containing 23 wt% SAS drug ((D_{60} = 66%). It was observed that, as soon as the SAS-DEM drug/FFL mixture was introduced into the dissolution medium, the lactose particles dissolved and all the drug particles deposited on the lactose were well dispersed in the dissolution medium. Higher drug loadings were associated with drug particle aggregates as observed in Figure 2.4c, which demonstrated relatively lower dissolution than the samples with lower drug loading (6 wt%). Overall enhancement in the drug dissolution was due to rapid dispersion or deagglomeration of the drug particles and also due to the improved wettability of the drug particles in the presence of a hydrophilic excipient, FFL. As the drug loading in the mixture is increased to 40%, there is a decrease in the dissolution rate (D_{60} = 64%) and, this is attributed to the agglomeration of the free drug at higher drug loadings as shown earlier in the SEM studies (Figure 2.4d). The physical mixture of drug/FFL at 25 wt% drug loading showed similar dissolution to that of SAS drug, indicating simple physical mixing with FFL was not effective in de-agglomerating the flaky drug particles. Figure 2.4e shows that the SAS drug and FFL excipient particles formed a random mixture, and the presence of drug agglomerates indicates efficient de-agglomeration of flaky drug particles was not achieved by simple physical mixing.

It was postulated that the addition of stabilizers could alter the surface morphology of the particles and also decrease their agglomeration, in turn increasing the dissolution of ITZ. Figure 2.12 presents the dissolution profiles of the SAS drug along with SDS as a stabilizer. There was no significant increase in the dissolution rate due to SDS in the SAS process. SEM images revealed no significant changes in the morphology of the particles and therefore dissolution rate was not altered much due to addition of

SDS. The dissolution profiles for SAS drug along with PLX as stabilizer are shown in Figure 2.13. It is evident from the results that there is no significant increase in the dissolution rate due to addition of PLX at 1 wt%, but at 10 wt% the dissolution of the drug increased by 2 fold (D_{30} = 78%) when compared to SAS drug (D_{30} = 35%). The increase in the dissolution of ITZ is due to a decrease in the particle size of the SAS drug with 10% PLX as shown in Table 2.1 and also due to sufficient wetting of the drug particles because of deposition on surrounding excipient particles. The physical mixture of the SAS drug with PLX in 10 wt% also shows a slight increase in the dissolution rate (D_{30} =54%) when compared to the SAS drug, this is due to improved wettability of ITZ by PLX. The dissolution profiles for drug/PLX/FFL mixtures were shown in Figure 2.14. The mixtures showed similar dissolution rates as that of 10 wt% PLX, and the results were as expected. The D_{60} values for the drug/10%wt PLX, drug/PLX/15% wt FFL and drug/PLX/50% wt FFL were 85%, 78% and 85%, respectively. The flowability of the powder should be much better due to addition of FFL and provides directly compressible blend for ITZ.

In conclusion, itraconazole microflakes were produced by the SAS process, and showed significant enhanced dissolution compared to the bulk drug. Production of micro flakes by SAS-DEM method with FFL prevents drug agglomeration and further enhanced the dissolution rate at lower drug loadings. PLX produced crystalline drug micro/nanoflakes in loose agglomerates with superior dissolution properties even at higher drug loadings. These flakes upon dispersion in water fragment and produce smaller flakes. The enhancement in the dissolution rate is due to decrease in particle size in presence of PLX and as well as sufficient wetting of the drug particles due to

surrounding excipient particles. XRD, DSC and FT-IR studies revealed that crystallinity of the drug is not altered. Further, ITZ did not undergo any specific chemical interactions with PLX and FFL by SAS-DEM method.

2.5 Acknowledgments

Financial supports from National Science Foundation (NIRT grant DMI-0506722) and from Harrison School of Pharmacy, Auburn University are appreciated. We would like to thank Mr. Adam Byrd, Dept. of Chemical Engineering, Auburn University for his assistance with surface area measurement.

2.6 References

1. Amidon GL, Lennernaes H, Shah VP, Crison JR. 1995. A theoretical basis for a biopharmaceutic drug classification: the correlation of in vitro drug product dissolution and in vivo bioavailability. Pharm Res 12(3):413-420.
2. Rogers TL, Gillespie IB, Hitt JE, Fransen KL, Crowl CA, Tucker CJ, Kupperblatt GB, Becker JN, Wilson DL, Todd C, Broomall CF, Evans JC, Elder EJ. 2004. Development and Characterization of a Scalable Controlled Precipitation Process to Enhance the Dissolution of Poorly Water-Soluble Drugs. Pharm Research 21(11):2048-2057.
3. Rasenack N, Mueller BW. 2002. Dissolution Rate Enhancement by in Situ Micronization of Poorly Water-Soluble Drugs. Pharm Res 19(12):1894-1900.
4. Jounela AJ, Pentikainen PJ, Sothmann A. 1975. Effect of particle size on the bioavailability of digoxin. Eur J Clin Pharmaco 8(5):365-370.

5. Liversidge GG, Cundy KC. 1995. Particle size reduction for improvement of oral bioavailability of hydrophobic drugs: I. Absolute oral bioavailability of nanocrystalline danazol in beagle dogs. Int J Pharm 125(1):91-97.

6. Vogt M, Kunath K, Dressman JB. 2008. Dissolution enhancement of fenofibrate by micronization, cogrinding and spray-drying: Comparison with commercial preparations. Eur J Pharm Biopharm 68(2):283-288.

7. Brewster ME, Loftsson T, Estes KS, Lin JL, Fridriksdottir H, Bodor N. 1992. Effect of various cyclodextrins on solution stability and dissolution rate of doxorubicin hydrochloride. Int J Pharm 79(2-3):289-299.

8. Badr-Eldin SM, Elkheshen SA, Ghorab MM. 2008. Inclusion complexes of tadalafil with natural and chemically modified beta-cyclodextrins. I: Preparation and *in-vitro* evaluation. Eur J Pharm Biopharm 70(3):819-827.

9. Sathigari S, Chadha G, Phillip LYH, Wright N, Parsons DL, Rangari VK, Fasina O, Babu RJ. 2009. Physicochemical characterization of efavirenz-cyclodextrin inclusion complexes. AAPS PharmSciTech 10(1):81-87.

10. Phillip LYH, Sathigari S, Jean LYJ, Ravis WR, Chadha G, Parsons DL, Rangari Vijay K, Wright N, Babu RJ. 2009. Gefitinib-cyclodextrin inclusion complexes: physico-chemical characterization and dissolution studies. Drug Dev Ind Pharm 35(9):1113-1120.

11. Joshi HN, Tejwani RW, Davidovich M, Sahasrabudhe VP, Jemal M, Bathala MS, Varia SA, Serajuddin ATM. 2004. Bioavailability enhancement of a poorly water-soluble drug by solid dispersion in polyethylene glycol-polysorbate 80 mixture. Int J Pharm 269(1):251-258.

12. Dannenfelser RM, He H, Joshi Y, Bateman S, Serajuddin ATM. 2004. Development of clinical dosage forms for a poorly water soluble drug I: application of polyethylene glycol-polysorbate 80 solid dispersion carrier system. J Pharm Sci 93(5):1165-1175.
13. Kennedy M, Hu J, Gao P, Li L, Ali-Reynolds A, Chal B, Gupta V, Ma C, Mahajan N, Akrami A, Surapaneni S. 2008. Enhanced Bioavailability of a Poorly Soluble VR1 Antagonist Using an Amorphous Solid Dispersion Approach: A Case Study. Mol Pharm 5(6):981-993.
14. Muhrer G, Meier U, Fusaro F, Albano S, Mazzotti M. 2006. Use of compressed gas precipitation to enhance the dissolution behavior of a poorly water-soluble drug: Generation of drug microparticles and drug-polymer solid dispersions. Int J Pharm 308(1-2):69-83.
15. Han HK, Choi HK. 2007. Improved absorption of meloxicam via salt formation with ethanolamines. Eur J Pharm Biopharm 65(1):99-103.
16. Gwak HS, Choi JS, Choi HK. 2005. Enhanced bioavailability of piroxicam via salt formation with ethanolamines. Int J Pharm 297(1-2):156-161.
17. O'Connor KM, Corrigan OI. 2001. Comparison of the physicochemical properties of the N-(2-hydroxyethyl)pyrrolidine, diethylamine and sodium salt forms of diclofenac. Int J Pharm 222(2):281-293.
18. Balakrishnan A, Rege BD, Amidon GL, Polli JE. 2004. Surfactant-mediated dissolution: Contributions of solubility enhancement and relatively low micelle diffusivity. J Pharm Sci 93(8):2064-2075.

19. Chavanpatil MD, Khdair A, Panyam J. 2007. Surfactant-polymer Nanoparticles: A Novel Platform for Sustained and Enhanced Cellular Delivery of Water-soluble Molecules. Pharm Res 24(4):803-810.

20. Chiou WL, Chen SJ, Athanikar N. 1976. Enhancement of dissolution rates of poorly water-soluble drugs by crystallization in aqueous surfactant solutions. I: sulfathiazole, prednisone, and chloramphenicol. J Pharm Sci 65(11):1702-1704.

21. Granero GE, Ramachandran C, Amidon GL. 2005. Dissolution and solubility behavior of fenofibrate in sodium lauryl sulfate solutions. Drug Dev Ind Pharm 31(9):917-922.

22. Wong SM, Kellaway IW, Murdan S. 2006. Enhancement of the dissolution rate and oral absorption of a poorly water soluble drug by formation of surfactant-containing microparticles. Int J Pharm 317(1):61-68.

23. Kawakami K, Miyoshi K, Ida Y. 2004. Solubilization behavior of poorly soluble drugs with combined use of Gelucire 44/14 and cosolvent. J Pharm Sci 93(6):1471-1479.

24. Viernstein H, Weiss-Greiler P, Wolschann P. 2003. Solubility enhancement of low soluble biologically active compounds-temperature and cosolvent dependent inclusion complexation. Int J Pharm 256(1-2):85-94.

25. Blagden N, de Matas M, Gavan PT, York P. 2007. Crystal engineering of active pharmaceutical ingredients to improve solubility and dissolution rates. Adv Drug Deliv Rev 59(7):617-630.

26. Jung J, Perrut M. 2001. Particle design using supercritical fluids: Literature and patent survey. J Supercrit Fluids 20(3):179-219.

27. Loth H, Hemgesberg E. 1986. Properties and dissolution of drugs micronized by crystallization from supercritical gases. Int J Pharm 32(2-3):265-267.

28. Foster NR, Dehghani F, Charoenchaitrakool KM, Warwick B. 2003. Application of dense gas techniques for the production of fine particles. AAPS PharmSci 5(2):1-7.

29. Jonghwi L. 2003. Drug nano and microparticles processed into solid dosage forms: physical properties. J Pharm Sci 92(10):2057-2068.

30. Farinha A, Bica A, Tavares P. 2000. Improved bioavailability of a micronized megestrol acetate tablet formulation in humans. Drug Dev Ind Pharm 26(5):567-570.

31. Sitruk-Ware R, Bricaire C, De Lignieres B, Yaneva H, Mauvais-Jarvis P. 1987. Oral micronized progesterone: Bioavailability pharmacokinetics, pharmacological and therapeutic implications-a review. Contraception 36(4):373-402.

32. Barrett AM, Dehghani F, Foster NR. 2008. Increasing the Dissolution Rate of Itraconazole Processed by Gas Antisolvent Techniques using Polyethylene Glycol as a Carrier. Pharm Res 25(6):1274-1289.

33. Reverchon E, Della PG. 2001. Supercritical fluids-assisted Micronization techniques: Low-impact routes for particle production. Pure Appl Chem 73(8):1293-1297.

34. Pasquali I, Bettini R, Giordano F. 2008. Supercritical fluid technologies: An innovative approach for manipulating the solid-state of pharmaceuticals. Adv Drug Deliv Rev 60(3):399-410.

35. Lengsfeld CS, Delplanque JP, Barocas VH, Randolph TW. 2000. Mechanism Governing Microparticle Morphology during Precipitation by a Compressed Antisolvent: Atomization vs Nucleation and Growth. J Phys Chem B 104(12):2725-2735.

36. Reverchon E, Torino E, Dowy S, Braeuer A, Leipertz A. 2010. Interactions of phase equilibria, jet fluid dynamics and mass transfer during supercritical antisolvent Micronization. Chem Eng J 156(2):446-458.

37. Perez de DY, Pellikaan HC, Wubbolts FE, Witkamp GJ, Jansens PJ. 2005. Operating regimes and mechanism of particle formation during the precipitation of polymers using the PCA process. J Supercrit Fluids 35(2):147-156.

38. Sacha GA, Schmitt WJ, Nail SL. 2006. Identification of critical process variables affecting particle size following precipitation using a supercritical fluid. Pharm Dev Technol 11(2):187-194.

39. Sacha GA, Schmitt WJ, Nail SL. 2006. Identification of physical-chemical variables affecting particle size following precipitation using a supercritical fluid. Pharm Dev. Technol 11(2):195-205.

40. Reverchon E, De Marco I, Torino E. 2007. Nanoparticles production by supercritical antisolvent precipitation: A general interpretation. J Supercrit Fluids 43(1):126-138.

41. Aguiar AJ, Zelmer JE, Kinkel AW. 1967. Deaggregation behavior of a relatively insoluble substituted benzoic acid and its sodium salt. J Pharm Sci 56(10):1243-1252.

42. Swanepoel E, Liebenberg W, de Villiers MM, Dekker TG. 2000. Dissolution properties of piroxicam powders and capsules as a function of particle size and the agglomeration of powders. Drug Dev Ind Pharm 26(10):1067-1076.

43. de Villiers MM. 1996. Influence of agglomeration of cohesive particles on the dissolution behavior of furosemide powder. Int J Pharm 136(1,2):175-179.

44. Kale K, Hapgood K, Stewart P 2009. Drug agglomeration and dissolution - What is the influence of powder mixing? Eur J Pharm Biopharm 72(1):156-164.

45. Harnby N. 2000. An engineering view of pharmaceutical powder mixing. Pharm Sci Technolo Today 3(9):303-309.

46. Sanganwar GP, Sathigari S, Babu RJ, Gupta RB. 2010. Simultaneous production and co-mixing of microparticles of nevirapine with excipients by supercritical antisolvent method for dissolution enhancement. Eur J Pharm Sci 39(1-3):164-174.

47. Hassan HA, Al-Marzouqi AH, Jobe B, Hamza AA, Ramadan GA. 2007. Enhancement of dissolution amount and in vivo bioavailability of itraconazole by complexation with beta -cyclodextrin using supercritical carbon dioxide. J Pharm Biomed Anal 45(2):243-250.

48. El Maghraby GM, Alomrani AH. 2009. Synergistic enhancement of itraconazole dissolution by ternary system formation with pluronic F68 and hydroxypropylmethylcellulose. Sci Pharm 77(2):401-417.

49. Liu D, Fei X, Wang S, Jiang T, Su D. 2006. Increasing solubility and dissolution rate of drugs via eutectic mixtures: itraconazole-poloxamer 188 system. Asian J Pharm Sci 1(3-4):213-221.

50. Mellaerts R, Mols R, Jammaer JAG, Aerts CA, Annaert P, Van Humbeeck J, Van den Mooter G, Augustijns P, Martens JA. 2008. Increasing the oral bioavailability of the poorly water soluble drug itraconazole with ordered mesoporous silica. Eur J Pharm Biopharm 69(1):223-230.

51. Mellaerts R, Aerts A, Caremans TP, Vermant J, Van den Mooter G, Martens JA, Augustijns P. 2010. Growth of Itraconazole Nanofibers in Supersaturated Simulated Intestinal Fluid. Mol Pharm 7(3):905-913.

52. Wulsten E, Kiekens F, van Dycke F, Voorspoels J, Lee G. 2009. Levitated single-droplet drying: Case study with itraconazole dried in binary organic solvent mixtures. Int J Pharm 378(1-2):116-121.

53. Higuchi T, Connors KA. 1965. Phase-solubility techniques. Adv Anal Chem Instr 4:117-212.

54. Shekunov BY, Chattopadhyay P, Tong HHY, Chow AHL. 2007. Particle Size Analysis in Pharmaceutics: Principles, Methods and Applications. Pharm Res 24(2):203-227.

55. Kim MS, Lee S, Park JS, Woo JS, Hwang SJ. 2007. Micronization of cilostazol using supercritical antisolvent (SAS) process: Effect of process parameters. Powder Technol 177(2):64-70.

56. Chattopadhyay P, Gupta RB. 2002. Protein nanoparticles formation by supercritical antisolvent with enhanced mass transfer. AIChE J 48(2):235-244.

57. Sanganwar GP, Gupta RB. 2008. Enhancement of shelf life and handling properties of drug nanoparticles: nanoscale mixing of itraconazole with silica. Ind Eng Chem Res 47(14):4717-4725.

58. Sinswat P, Gao X, Yacaman MJ, Williams RO, Johnston KP. 2005. Stabilizer choice for rapid dissolving high potency itraconazole particles formed by evaporative precipitation into aqueous solution. Int J Pharm 302(1-2):113-124.

59. Noyes AA, Whitney WR. 1897. The rate of solution of solid substances in their own solutions. J Am Chem Soc 19(12):930-934.

Table 2.1 Particle size distribution of Itraconazole in various formulations

Sample	d_{50} (μm)	d_{90} (μm)
ITZ, micronized	1.55 ± 0.49	10.31± 2.30
ITZ, SAS	0.94 ± 0.05	5.09 ± 0.39
ITZ + FFL SAS-DEM (6% drug loading)	0.82 ± 0.06	3.49 ± 0.84
ITZ + FFL SAS-DEM (23% drug loading)	1.73 ± 0.83	6.28 ± 0.86
ITZ + FFL SAS-DEM (40% drug loading)	0.90 ± 0.05	6.75 ± 0.61
ITZ + 10% PLX	0.82 ± 0.01	3.45 ± 0.19
ITZ + 1% SDS	0.89 ± 0.06	4.00 ± 0.18
ITZ + 10% SDS	0.73 ± 0.02	4.25 ± 0.60
ITZ + 10% PLX + FFL SAS-DEM (15% drug loading)	0.85 ± 0.03	2.66 ± 0.13
ITZ + 10% PLX + FFL SAS-DEM (50% drug loading)	0.86 ± 0.03	4.32 ± 0.15

Table 2.2 Relative standard deviation (RSD) at various drug loadings with excipient(s)

Mean Drug Loading (wt. %)	**RSD (%)**
Drug /FFL by SAS-DEM	
6	1.17
23	4.24
40	1.28
Drug + FFL+ PLX by SAS-DEM	
50	3.95

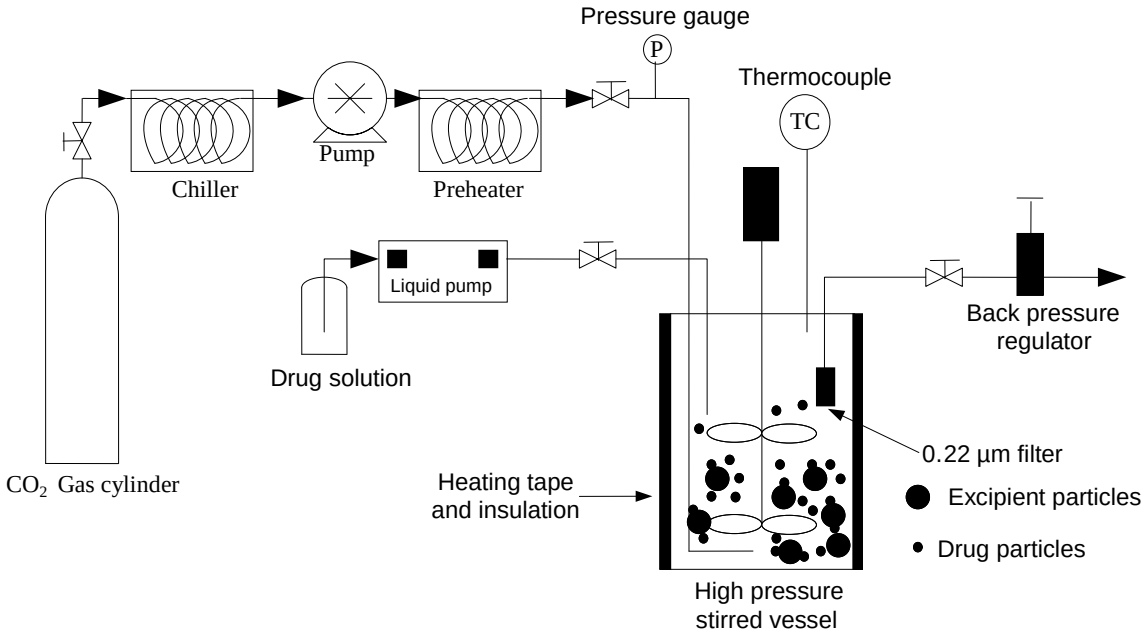

Figure 2.1 Apparatus for simultaneous particle formation and mixing using supercritical antisolvent (SAS-DEM)[46]

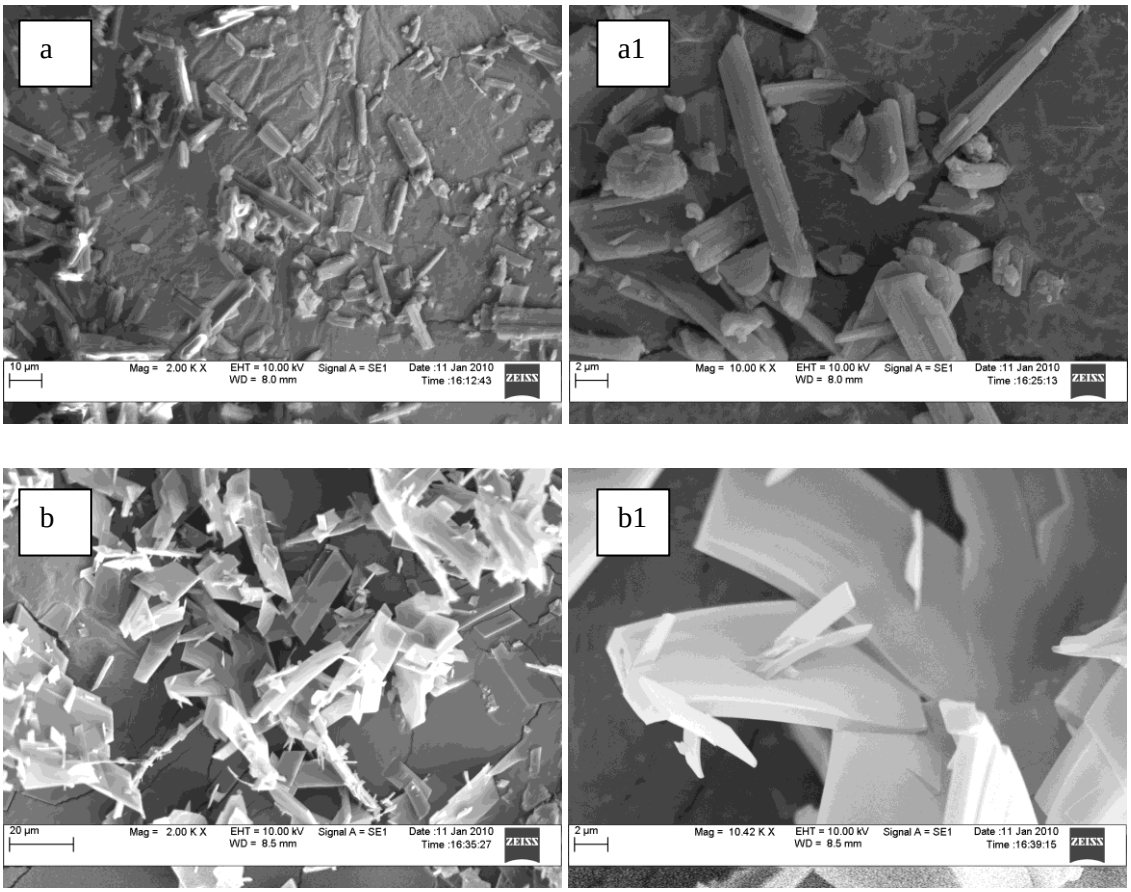

Figure 2.2 SEM images of (a) supplier drug, (a1) supplier drug at a higher magnification, (b) drug produced by SAS, (b1) drug produced by SAS at a higher magnification showing agglomerates of several micron/nano sized particles.

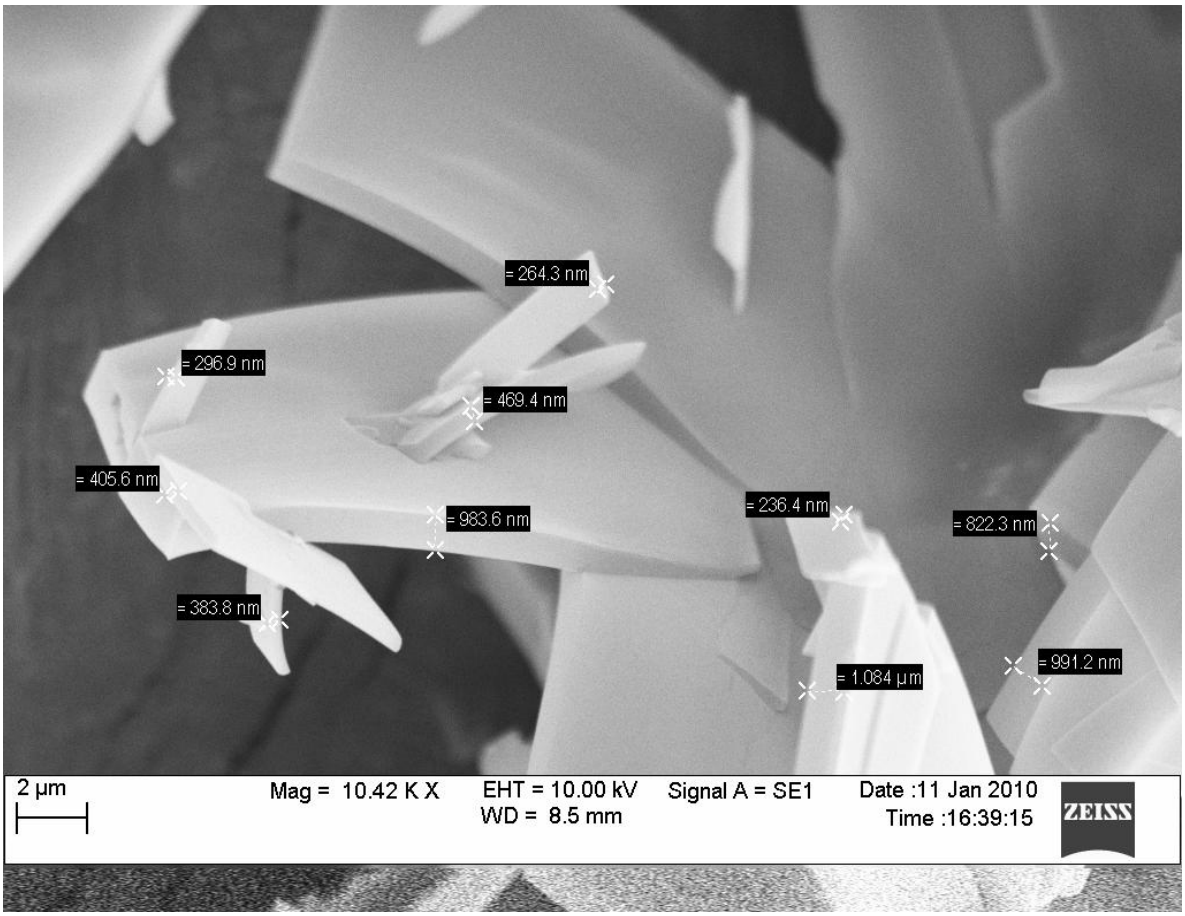

Figure 2.3 SEM image of drug agglomerate produced by SAS, the agglomerate consists of flakes in submicron thicknesses.

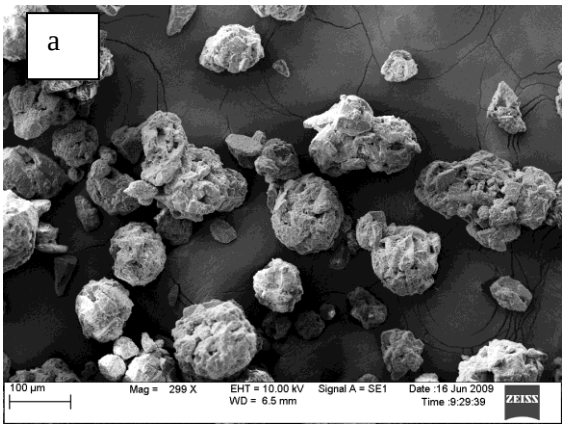
a
100 µm
Mag = 299 X
EHT = 10.00 kV
WD = 6.5 mm
Signal A = SE1
Date :16 Jun 2009
Time :9:29:39
ZEISS

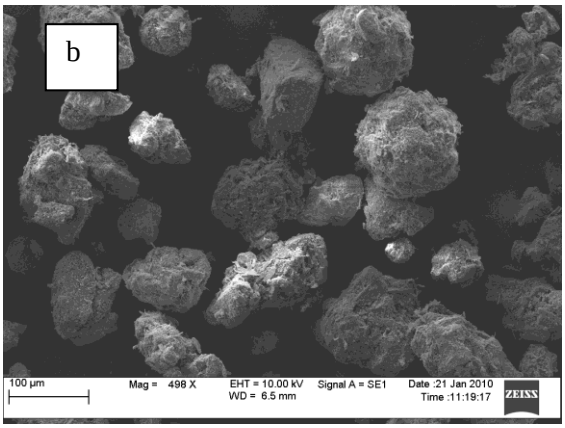
b
100 µm
Mag = 498 X
EHT = 10.00 kV
WD = 6.5 mm
Signal A = SE1
Date :21 Jan 2010
Time :11:19:17
ZEISS

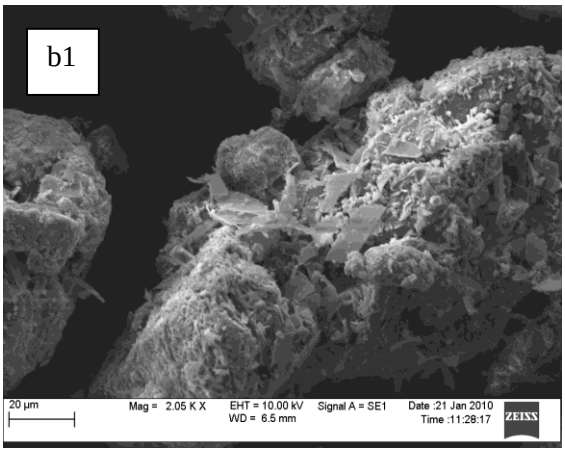
b1
20 µm
Mag = 2.05 K X
EHT = 10.00 kV
WD = 6.5 mm
Signal A = SE1
Date :21 Jan 2010
Time :11:28:17
ZEISS

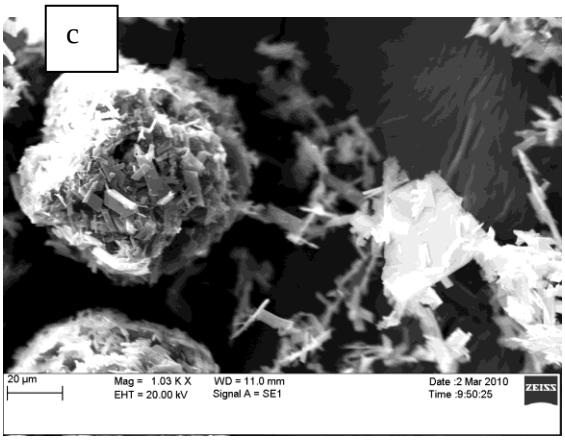
c
20 µm
Mag = 1.03 K X
EHT = 20.00 kV
WD = 11.0 mm
Signal A = SE1
Date :2 Mar 2010
Time :9:50:25
ZEISS

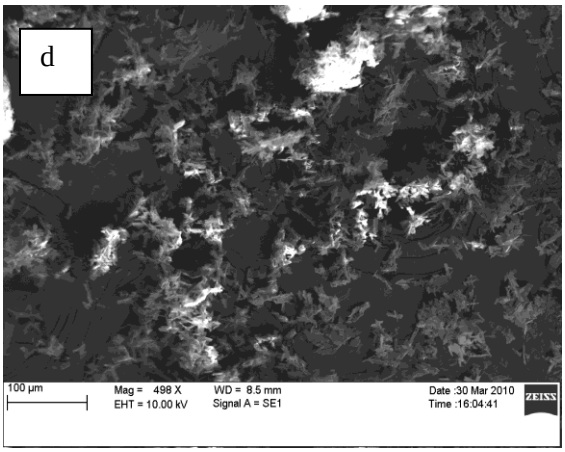
d
100 µm
Mag = 498 X
EHT = 10.00 kV
WD = 8.5 mm
Signal A = SE1
Date :30 Mar 2010
Time :16:04:41
ZEISS

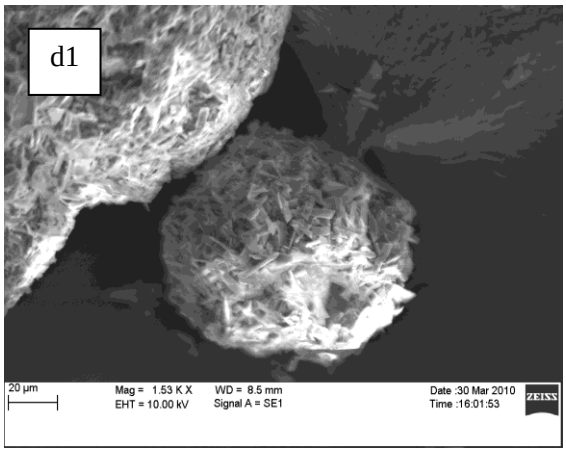
d1
20 µm
Mag = 1.53 K X
EHT = 10.00 kV
WD = 8.5 mm
Signal A = SE1
Date :30 Mar 2010
Time :16:01:53
ZEISS

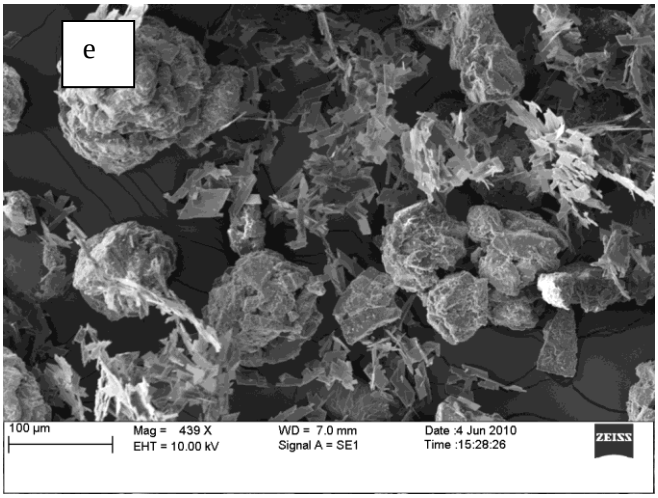

Figure 2.4 SEM images of drug and lactose mixture prepared by SAS-DEM method (a) lactose particles (b) flaky drug particles deposited on the surface of larger lactose particles at 6 wt % in the mixture (b1) higher magnification of (b) showing individual lactose particle and flaky drug particles on the surface of lactose (c) flaky drug particles covering the entire surface of lactose at 23 wt % in the mixture, and few agglomerates of flaky structures (d) presence of flaky agglomerates at drug loading of 40 wt % (d1) higher magnification of (d) showing entire surface of lactose covered by drug flakes at 40 wt % drug loading (e) Physical mixture of drug (by SAS) and FFL at 25 wt % of drug loading.

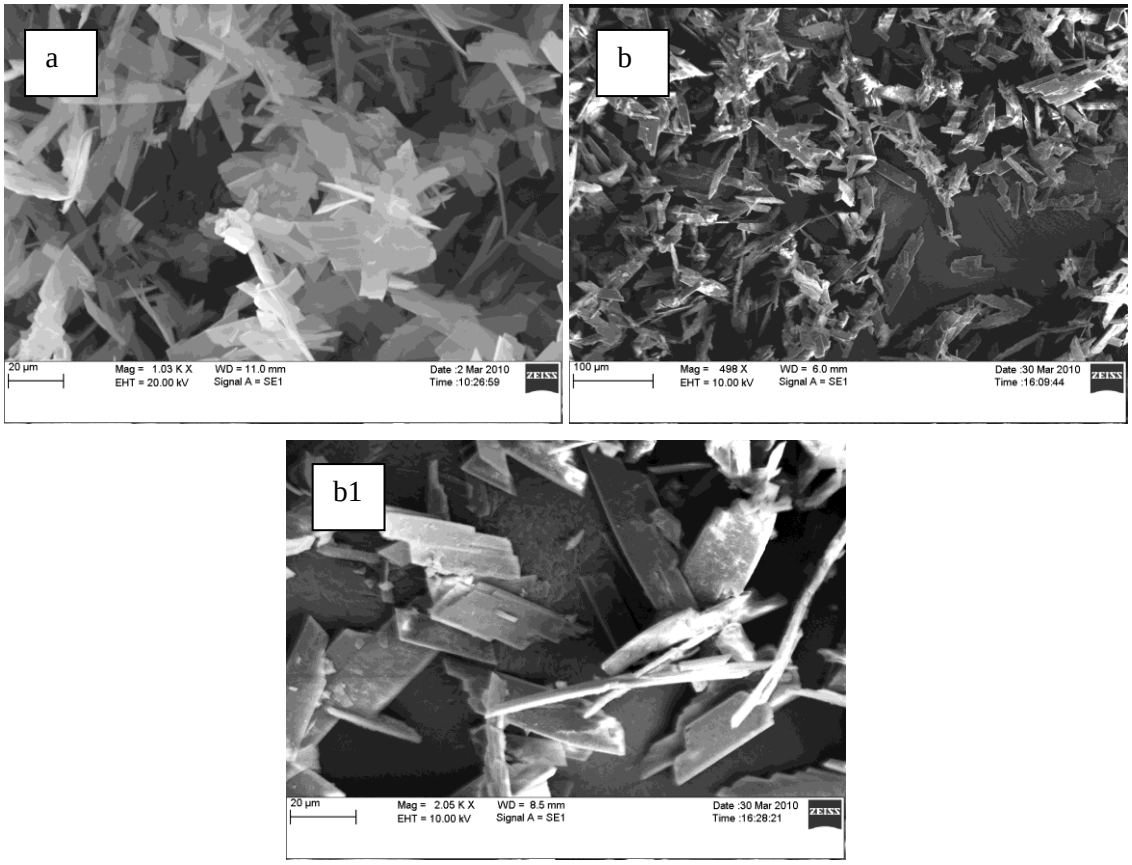

Figure 2.5 SEM images of drug and SDS stabilizer prepared by SAS method (a) SAS drug with 1% w/w of stabilizer, showing agglomerates of flaky shaped drug particles, (b) SAS drug with 10% w/w of stabilizer, showing de-aggregation of micro flakes, and (b1) higher magnification of individual drug flakes.

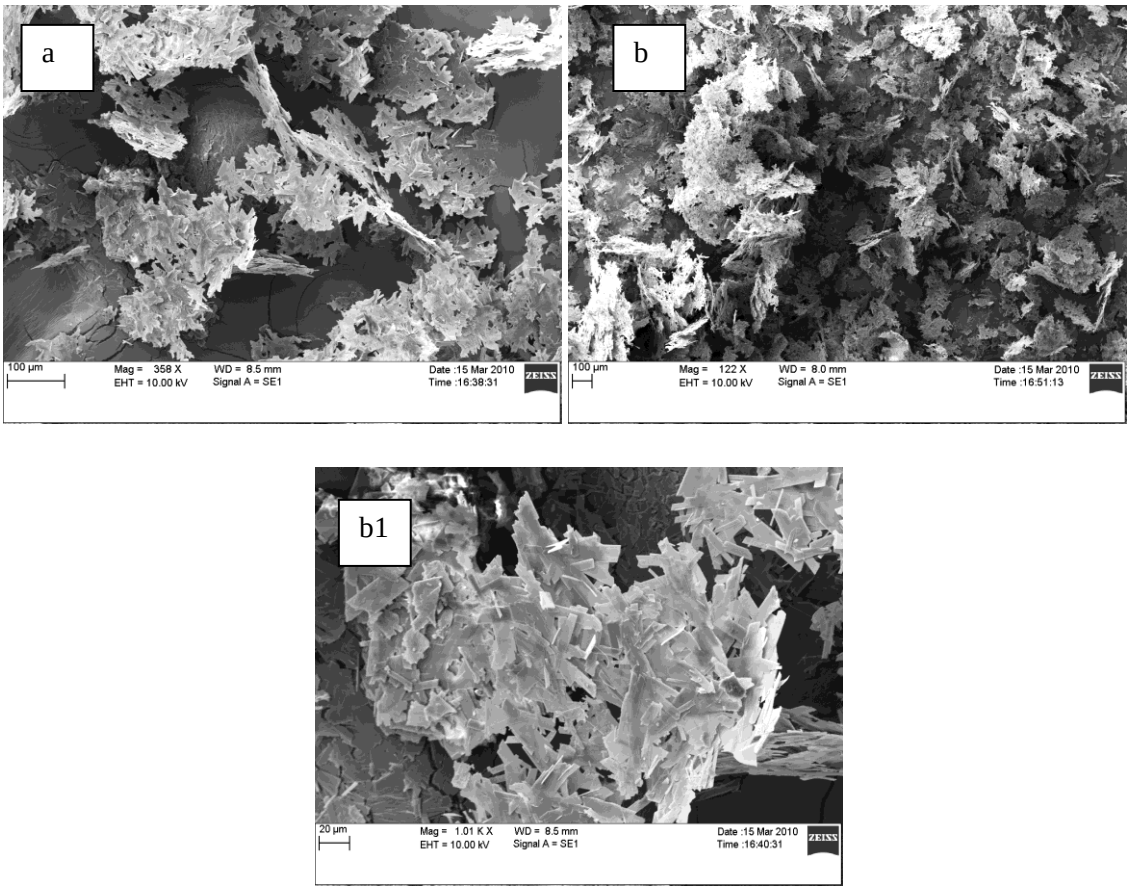

Figure 2.6 SEM images of drug and PLX stabilizer prepared by SAS method (a) SAS drug with 1% w/w of stabilizer, showing large agglomerates of flaky shaped drug particles, (b) SAS drug with 10% w/w of stabilizer, showing agglomerated flakes, and (b1) higher magnification of b.

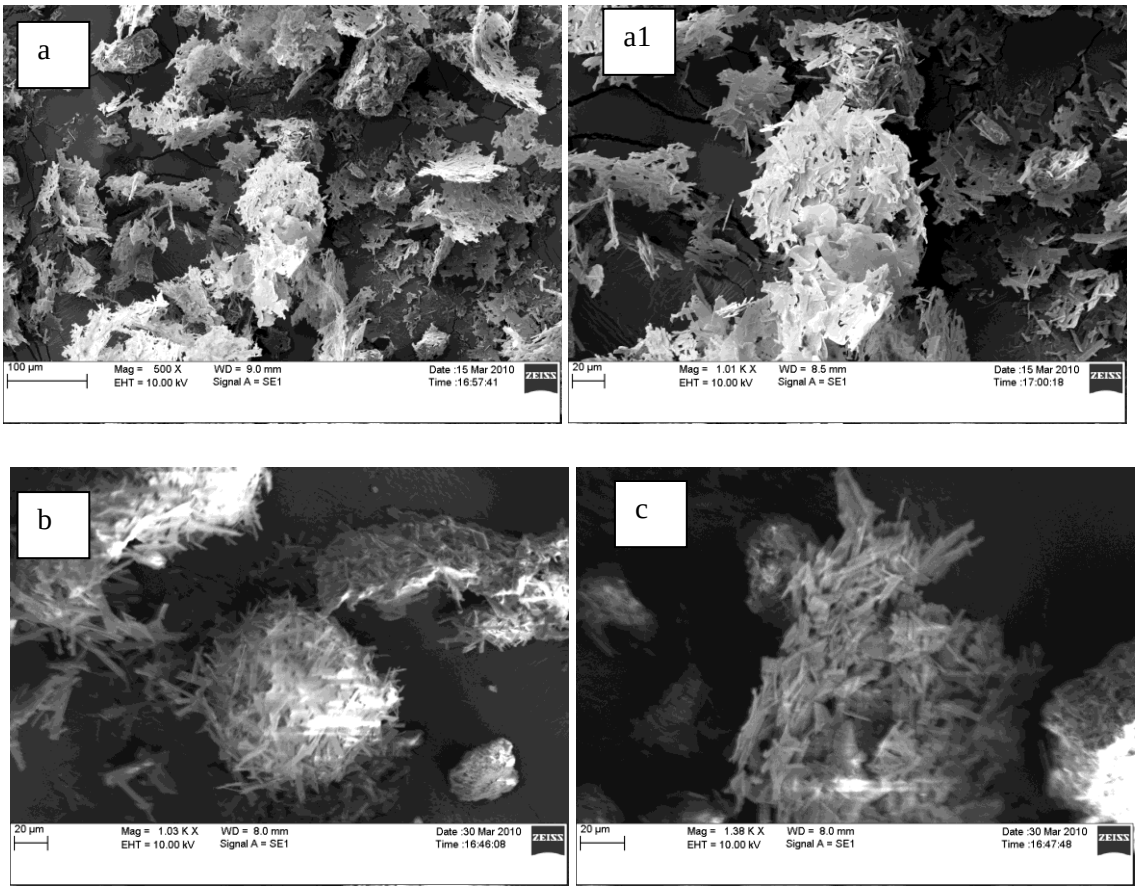

Figure 2.7 SEM images of drug/PLX and lactose mixture prepared by SAS-DEM method (a) flaky agglomerates of drug along with PLX, and also deposited on lactose particles, (a1) higher magnification of (a) showing flaky drug agglomerates entirely deposited on the surface of larger lactose particles at 15 wt % in the mixture, (b) lactose particle fully covered with flaky drug particles at 50 wt % in the mixture and also showing agglomerates of flaky structures, and (c) presence of flaky drug agglomerates at drug loading of 50 wt %.

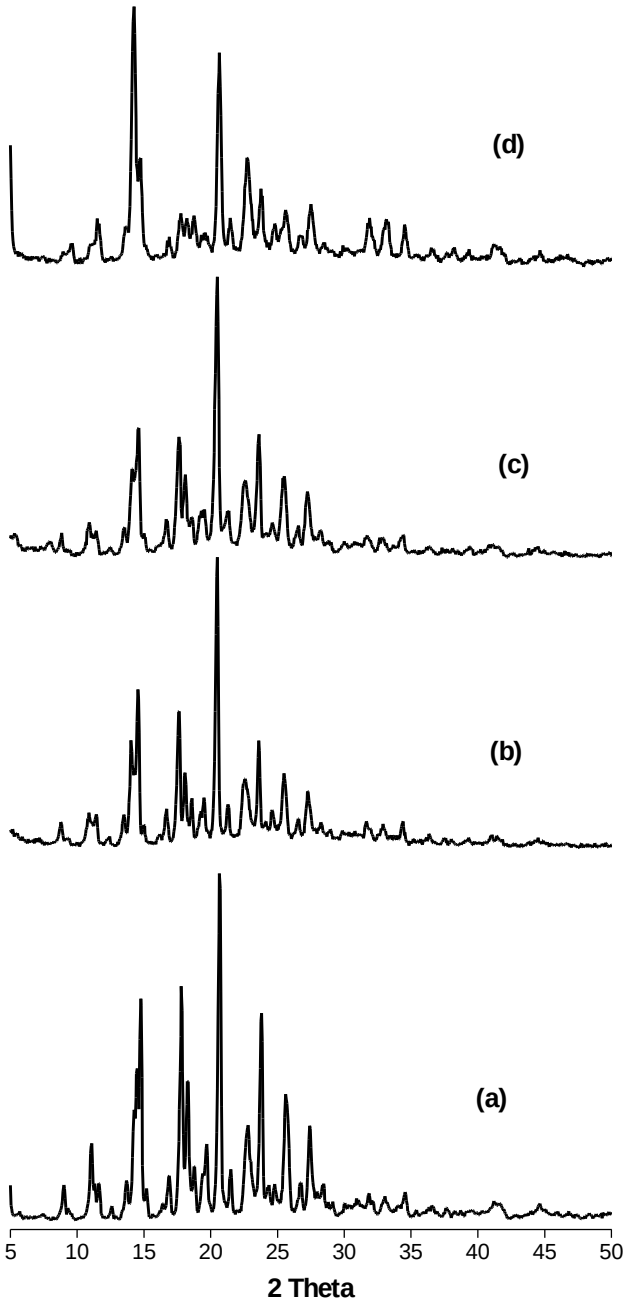

Figure 2.8 XRD patterns of (a) supplier drug, (b) SAS drug, (c) SAS drug + 10 wt % SDS, and (d) SAS drug + 10 wt % PLX.

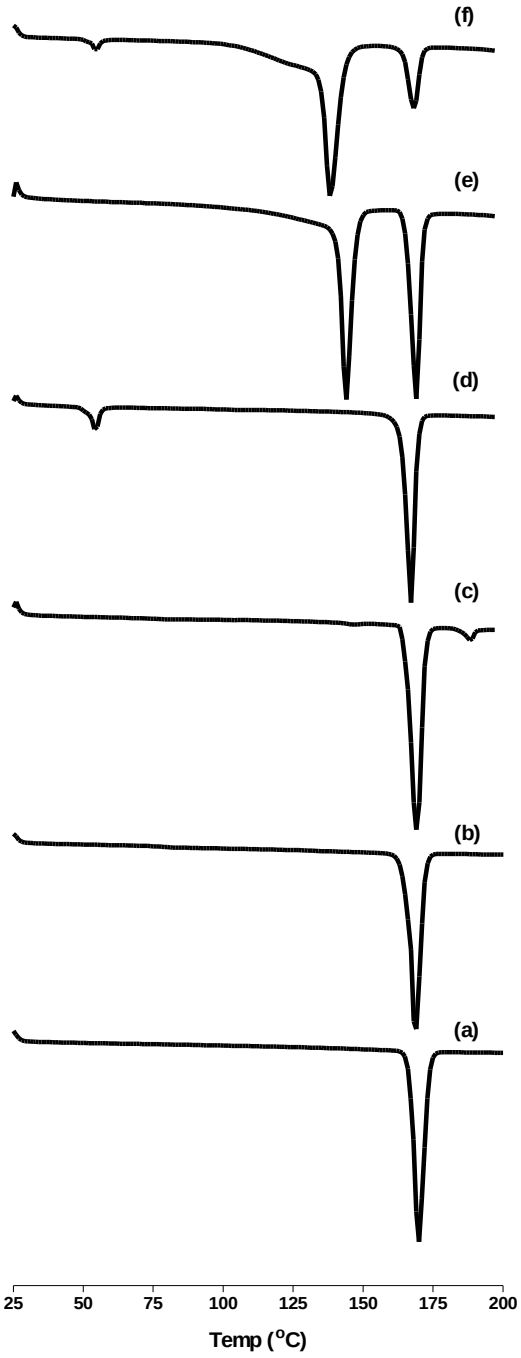

Figure 2.9 DSC thermographs of (a) supplier drug, (b) SAS drug, (c) SAS drug + 10 wt % SLS, (d) SAS drug + 10 wt % PLX, (e) SAS-DEM products of drug/FFL- 40 wt. % drug loading, and (f) SAS-DEM products of drug/PLX/FFL- 15 wt. % drug loading.

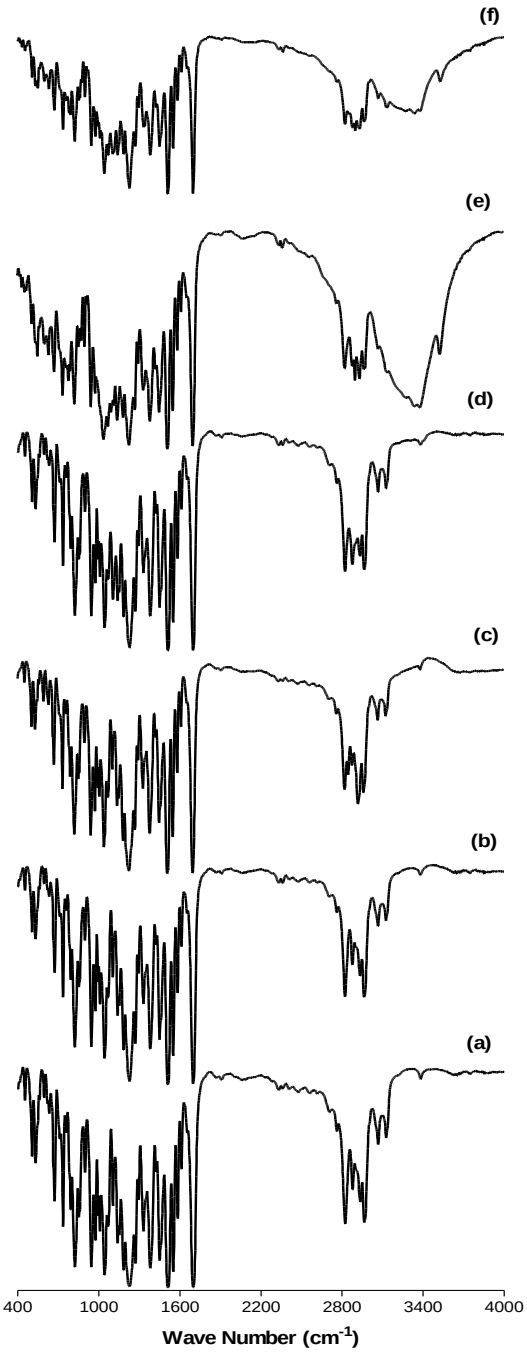

Figure 2.10 FT-IR spectra of (a) supplier drug, (b) SAS drug, (c) SAS drug + 10 wt % SLS, (d) SAS drug + 10 wt % PLX, (e) SAS-DEM products of drug/FFL- 40 wt. % drug loading, and (f) SAS-DEM products of drug/PLX/FFL- 15 wt. % drug loading.

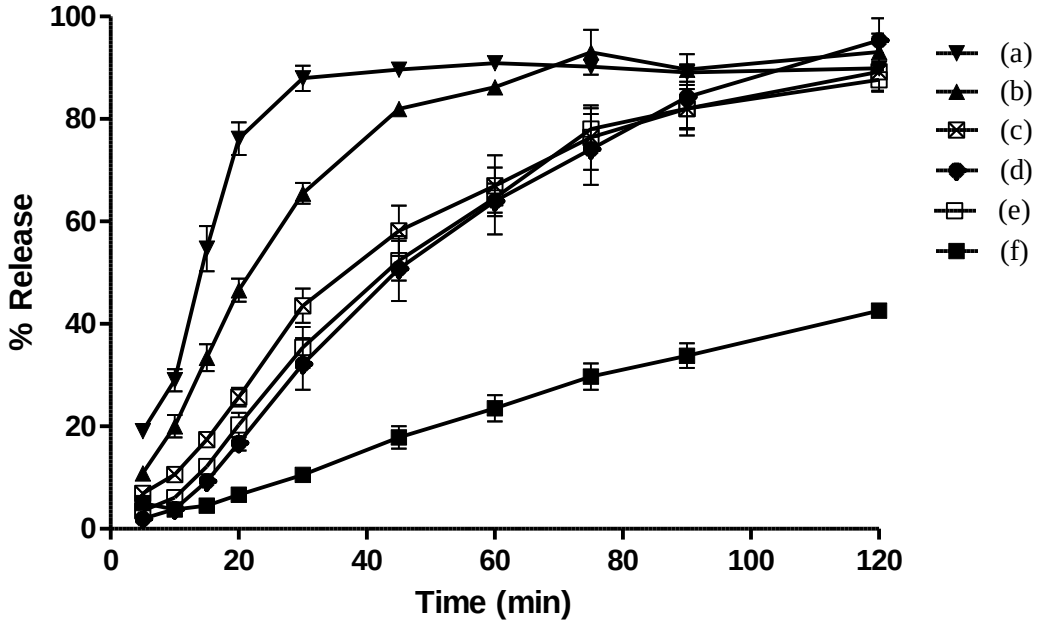

Figure 2.11 Dissolution profiles (from top to bottom) of (a) SAS-DEM product:lactose + 6 wt. % drug, (b) SAS-DEM product: lactose + 23 wt. % drug, (c) physical mixture: lactose + 25 wt. % drug, (d) SAS-DEM product: lactose + 40 wt. % drug, (e) SAS drug, and (f) Supplier drug.

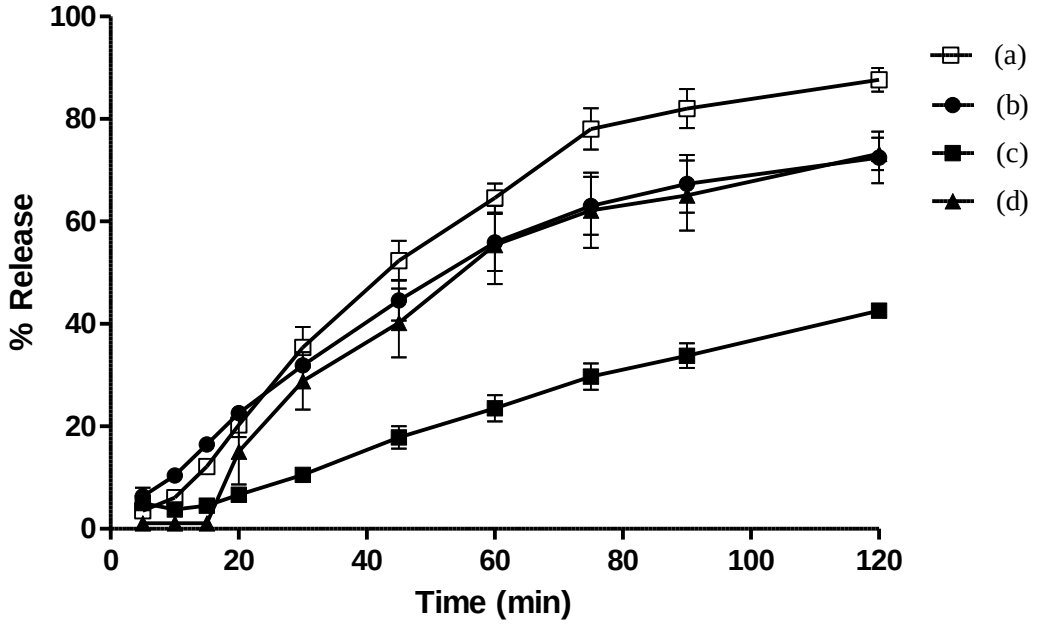

Figure 2.12 Dissolution profiles (from top to bottom) of (a) SAS drug, (b) SAS drug + 10 wt % SDS (c) SAS drug + 1 wt % SDS, and (d) Supplier drug.

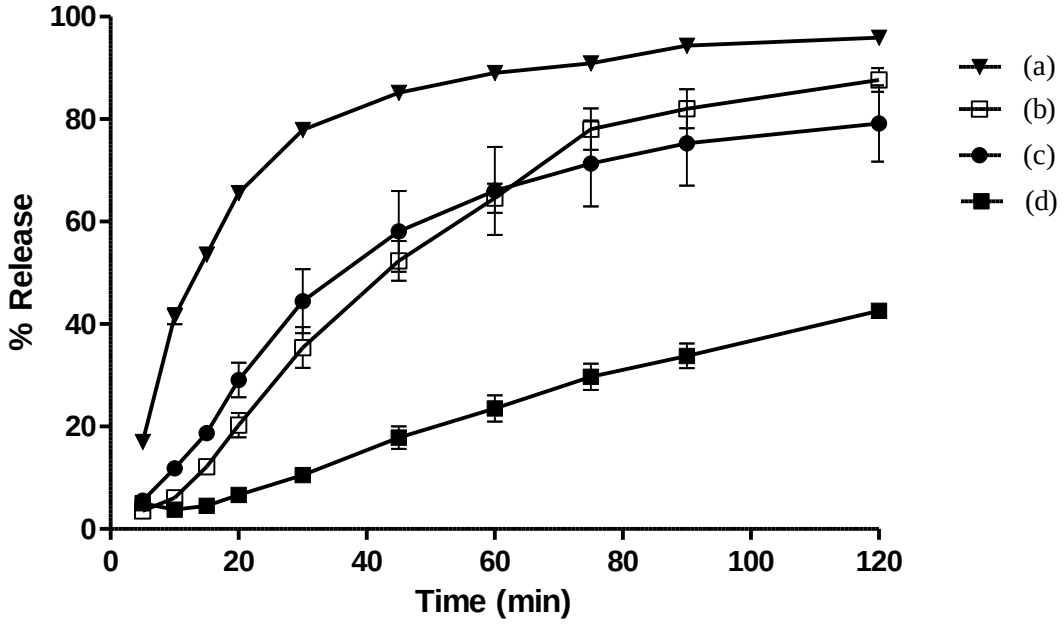

Figure 2.13 Dissolution profiles (from top to bottom) of (a) SAS drug + 10 wt % PLX, (b) SAS drug, (c) SAS drug + 1 wt % PLX, and (d) Supplier drug.

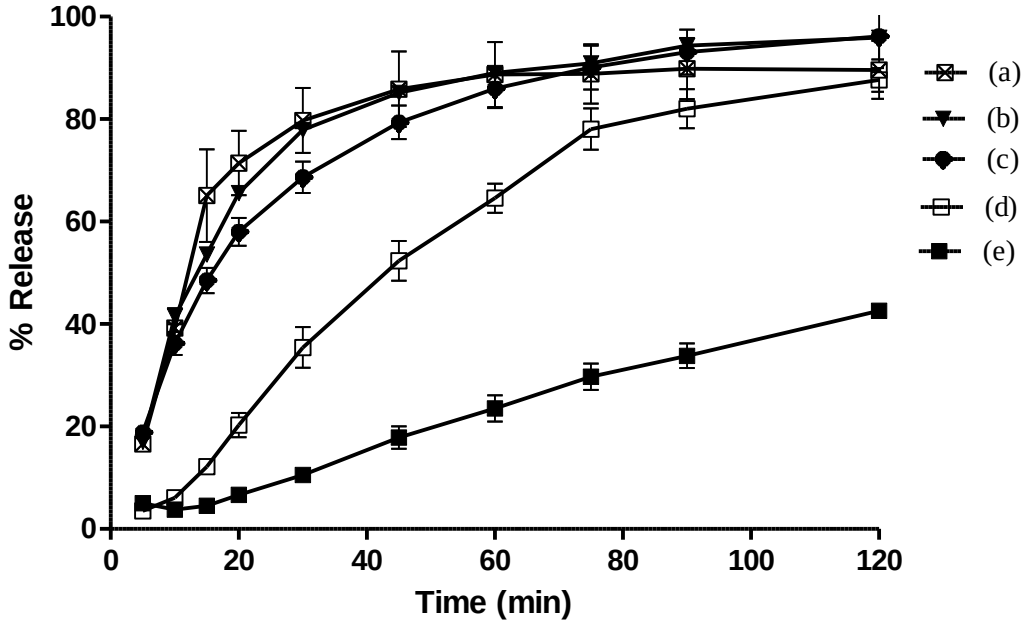

Figure 2.14 Dissolution profiles (from top to bottom) of SAS-DEM formulations (a) SAS drug + 10 wt % PLX + FFL – 50 wt % drug loading , (b) SAS drug + 10 wt % PLX, (c) SAS drug + 10 wt % PLX + FFL – 15 wt % drug loading, (d) SAS drug, and (e) Supplier drug.

3. Drug Polymer Miscibility Studies: Glass Transitions in Binary Efavirenz + Polymer Systems

3.1 Abstract

To evaluate miscibility, glass transition temperatures T_g have been determined for two binary polymer (Plasdone S-630 or Eudragit® E) + drug systems as a function of composition. Each polymer serves for the dispersion of the anti-HIV drug Efavirenz. In both systems the T_g *vs*. drug concentration diagrams are s-shaped. T_gs of Efavirenz + Plasdone mixtures with drug mass fraction below $\varphi_{drug} = 0.6$ are above linear values. This implies enhanced thermal and mechanical stability – an advantage for the drug –polymer solid dispersion. In the other system, a strong negative deviation of T_gs is observed over the entire compositional range and explained by positive excess mixing volumes. Several equations are used to represent T_g *vs*. composition diagrams, but only one (Brostow et al. Mater Lett 2008;62:3152) provides reliable results.

Keywords: glass transition temperature; drug encapsulation; miscibility; Efavirenz

3.2 Introduction

The dispersion of small drug molecules in polymeric matrices has long been of interest in the design of various drug delivery systems such as medicated contact lenses,[1-3] drug eluting stents[4,5] biodegradable implants,[6,7] transdermal patches,[8,9] and oral

formulations.[10,11] For poorly water soluble drugs dispersion or intimately mixing of crystalline drug in amorphous polymers to form molecular level solid dispersions is one of the techniques to enhance the dissolution rate and /or bioavailability.[11,12] The drug is stabilized in the amorphous form when dispersed into a polymer matrix. Amorphous drugs are advantageous over their crystalline counter parts with higher solubility, faster dissolution rate and enhanced oral bioavailability.[13] Miscibility of the drug and polymer at molecular level is one of the critical attributes that affect the stability of the solid dispersions.[14] An immiscible system could lead to recrystallization of the drug during storage. Presently the most common technique used to determine miscibility or homogeneity of this type of mixture is differential scanning calorimetry, that measures/determines the glass transition temperature (T_g) of the mixture.[13] Miscible dispersions are usually characterized by a single T_g value intermediate to those of the polymer and active pharmaceutical ingredient (API), as opposed to two T_g's values observed, corresponding to the API and polymer phase, in a phase separated system.[15]

The T_g is the most important feature of non-crystalline materials, including polymers and polymer-based composites.[16-18] The underlying mechanism demonstrates high sensitivity to even subtle modifications of structure and interactions. Increasing demand for polymer-based materials with predefined properties causes more and more polymer *blends* being made, and examined to assert miscibility of their constituents. Typically, fully miscible binary (A + B) blends show a single T_g value varying with the composition, say mass fraction φ_B, from $T_{g,A}$ to $T_{g,B}$. Compatible (partly miscible) blends exhibit two composition-dependent transitions, while incompatible blends show two glass transitions ($T_{g,A}$ and $T_{g,B}$) unaffected by the composition.

Fusion or solvent evaporation dispersion methods can be used to incorporate drugs into polymers. The use of a hot-melt extrusion (HME) technique has several advantages over traditional pharmaceutical processing techniques, such as the absence of solvents, few processing steps, continuous operation, formation of solid dispersions and improved drug dissolution and bioavailability.[19] As already noted, miscibility can be verified by $T_g(\varphi)$ determination.

Efavirenz is a non nucleoside reverse transcriptase inhibitor used as a part of an antiretroviral therapy for the treatment of human immunodeficiency virus (HIV) type 1 infection.[20] The chemical formula of the drug is given in Figure 1. This drug has been classified as a Biopharmaceutics Classification System (BCS) Class-II compound with good permeability but poor aqueous solubility with a dissolution rate dependent absorption.[21,22] The dissolution of efavirenz can be increased by preparation of HME blends of this drug and polymers. The polymers selected were Eudragit E (a low T_g polymer) and Plasdone S-630 (a high T_g polymer).

We present here the results of Efavirenz drug + polymer systems. Both systems have shown miscibility, but unusual s-shaped $T_g(\varphi)$ diagrams. With anomalous $T_g(\varphi)$ plots often reported for binary blends, the best option would be representing experimental data by a *single* analytical equation. Then, among others, development of drug + polymer dispersion systems would be significantly facilitated since the polymer concentration in the capsule has to be optimized. We describe below the drug + polymer pairs and the method of determination of $T_g(\varphi)$ used. Accordingly, we list important $T_g(\varphi)$ equations and apply them to evaluate their reliability in representation of $T_g(\varphi)$ diagrams.

3.3 Materials and methods

3.3.1 *Materials*

Efavirenz was a generous gift from Aurobindo Pharma Co. (Hyderabad, India). Eudragit EPO and Plasdone S-630 were provided as gift samples by Evonik Industries (Piscataway, NJ) and ISP Technologies Inc. (Wayne, NJ), respectively.

3.3.2 *Preparation of binary physical mixtures*

The drug and polymer physical mixtures were prepared by geometrically mixing in different ratios. The samples were thoroughly mixed with spatula and passed through a 60 mesh screen, and then further vortex mixed for 5 minutes. The samples were prepared in 0:1, 1:4, 1:1, 4:1 and 1:0 ratio of the drug to the polymer.

3.3.3 *Characterization of the physical mixtures by thermal analysis*

To determine the T_g of the mixtures, thermal analysis was carried out using a Differential Scanning Calorimeter (model Q200, TA instruments, New Castle, DE). Samples were prepared in hermetically sealed pans and subjected to a heat-cool-heat cycle at a rate of 10^oC/min to determine the glass transition temperatures (T_g). Data analysis for all measurements was performed using Universal Analysis 2000 software (TA instruments). The single T_g values reported here correspond to the midpoint temperature of the heat capacity change during DSC scans. Theoretical and experimental T_g values of the drug /polymer binary mixtures were compared to evaluate the influence of the drug content on the T_g of the blend.

3.4 $T_g(\varphi)$ equations

In Table 3.1 we have tabulated several T_g equations for miscible binary polymer blends, ending the list with our own equation. We have discussed previously origins of the above equations.[31] The Couchman and Karasz equation requires the knowledge of changes in heat capacities, often not available (T_g values from dielectric or dynamic mechanical relaxation). Gordon-Taylor, Jenckel-Heusch, and Utracki equations can only represent *either positive or negative* deviations from linearity, and–-as happens also with the Fox equation–-are inapplicable to our s-shaped diagrams. In the following section we confront the remaining equations with experiment.

3.5 Calculations and Results

Figure 3.4 presents the results for the miscible Efavirenz + Plasdone S-630 copovidone blend. The success of each representation of experimental data is judged by the coefficient of determination R^2 (= 1 for the perfect fit). We see clear divergence from the Fox, Gordon-Taylor and Kwei equations. The Brekner-Schneider-Cantow equation with K_1= -0.4±0.2 and K_2= -0.9±0.1 (R^2=0.997), provides decent description of the data - slightly inferior to that attained by our equation with a_0= 8±1, a_1= -32±3 and a_2= -39±7 (R^2=1). The deviation of the blend T_g from linearity (insert in Figure 3.4) demonstrates a sign inversion, with positive deviations below φ_{drug} = 0.6. In combination with the $a_1 < 0$ estimate,[31] the above behavior implies an enhancement of the thermal and mechanical stability at low drug loadings – an advantage for the intended drug encapsulation application.

Figure 3.5 presents results for the miscible Efavirenz + Eudragit® E system. The strong sigmoid– negative deviation from the linear mixing rule *cannot* be accounted for by any of the Gordon-Taylor, Kwei or BSC equations. For the latter equation, the fitting parameters are K_1= 0.8±1.4 and K_2= 9.3±2.7 (R^2=0.911). Application of our equation provided perfect description (R^2 = 1) and an interesting set of parameter values (a_0= -37.0±0.1, a_1= 60.7±0.1 and a_2= -75.1±0.1).

The behavior seen in Figure 3.5 can be explained in terms of excess volume V^E:

$$V^E = V - \varphi_A V_A - \varphi_B V_B \qquad 9$$

Where V pertains to the blend and all volumes are specific per 1 g. $V^E > 0$ means more space for chain relaxations with a concomitant lowering of T_g. The presence of longer lateral groups in Eudragit® E, compared to those found in Plasdone, gives a reason for the dissimilar $T_g(\varphi)$ dependences, by preventing packed chain conformations. We recall that in the glassy state we have nearly tetrahedral Delaunay simplices (duals of Voronoi polyhedral)[32] while in the liquid state there are less regular simplices forming percolation systems.[33] The latter require more space; hence $V^E > 0$ favors their formation.

Strong negative deviation from linearity has also been reported for homogeneous solid dispersions of steroid hormone 17β-Estradiol in Eudragit® RS (ERS) copolymer.[34] This dependence is also more effectively described using Eq. 8 in Table 3.1 (see the insert in Figure 3.5), with a_0= -37.2±2.1, a_1= 14.3±4.6 and a_2= 34.4±11.4 (R^2=0.986). The significance of the $V^E > 0$ effect is further demonstrated in this last system - given the occurrence of hydrogen-bonding intercomponent interactions.[34] Thus, while our experiments have been on two systems, here we have a third drug + polymer system for which our Eq. 8 in Table 3.1 provides nearly perfect results.

In conclusion, miscibility has been reported for drug + polymer mixtures and their irregular $T_g(\varphi)$ diagrams were analyzed. Eq. 8 in Table 3.1 has been shown to be applicable also to highly asymmetric s-shaped $T_g(\varphi)$ dependences – where other equations fail – and to work when one of the components is not a polymer but a low molecular mass organic compound, namely a drug. The number of parameters needed using Eq. 8 in Table 3.1 is indeed a measure of the system complexity .[35,36]

3.6 References

1. Gulsen D, Li CC, Chauhan A. 2005. Dispersion of DMPC liposomes in contact lenses for ophthalmic drug delivery. Curr Eye Res 30(12):1071-1080.
2. Zelenskaia MV, Baru EF, Kivaev AA, Suprun AV, Riabtseva AA. 1986. Soft contact lenses impregnated with hypotensive preparations in the treatment of glaucoma. Vestn Oftalmol 102(3):14-17.
3. Kaur IP, Kanwar M. 2002. Ocular preparations: the formulation approach. Drug Dev Ind Pharm 28(5):473-493.
4. Nakazawa G, Finn AV, Kolodgie FD, Virmani R. 2009. A review of current devices and a look at new technology: drug-eluting stents. Expert Rev Med Devices 6(1):33-42.
5. Parker T, Dave V, Falotico R. Polymers for drug eluting stents. Curr Pharm Des 16(36):3978-3988.
6. Al Malyan M, Becchi C, Nikkola L, Viitanen P, Boncinelli S, Chiellini F, Ashammakhi N. 2006. Polymer-based biodegradable drug delivery systems in pain management. J Craniofac Surg 17(2):302-313.

7. Lee SS, Hughes P, Ross AD, Robinson MR. Biodegradable implants for sustained drug release in the eye. Pharm Res 27(10):2043-2053.
8. Winblad B, Machado JC. 2008. Use of rivastigmine transdermal patch in the treatment of Alzheimer's disease. Expert Opin Drug Deliv 5(12):1377-1386.
9. Valenta C, Auner BG. 2004. The use of polymers for dermal and transdermal delivery. Eur J Pharm Biopharm 58(2):279-289.
10. Serajuddin AT. 1999. Solid dispersion of poorly water-soluble drugs: early promises, subsequent problems, and recent breakthroughs. J Pharm Sci 88(10):1058-1066.
11. Vasconcelos T, Sarmento B, Costa P. 2007. Solid dispersions as strategy to improve oral bioavailability of poor water soluble drugs. Drug Discov Today 12(23-24):1068-1075.
12. Leuner C, Dressman J. 2000. Improving drug solubility for oral delivery using solid dispersions. Eur J Pharm Biopharm 50(1):47-60.
13. Qian F, Huang J, Hussain MA. Drug-polymer solubility and miscibility: Stability consideration and practical challenges in amorphous solid dispersion development. J Pharm Sci 99(7):2941-2947.
14. Qian F, Huang J, Zhu Q, Haddadin R, Gawel J, Garmise R, Hussain M. Is a distinctive single Tg a reliable indicator for the homogeneity of amorphous solid dispersion? Int J Pharm 395(1-2):232-235.
15. Ivanisevic I. Physical stability studies of miscible amorphous solid dispersions. J Pharm Sci 99(9):4005-4012.

16. Brostow W. 2000. Performance of plastics, Munich-Cincinnati: Hanser publishing Co.

17. Gedde UW. 2001. Polymer Physics, 2nd ed., Dordrecht: Kluwer Academy.

18. Bunsell AR, Renard J. 2005. Fundamentals of fibre reinforced composite materials, Bristol-Philadelphia: Institute of Physics.

19. Crowley MM, Zhang F, Repka MA, Thumma S, Upadhye SB, Battu SK, McGinity JW, Martin C. 2007. Pharmaceutical applications of hot-melt extrusion: part I. Drug Dev Ind Pharm 33(9):909-926.

20. Maurin MB, Rowe SM, Blom K, Pierce ME. 2002. Kinetics and mechanism of hydrolysis of efavirenz. Pharmaceutical Research 19(4):517-522.

21. Kasim NA, Whitehouse M, Ramachandran C, Bermejo M, Lennernas H, Hussain AS, Junginger HE, Stavchansky SA, Midha KK, Shah VP, Amidon GL. 2004. Molecular properties of WHO essential drugs and provisional biopharmaceutical classification. Mol Pharm 1(1):85-96.

22. Takano R, Sugano K, Higashida A, Hayashi Y, Machida M, Aso Y, Yamashita S. 2006. Oral absorption of poorly water-soluble drugs: computer simulation of fraction absorbed in humans from a miniscale dissolution test. Pharm Res 23(6):1144-1156.\

23. Fox GT. 1956. Influence of diluent and of copolymer composition on the glass temperature of a polymer system. Bull Am Phys Soc 1 :123.

24. Gordon M, Taylor JS. 1952. Ideal copolymers and the second-order transitions of synthetic rubbers I. Noncrystalline copolymers. J Appl Chem 2:493-500.

25. Jenckel E, Heusch R. 1953. Lowering the freezing temperature of organic glasses with solvents. Kolloid-Z 130:89-105.

26. Couchman PR, Karasz FE. 1978. Classical thermodynamic discussion of effect of composition on glass transition temperatures. Macromolecules 11(1):117-119.

27. Utracki LA. 1989. Polymer alloys and blends: Thermodynamic and Rheology. Hanser Publishers, germany.

28. Kwei TK. 1984. The effect of hydrogen bonding on the glass transition temperatures of polymer mixtures. J Polym Sci Lett 22:307-313.

29. Brekner MJ, Schneider A, Cantow HJ. 1988. Approach to the composition dependence of the glass transition temperature of compatible polymer blends. Polymer 78:78-85.

30. Brostow W, Chiu R, Kalogeras IM, Vassilikou-Dova A. 2008. Prediction of glass transition temperatures: binary blends and copolymers. Mater Lett 62:3152-3155.

31. Kalogeras IM, Brostow W. 2009. Glass transition temperatures in binary polymer blends. J Polym Sci Phys 47:80-95.

32. Brostow W, Castano VM.1999. Voronoi Polyhedra as a Tool for Dealing with Spatial Structures of Amorphous Solids, Liquids and Dense Gases. J Mater Ed 21:297-304.

33. Medevedev NN, Geiger A, Brostow W. 1990. Distinguishing liquids from amorphous solids: percolation analysis on the voronoi network. J Chem Phys 93:8337-8342.

34. Wiranidchapong C, Rades T, Kulvanich P, Tucker IG. 2009. Method of preparation does not affect the miscibility between steroid harmone and polymethacrylate. Thermochim Acta 485:57-64.

35. ElMiloudi K, Djadoun S, Sbirrazzuoli N, Geribaldi S. 2009. Miscibility and phase behavior of binary and ternary homoblends of poly (styrene-co-acrylic acid), poly (styrene-co-N, N-dimethylacylamide) and poly (styrene-co-4-vinylpyridine). Thermochimica Acta 483:49-54.

36. ElMiloudi K, Djadoun S. 2009. A thermodynamic analysis of specific interactions in homoblends of poly(styrene-co-4-vinylpyridine) and poly(styrene-co-methacrylic acid). J Polym Sci Phys 47:923-931.

Table 3.1 Equations proposed for glass transition temperatures of binary mixtures. φ_i , x_i, $\Delta C_{p,i}$ and $T_{g,i}$ are, respectively, the weight fraction, the molar fraction, the difference between the heat capacity of the liquid and the heat capacity of the glass forms, and the glass transition temperature of the *i*-th component.

Function's name	Functional form	Fitting parameters	Eq. No.
Fox [23]	$\frac{1}{T_g} = \frac{\varphi_A}{T_{g,A}} + \frac{1-\varphi_1}{T_{g,B}}$	-	1
Gordon-Taylor[24]	$T_g = \frac{\varphi_A T_{g,A} + k_{GT}(1-\varphi_A)T_{g,B}}{\varphi_A + k_{GT}(1-\varphi_A)}$	k_{GT}	2
Jenckel-Heusch[25]	$T_g = \varphi_A T_{g,A} + (1-\varphi_A)T_{g,B} + b(T_{g,B} - T_{g,A})\varphi_A(1-\varphi_A)$	b	3
Couchman-Karasz[26]	$\ln T_g = \frac{x_A \Delta C_{p,A} \ln T_{g,A} + \Delta C_{p,B}(1-x_A)T_{g,B}}{x_A \Delta C_{p,A} + (1-x_A)\Delta C_{p,B}}$	-	4
Utracki[27]	$T_g = [1 + K^*\varphi_A(1-\varphi_A)]\left[\varphi_A T_{g,A}^{3/2} + (1-\varphi_A)T_{g,B}^{3/2}\right]^{2/3}$	K^*	5
Kwei[28]	$T_g = \frac{\varphi_A T_{g,A} + k_{Kw}(1-\varphi_A)T_{g,B}}{\varphi_A + k_{Kw}(1-\varphi_A)} + q\varphi_A(1-\varphi_A)$	k_{Kw}, q	6
Brekner-Schneider-Cantow (BSC)[29]	$T_g = T_{g,A} + (T_{g,B} - T_{g,A})[(1+K_1)\varphi_{B,c}) - (K_1 + K_2)\varphi_{B,c}^2 +$; $\varphi_{B,c} = \frac{k\varphi_B}{\varphi_A + k\varphi_B}$, $k \approx \frac{T_{g,A}}{T_{g,B}}$	K_1, K_2	7
Our equation[30, 31]	$T_g = \varphi_A T_{g,A} + (1-\varphi_A)T_{g,B} + \varphi_A(1-\varphi_A)\left[a_0 + a_1(2\varphi_A - 1)\right.$	a_0, a_1, a_2	8

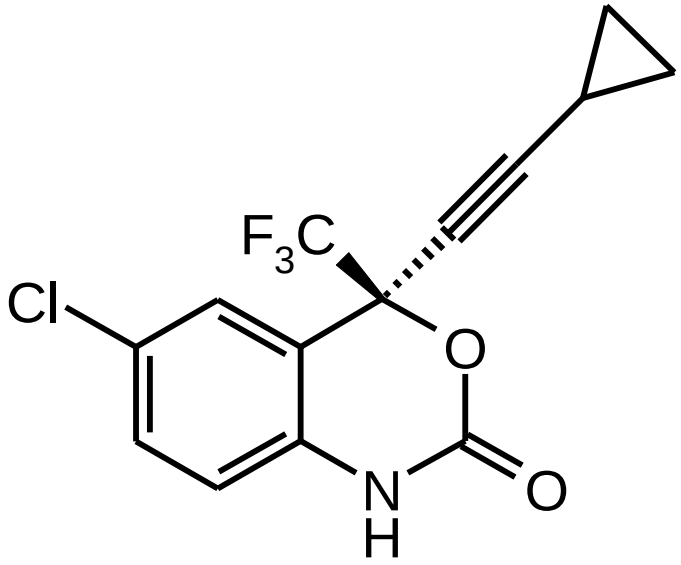

Figure 3.1 Structure of efavirenz

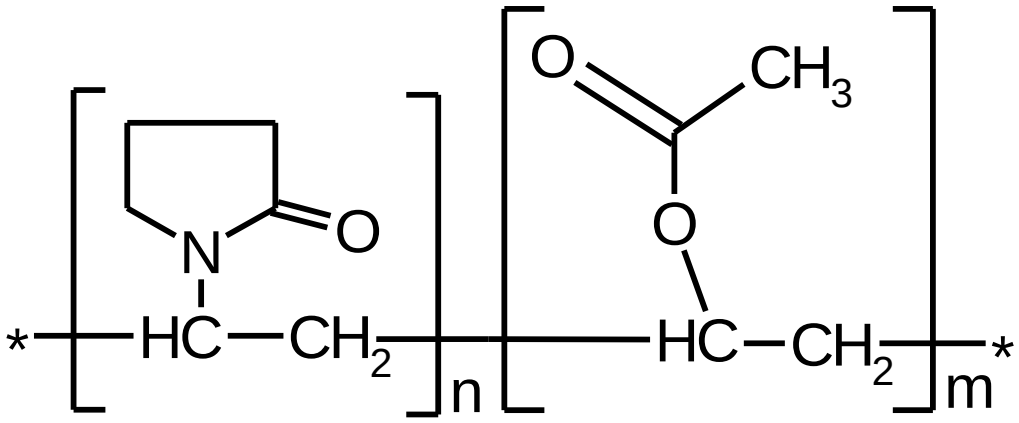

Figure 3.2 Structure of Plasdone S-630

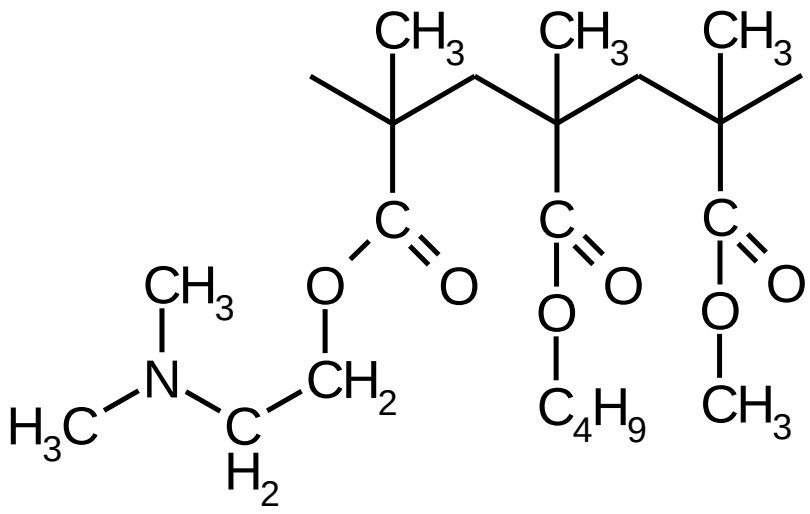

Figure 3.3 Structure of eudragit E

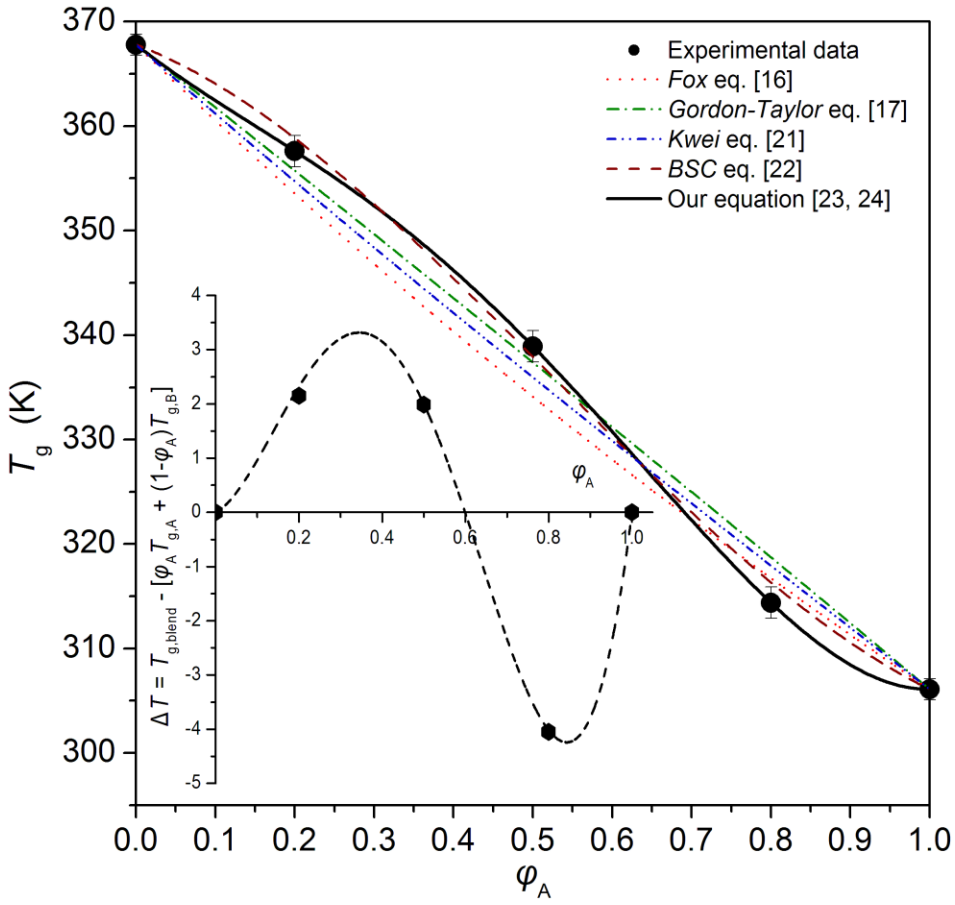

Figure 3.4 Glass transition temperatures vs. drug concentration for the miscible Efavirenz + PLS S-630 copovidone blends. The deviation from linearity, $\Delta T = T_{g,blend} - [\varphi_A T_{g,A} + (1 - \varphi_A) T_{g,B}]$ vs. φ_A, is shown in the insert.

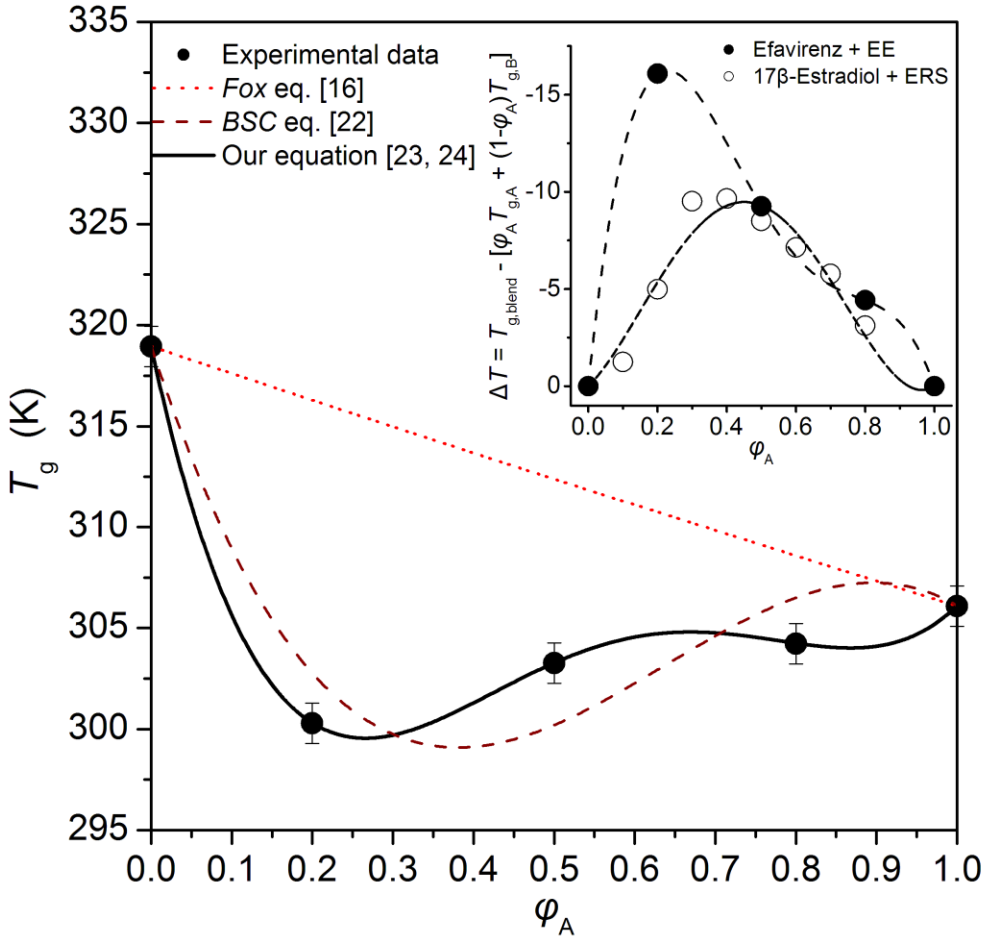

Figure 3.5 Compositional variation of the glass transition temperature for the miscible Efavirenz + Eudragit® E blends. Deviations from linearity (ΔT vs. φ_A) for drugs incorporated in different Eudragit matrices are compared in the insert.

4. Amorphous State Characterization of Efavirenz - Polymer Hot Melt Extrusion Systems for Dissolution Enhancement

4.1 Abstract

The aim of this study was to improve the dissolution rate of a poorly water soluble drug, efavirenz (EFV), by formulating a physically stable, amorphous, glassy solid solution with polymers. Hot melt extrusion (HME) was used to separately prepare solid solutions of EFV with Eudragit EPO (a low Tg polymer) and Plasdone S-630 (a high Tg polymer). Similarly, binary physical mixtures of drug and the respective polymer were also prepared. These systems were characterized for thermal and rheological properties as a function of drug concentration to understand the miscibility and processibility by hot melt extrusion. The melt extrudates were characterized for dissolution and solid state stability upon storage at room temperature for nine months. All samples were analyzed by differential scanning calorimetry (DSC), x-ray diffraction (XRD), fourier-transform infrared spectroscopy (FTIR) and dissolution studies. Thermal and rheological studies revealed that the drug is miscible with both polymers and a decrease in melt viscosity was observed as the drug concentration increased due to plasticization of the polymers by the drug. XRD and DSC studies confirmed that the drug was converted to its amorphous state during the extrusion process and retained its glassy state during storage suggesting good physical stability. The dissolution rate of EFV from

the hot melt extrudates was significantly higher than its crystalline form and corresponding physical mixtures due to the amorphous state of the drug. FTIR studies revealed an interaction between the EFV and Plasdone S-630 which reduced the molecular mobility and prevented crystallization upon storage. EFV and Eudragit EPO systems lack specific interactions, but are less susceptible to crystallization due to the antiplasticization effect of the polymer.

4.2 Introduction

Efavirenz (EFV) is a non nucleoside reverse transcriptase inhibitor (NNRTI) used for the treatment of human immunodeficiency virus (HIV) type 1 infection.[1] Despite being widely used clinically, this drug has very low oral bioavailability (40-45%) and high inter (56%) and intra (22%) individual variability.[2,3] This drug has been classified as a Biopharmaceutics Classification System (BCS) Class-II compound with good permeability but poor aqueous solubility with a dissolution rate dependent absorption.[4,5] The very low aqueous solubility (~3-9 μg/ml) hinders its administration, oral absorption and bioavailability.[6] By improving dissolution, it is possible to enhance its oral bioavailability and reduce side effects.[7] In general, an intrinsic dissolution rate less than 0.1 mg/min/cm^2 could be a rate limiting factor for oral drug absorption.[8] EFV has a very low intrinsic dissolution rate of 0.037 mg/cm^2/min, which suggests dissolution rate-limited absorption problems for this drug.[9] Polymeric micellar solubilization and cyclodextrin complexation have significantly increased the solubility of EFV.[3,9]

Hot melt extrusion (HME) is a promising method to enhance the dissolution of poorly soluble drugs.[10] The improvement in dissolution by HME can be attributed to

improved wetting of the drug, deagglomeration and micellization of the drug with hydrophilic polymers.[11] The pharmaceutical potential of amorphous drug-polymer dispersions was realized with an NNRTI, etravirine (Intelence®), which is formulated in the amorphous form by the spray drying method. Upon oral administration, this dosage form provided several fold higher plasma concentrations above the viral inhibitory concentration, as compared to the crystalline form of the drug.[12]

Amorphous drug substances are physically unstable due to their high energy state and tend to recrystallize upon storage.[13] In order to stabilize these systems, various polymer carriers have been used because they readily generate amorphous forms and may be able to retain the amorphous nature of the drug upon storage.[14-16] The long polymeric chains can sterically hinder the association between drug molecules and thereby inhibit the recrystallization of drug. In addition, the interaction between the drug and polymer provides an increased energy barrier for nucleation and consequently enhances the physical stability.[12] In order to achieve a single amorphous drug-polymer phase, a certain degree of solid solubility, miscibility and kinetic stabilization is required.[17] The amorphous solid solutions are often supersaturated and hence the kinetic stabilization plays an important role in the physical stability of the amorphous drug. To obtain sufficient kinetic stabilization, a high glass transition temperature is an invaluable property for a given polymer. The presence of functional groups that are either donors or acceptors for hydrogen bonds provide specific interactions to increase the drug solubility in the polymer and inhibit phase separation and crystallization of a drug from glass solution.[17-19]

The primary objective of this study is to characterize amorphous EFV - polymer systems prepared by HME in order to enhance the dissolution of the drug. HMEs of the EFV were formulated using Eudragit EPO (a low T_g polymer) and Plasdone S-630 (a high T_g polymer) as hydrophilic carriers (Table 4.1). These polymers - drug solid dispersions were evaluated for physical chemical interactions and drug dissolution profiles in comparison with the corresponding physical mixtures (PMs). In addition, the amorphous state stability of the drug in HME dispersions was monitored at room temperature for nine months.

4.3 Materials and methods

4.3.1 *Materials*

Efavirenz was a generous gift from Aurobindo Pharma Co. (Hyderabad, India). Eudragit EPO and Plasdone S-630 were provided as gift samples by Evonik Industries (Piscataway, NJ) and ISP Technologies Inc. (Wayne, NJ), respectively. All reagents and chemicals used were of analytical grade.

4.3.2 *Solubility parameter calculations*

Solubility parameter (δ) for EFV was performed by the group contribution method using molecular modeling pro software (ChemSW, Fairfield, CA). The solubility parameters for the polymers were taken from the literature and matched to the EFV by observing the relative difference in total, Δδ.

4.3.3 *Density measurements*

The true density of the EFV and polymers were determined in duplicate using a gas displacement pycnometer (Accupyc 1330, Micromeritics, Norcross, GA).

4.3.4 *Preparation of binary physical mixtures*

The drug was triturated with the polymer (Eudragit EPO or Plasdone S-630) using a mortar and pestle and these mixtures were passed through a number 60 sieve. These mixtures were further blended on a vortex mixer for 5 minutes. The samples were prepared in 20%, 50% and 80% drug loadings.

4.3.5 *Characterization of binary physical mixtures*

In order to evaluate the miscibility of the drug and polymers and to determine extrudability of the physical mixtures, thermal and rheological studies were performed.

4.3.5.1 *Thermal analysis*

Thermal analysis was carried out using a Differential Scanning Calorimeter (Model: Q200, TA instruments, New Castle, DE). Samples were prepared in hermetically sealed pans and subjected to a heat-cool-heat cycle at a rate of 10^{o}C/min to determine the glass transition temperatures (T_g). Theoretical and experimental T_g values of the drug /polymer binary mixtures were compared to evaluate the influence of the drug content on the T_g of the blend.

4.3.5.2 *Rheological Studies*

The rheological properties of the polymers and binary mixtures were studied using a rotational rheometer (MCR301, Anton Paar, Ashland VA). Measurements were made using 25 mm parallel plates under controlled strain and steady shear. The shear rate employed was from 0.01 to 100 s^{-1}. The measured and calculated parameters were zero shear viscosity (η_o) and activation energy (Ea). η_o was obtained from the plot of viscosity as a function of shear rate at a constant temperature. The 'Ea' is indicative of the energy needed to initiate the flow of the melt and was calculated by plotting the viscosity of the binary mixtures and polymers as a function of temperature (1/T).[20]

4.3.6 *Preparation of Hot Melt Extrudates*

Composites of drug and polymer in a 1:1 ratio were prepared by using a Haake Minilab twin screw extruder (Thermo Fisher Scientific, Pittsburgh, PA) with counter rotating screws at 50 rpm. The temperatures for processing were selected based on the T_g of the polymers and melting point of the drug. As a general rule, an extrusion process should be conducted at temperatures 20 - 40^oC above the T_g of the polymer and at a temperature close to the melting point of the drug. The temperatures employed were 120^oC and 140 ^oC for Eudragit EPO and Plasdone S-630 systems, respectively.

4.3.7 *Characterization of Hot Melt Extrudates*

The melt extrudates were ground to a fine powder using a mortar and pestle and passed through a number 60 sieve. The formulations were analyzed for drug content and saturation solubility and further characterized by differential scanning calorimetry (DSC),

X-ray Diffraction (XRD), Fourier-Transform Infrared Spectroscopy (FT-IR) and dissolution studies.

4.3.7.1 *Drug Content*

Samples equivalent to 10 mg of EFV were dissolved in 5 ml of methanol and appropriately diluted and the drug content was determined by UV- spectrophotometer at 246 nm (Jasco V680 spectrophotometer, Tokyo, Japan).

4.3.7.2 *Saturation Solubility*

An excess amount of the formulation was added to 5 ml of the 0.01N HCl with 0.2% sodium lauryl sulfate in water solution and sonicated for 30 min for 3 times at 3 h intervals. After equilibration for 24 h, the samples were filtered through 0.45 µm pore size nylon filters (Whatman International, England), suitably diluted and analyzed spectrophotometrically at 246 nm.

4.3.7.3 *DSC Studies*

The samples were sealed in aluminum hermetic pans and the DSC thermograms were recorded at a heating rate of 10^{o}C/min from 25^{o}C to 250^{o}C as described in section 2.5.1.

4.3.7.4 *XRD Studies*

X-ray powder diffraction patterns of the samples were obtained with a Rigaku XRD analyzer (Rigaku Americas, The Woodlands, TX) using a Cu Kα radiation source at

40 kV, 40 mA, and a miniflex goniometer. The diffraction patterns were obtained in 2θ range of 5–50° using a 0.05° step size and 2°/min scan speed.

4.3.7.5 *Dissolution Studies*

The dissolution studies of the formulations were performed using USP dissolution rate testing equipment, Type 2 (Hansen Research, Chatsworth, CA) at a temperature of 37^{o}C and a stirring rate of 50 rpm. The dissolution medium was 900 ml of 0.01N HCl with 0.2% sodium lauryl sulfate (SLS) in water. A sample equivalent to 10 mg of the drug was sprinkled on top of the dissolution medium and liquid samples were withdrawn at time intervals of 5, 10, 15, 20, 30, 45, 60, 90 and 120 minutes. The samples were filtered using 0.45 µm pore size nylon filters (Whatman International, England) and drug concentrations were measured using an UV spectrophotometer at 246 nm (Jasco V680 spectrophotometer, Tokyo, Japan).

4.3.7.6 *FT-IR Studies*

Infrared spectra of the drug, pure polymers and the formulations were obtained using an FT-IR apparatus (Nicolet IR 100 Spectrophotometer, Thermo Scientific, USA). The samples were mixed with KBr (1:100 ratio) and pellets were prepared in the sample holder. Spectra were recorded in transmission mode from 4000 to 400 cm^{-1} wave number range using 64 sample/background scans and 2 cm^{-1} resolution.

4.3.8 *Stability Studies*

The stability studies were conducted to determine the effect of aging on the physical and chemical stability of the drug in various formulations. The solid solutions were stored in screw capped glass vials placed at ambient room temperature (~23^{o}C) and a relative humidity of ~ 30-40%. The samples collected at 3, 6 and 9 month intervals were characterized by DSC, XRD, drug content and dissolution studies and compared with the initial formulations.

4.4 Results and Discussion

4.4.1 *Solubility Parameter Calculations*

Solubility parameter (δ) is a measure of the cohesive energy of the material. The cohesive energy represents the amount of energy needed to separate the constituents of atoms or molecules of the material to a distance where the atoms/molecules possess no potential energy. It is the net effect of all interatomic molecular interactions including van der Waals interactions, covalent bonds, ionic bonds, hydrogen bonds, electrostatic interactions, induced dipole and permanent dipole interactions.[21] The cohesive energy of a material can be quantified in a number of ways. The most common approach is to use the solubility parameter. The solubility parameter values of EFV and polymers and their relative $\Delta\delta$ are given in Table 4.1. The calculated solubility parameter for EFV is 24.55 MPa$^{1/2}$ and literature values for the polymers are 20.55 and 22.94 MPa$^{1/2}$ for Eudragit EPO and Plasdone S-630, respectively.[20] Compounds with similar values for solubility parameters are likely to be miscible because the energy of mixing within the components is balanced by the energy released by the interaction between the components.[19] It has

also been postulated that compounds with a $\Delta\delta$ < 7.0 $MPa^{1/2}$ are likely to be miscible while compounds with a $\Delta\delta$ > 10.0 $MPa^{1/2}$ are likely to be immiscible.[22] In this study, both polymers exhibited $\Delta\delta$ < 4 $MPa^{1/2}$ and were likely to be miscible and were expected to form a solid solution when melt extruded with the drug.

4.4.2 *Characterization of Binary Mixtures*

4.4.2.1 *Thermal Analysis by DSC*

Drug-polymer miscibility is the key factor for the stability of amorphous pharmaceutical solid dispersion systems; partial miscibility or poor solubility can result in the formation of concentrated drug domains that may be prone to recrystallization after production and during storage.[23] Miscibility of the drug with the polymer can be assessed based upon the shift in melting endotherm or glass transition temperature of the drug, [24] or can be predicted theoretically using the Gordon-Taylor equation based on the T_g, densities and weight fractions of the pure components.[25]

$$Tgmix = \frac{T_{g1}W_1 + T_{g2}KW_2}{W_1 + W_2} \qquad (1)$$

$$K = \frac{T_{g1} \times \rho_1}{T_{g2} \times \rho_2} \qquad (2)$$

Where T_g is the glass transition temperature, W_1 and W_2 are the weight fractions of the components and K is the parameter calculated from the densities (ρ) and T_g of the amorphous components.

The experimentally obtained T_g values are shown in Table 4.2. Amorphous EFV produced by heat quenching in the DSC cycle showed a T_g of 33°C and the amorphous

polymers showed a T_g of 45.95 and 94.79^oC for Eudragit EPO and Plasdone S-630, respectively. A single T_g was observed for all the ratios of drug–polymer binary mixtures. This suggests the miscibility of drug and polymer in the given ratios and presence of a single phase in all the systems. According to the Gordon–Taylor equation, if the drug and polymer are miscible, the binary mixture will exhibit a single T_g that ranges between the T_g of the pure components and is dependent on the relative proportion of each component. As shown in Figure 4.1(a), in the case of Plasdone S-630, the experimentally determined T_g of the binary mixtures is below the T_g of the pure polymer suggesting a plasticization effect of the drug on the polymer. The experimentally derived T_g values showed a positive deviation from the theoretical values determined by the Gordon-Taylor equation. This suggests the existence of drug-polymer interactions and which enhanced thermal and mechanical stability are achieved at lower drug loadings. Interactions between unlike components typically result in a lower free volume, less flexibility for molecular rearrangement, and experimental T_g values that exceed those prediction by the Gordon-Taylor equation.[26]

Similar results were obtained with the Eudragit EPO systems (Fig. 4.1(b) and Table 4.2). A single T_g was observed for all the systems suggesting miscibility of the binary systems. The T_g of the mixtures is lower than that of the pure Eudragit EPO polymer indicting a plasticization effect of EFV on the Eudragit EPO polymer. The observed T_g values were significantly lower than the theoretical values suggesting the free volume in the homogenous phase is larger than that in the ideal mixture. The presence of longer lateral groups in Eudragit EPO compared to those found in Plasdone S-630 explains the dissimilar T_g dependences, by preventing packed chain conformations.

Other phenomena may also have contributed to the observed behavior. Water is a well known plasticizer and could be present in the hydrophilic polymer. This could have resulted in lower T_g values in the binary mixtures; the experiments were carried out in closed pans that did not allow the evaporation of water during the DSC measurement.

4.4.2.2 *Rheological Evaluation of Binary Mixtures*

The rheological behavior of binary mixtures was evaluated by zero shear viscosity (η_o) and activation energy (Ea) parameters. η_o is considered the most useful parameter in correlating the rheological properties of the material to the HME and it is also useful in assessing drug-polymer miscibility.[20] With increasing shear rate, the polymers and binary mixtures display a Newtonian plateau that transitions to shear thinning behavior as described by the Cross model (Eqn 3).

$$\eta = \eta_\infty + \frac{\eta_\circ - \eta_\infty}{1 + (C\dot{\gamma})^m} \quad (3)$$

Where, η, η_o, and η_∞ are the viscosity, zero shear viscosity, and infinite shear viscosity respectively, $\dot{\gamma}$ is the shear rate, and *C* and *m* are the Cross constants; the constants are listed in Table 4.3. The binary mixture of 80% EFV – 20% Plasdone S-630 displayed Newtonian behavior over the entire range of applied shear rate and, thus, is not represented by Cross model.

Zero shear viscosity for Eudragit EPO pure polymer and its binary mixtures, and Plasdone S-630 and its binary mixtures are shown in Figure 4.2. The addition of 20% EFV to Eudragit EPO results in a drastic decrease in η_o, indicating the solubilization of

the drug in the polymer which disrupts the polymer structure which decreases viscosity. As the drug loading is increased to 50%, η_o further decreases relative to the 20% loading. Surprisingly, at higher drug loading of 80%, η_o increased slightly. This may be attributed to inadequate mixing of EFV and Eudragit EPO. In the case of EFV – Plasdone S-630 binary systems η_o continuously decreases with drug loading, signifying the solubilization and plastifying effect of the the drug in the polymer.

The E_a for EFV - Eudragit EPO and EFV – Plasdone S-630 binary systems are shown in Figures 4.3(a) and 4.3(b), respectively. In both cases as the drug concentration was increased, the E_a decreased, suggesting plasticization of EFV on both polymers. This is supported by the DSC results. The 1:1 and 4:1 binary physical mixtures of the drug with both polymers exhibited lower activation energy. This suggested that at least a drug loading of 50 % w/w was needed to decrease the viscosity of the system and ensure the flow of the melt in the extrusion process.

4.4.3 *Characterization of Extrudates*

The extrusion temperatures of 120^{o}C for Eudragit EPO and 140 ^{o}C for Plasdone S-630 were used for processing the samples and it was observed that the polymers and drug were stable at these high temperatures.

Transparent extrudates were produced with both polymers at 50 wt% drug loading. The obtained extrudates were triturated in a mortar with a pestle and passed through a 60 mesh sieve. The drug content in the extrudates was found to be in the range of 96 – 103% of the theoretical amount indicating a relatively homogenous mixture.

4.4.3.1 *DSC Studies*

The DSC thermograms of EFV, Eudragit EPO, and their physical mixture, and HME formulations are shown in Figure 4.4. Crystalline EFV was characterized by a single, sharp melting endotherm at 137^{o}C (ΔH 513.2 J/g). Eudragit EPO is an amorphous polymer and therefore lacked a distinct endotherm. The melting endotherm of the EFV in the physical mixture occurred at 121^{o}C, whereas the melt extrudate had no distinct melting endotherm for the drug. This indicated the drug has been converted into the amorphous form during melt extrusion. Figure 4.5 shows the DSC thermograms of EFV, Plasdone S-630, their physical mixture, and HME formulations. Plasdone S-630 is an amorphous polymer with no melting endotherm, whereas the physical mixture of EFV and Plasdone S-630 showed a broad endotherm between 100 to 110^{o}C. The disappearance of the melting endotherm in the DSC scan of HME suggested that the drug has been converted to the amorphous form during the extrusion process.

4.4.3.2 *XRD Studies*

XRD patterns of EFV, EFV- Eudragit EPO physical mixture, and HME binary systems are shown in Figure 4.6. The diffractogram of EFV shows multiple peaks indicating the crystalline nature of the drug. Several distinct peaks similar to crystalline EFV were observed in the physical mixture again indicating the crystalline nature of the drug in the mixture. In the case of melt extrudates, the characteristic peaks of EFV disappeared indicating the amorphous nature of EFV with Eudragit EPO after HME.

The XRD patterns of EFV, EFV - Plasdone S-630 physical mixture and HME binary systems are shown in Figure 4.7. Several distinct peaks similar to crystalline EFV

were observed in the physical mixture indicating the crystalline nature of the drug in the mixture. Plasdone S-630 melt extrudates had no distinct peaks indicating the amorphous nature of the HME formulation.

4.4.3.3 *FTIR Studies*

Infrared spectroscopy has been widely used to investigate drug-polymer interactions in solid dispersion systems.[27] In order to evaluate any possible chemical interactions between the drug and carriers, FTIR spectra of EFV, physical mixtures and HME formulations were examined. The spectra are shown in Figures 4.8 and 4.9 for Eudragit EPO and Plasdone S-630 formulations, respectively. IR spectrum of EFV presented characteristic peaks alkyne at 2250 cm^{-1} and C-F stretch in the range of 1000-1400 cm^{-1}. N-H stretch in the range of 3300-3400 cm^{-1} overlapped the C-H stretch at 2850 - 3000 cm^{-1}. The Eudragit EPO exhibited C=O stretch at 1750 cm^{-1} and C-H stretching (N-methylamino) at 2750-2850 cm^{-1} (Fig. 4.8b) and Plasdone S-630 spectra showed C=O stretch at 1680 cm^{-1} (Fig. 4.9b). As shown in Figure 4.8, the spectra of EFV - Eudragit EPO physical mixture and HME formulations are identical. The EFV skeleton stretching vibrations are not affected by the addition of polymer suggesting no interaction between the polymer and drug in the physical and HME mixtures. Plasdone S-630 has two groups (=N- and C=O) that can potentially form hydrogen bonds with EFV in the HME formulations. The carbonyl group is more favorable for hydrogen bonding and intermolecular interactions than the nitrogen atom because of steric hindrance. For HME formulations the N-H stretching's bands broadened and the intensity of the bands decreased indicating some degree of interaction between the proton donating groups (-

NH) of EFV and the proton accepting groups(C=O) in the Plasdone S-630 polymer. These results support the positive deviation of the experimental T_g values with the theoretically predicted values by the Gordon –Taylor equation.

4.4.4 *Dissolution Studies*

Figure 4.10 shows the dissolution profiles of Eudragit EPO based physical mixture, HME formulations and EFV. Due to the extreme low solubility of the drug, 0.2% w/v SLS was added to the dissolution medium to maintain sink conditions. EFV is a poorly soluble drug with a solubility of 9.2 µg/ml in water.[1] The saturation solubility of the EFV was increased by the addition of SLS to the dissolution medium to be 197 µg/ml. The dissolution of the HME formulations (D_{30}= 96%) was ~2 fold higher than EFV alone (D_{30}= 43%) and the corresponding physical mixture (D_{30}= 45%). The increase in the dissolution rate in the case of the HME formulation is attributed to the amorphous state of the drug that offers a lower thermodynamic barrier to dissolution and the formation of a glassy solution where the drug is molecularly dispersed in the polymer. The higher apparent solubility and increase in dissolution rate for amorphous materials is well known and has been extensively documented.[28,29] The enhancement in solubility is the result of the disordered structure of the amorphous solid. Due to the short range intermolecular interactions in an amorphous system no lattice energy has to be overcome, whereas in the crystalline material the lattice has to be disrupted for the material to dissolve.[30] Solubility and dissolution rate of the drug was not enhanced by simple physical mixing with the polymer. Though SLS provided sufficient wetting of the drug

particles as observed during dissolution studies, the hydrophilic polymer, Eudragit EPO, in the physical mixture did not further enhance the dissolution of EFV.

The dissolution profiles of the EFV - Plasdone S-630 physical mixture, their HME formulations and pure EFV are shown in Figure 4.11. The dissolution of the HME formulation (D_{30}= 82 %) was ~1.7 fold higher than its corresponding physical mixture (D_{30}= 47 %) or EFV alone (D_{30}= 43%). The enhancement in dissolution in Plasdone S-630 extrudates is also due to the conversion of crystalline drug into the amorphous state. The differences in the dissolution profile between the two polymer systems are due to the solubility/dissolution nature of the polymer in the dissolution medium. Dissolution of the drug in Eudragit EPO is governed by the carrier, where as in the case of Plasdone S-630 systems the dissolution rate is governed by solubilization of the polymer to create a hydrotropic environment for the insoluble drug. Thus, for Eudragit systems the dissolution is predominantly carrier controlled, whereas for Plasdone S-630 systems the drug dissolution is predominantly drug controlled.[31] It was observed in the dissolution studies that Plasdone S-630 dissolved rapidly leaving the drug as a fine precipitate than the crystalline drug in the physical mixtures. In the case of Eudragit EPO systems, the polymer dissolved much slower because the polymer dissolution is pH dependent. Precipitation of the EFV was not observed in the dissolution medium with Eudragit EPO systems. Similar dissolution results were reported for itraconazole extrusion systems with polymers.[32]

4.4.5 *Stability on Storage*

Glassy solid solutions are thermodynamically metastable systems that favor the conversion of amorphous form into the crystalline form under storage.[33] To evaluate the physical state of the drug, the formulations were characterized by XRD and DSC after storage for 9 months. The dissolution stability was also evaluated for both initial and aged samples. As shown in the DSC thermograms in Figures 4.4 and 4.5, both HME formulations after storage were similar to the initial formulations and did not show any melting endotherm. This indicated an amorphous state of the drug in the aged samples. The XRD results as shown in Figures 4.6 and 4.7 demonstrate similar diffractograms of aged as compared to fresh HME formulations, indicating the amorphous nature of the EFV. Both DSC and XRD results on aged samples confirmed that there was no recrystallization of the amorphous drug in the HME formulations suggesting good physical stability. The dissolution profiles of aged samples relative to fresh HME formulations further proved that the amorphous state of the drug was maintained in the aged formulations. The enhanced physical stability of the HME formulations upon storage is attributed to drug polymer interactions and antiplasticization effect of the polymer. Plasdone S-630 systems had strong intermolecular interactions, particularly hydrogen bonding between amorphous EFV and the polymer. These might further reduce the molecular mobility and retarded recrystallization during storage. Though there were no strong inter-molecular interactions in the Eudragit EPO systems, the physical stability of this formulation may be due to the antiplasticization effect of the polymer on the drug.

4.5 Conclusion

Dissolution rate enhancement of EFV was obtained by preparing amorphous glassy solutions with Eudragit EPO and Plasdone S-630 polymers by melt extrusion. The crystalline EFV was converted to the amorphous state during the extrusion process with both polymers. Enhanced physical stability of the Plasdone S-630 HME formulation is attributed to drug-polymer interactions. For Eudragit EPO, the HME formulation is less susceptible to recrystallization perhaps due to the antiplasticization effect of the polymer.

4.6 Acknowledgements

The authors are thankful to Aurobinda Pharma (Hyderabad, India), ISP Technologies (Wayne, NJ) and Evonik Industries (Piscataway, NJ). Financial support from the Harrison School of Pharmacy, Auburn University is highly appreciated.

4.7 References

1. Maurin MB, Rowe SM, Blom K, Pierce ME. 2002. Kinetics and mechanism of hydrolysis of efavirenz. Pharmaceutical Research 19(4):517-522.
2. Gazzard B, Bernard AJ, Boffito M, Churchill D, Edwards S, Fisher N, Geretti AM, Johnson M, Leen C, Peters B, Pozniak A, Ross J, Walsh J, Wilkins E, Youle M. 2006. British HIV Association (BHIVA) guidelines for the treatment of HIV-infected adults with antiretroviral therapy (2006). HIV Med 7(8):487-503.
3. Chiappetta DA, Hocht C, Sosnik A. 2002. A highly concentrated and taste-improved aqueous formulation of efavirenz for a more appropriate pediatric management of the anti-HIV therapy. Curr HIV Res 8(3):223-231.

4. Kasim NA, Whitehouse M, Ramachandran C, Bermejo M, Lennernas H, Hussain AS, Junginger HE, Stavchansky SA, Midha KK, Shah VP, Amidon GL. 2004. Molecular properties of WHO essential drugs and provisional biopharmaceutical classification. Mol Pharm 1(1):85-96.
5. Takano R, Sugano K, Higashida A, Hayashi Y, Machida M, Aso Y, Yamashita S. 2006. Oral absorption of poorly water-soluble drugs: computer simulation of fraction absorbed in humans from a miniscale dissolution test. Pharm Res 23(6):1144-1156.
6. Sosnik A, Chiappetta DA, Carcaboso AM. 2009. Drug delivery systems in HIV pharmacotherapy: what has been done and the challenges standing ahead. J Control Release 138(1):2-15.
7. Vasconcelos T, Sarmento B, Costa P. 2007. Solid dispersions as strategy to improve oral bioavailability of poor water soluble drugs. Drug Discov Today 12(23-24):1068-1075.
8. Kaplan SA. 1972. Biopharmaceutical considerations in drug formulation design and evaluation. Drug Metab Rev 1: 15-34.
9. Sathigari S, Chadha G, Lee YH, Wright N, Parsons DL, Rangari VK, Fasina O, Babu RJ. 2009. Physicochemical characterization of efavirenz-cyclodextrin inclusion complexes. AAPS PharmSciTech 10(1):81-87.
10. Crowley MM, Zhang F, Repka MA, Thumma S, Upadhye SB, Battu SK, McGinity JW, Martin C. 2007. Pharmaceutical applications of hot-melt extrusion: part I. Drug Dev Ind Pharm 33(9):909-926.

11. Chokshi RJ, Zia H, Sandhu HK, Shah NH, Malick WA. 2007. Improving the dissolution rate of poorly water soluble drug by solid dispersion and solid solution: pros and cons. Drug Deliv 14(1):33-45.
12. Yang J, Grey K, Doney J. 2010. An improved kinetics approach to describe the physical stability of amorphous solid dispersions. Int J Pharm 384(1-2):24-31.
13. Hancock BC, Zografi G. 1997. Characteristics and significance of the amorphous state in pharmaceutical systems. J Pharm Sci 86:1-12.
14. Leuner C, Dressman J. 2000. Improving drug solubility for oral delivery using solid dispersions. Eur J Pharm Biopharm 50(1):47-60.
15. Serajuddin AT. 1999. Solid dispersion of poorly water-soluble drugs: early promises, subsequent problems, and recent breakthroughs. J Pharm Sci 88(10):1058-1066.
16. Konno H, Taylor LS. 2006. Influence of different polymers on the crystallization tendency of molecularly dispersed amorphous felodipine. J Pharm Sci 95(12):2692-2705.
17. Janssens S, Van den Mooter G. 2009. Review: physical chemistry of solid dispersions. J Pharm Pharmacol 61(12):1571-1586.
18. Marsac PJ, Shamblin SL, Taylor LS. 2006. Theoretical and practical approaches for prediction of drug-polymer miscibility and solubility. Pharm Res 23(10):2417-2426.
19. Matsumoto T, Zografi G. 1999. Physical properties of solid molecular dispersions of indomethacin with poly(vinylpyrrolidone) and poly(vinylpyrrolidone-co-vinyl-acetate) in relation to indomethacin crystallization. Pharm Res 16(11):1722-1728.

20. Chokshi RJ, Sandhu HK, Iyer RM, Shah NH, Malick AW, Zia H. 2005. Characterization of physico-mechanical properties of indomethacin and polymers to assess their suitability for hot-melt extrusion processs as a means to manufacture solid dispersion/solution. J Pharm Sci 94(11):2463-2474.

21. Hancock BC, York P, Rowe RC. 1997. The use of solubility parameters in pharmaceutical dosage form design. International Journal of Pharmaceutics 148(1):1-21.

22. Greenhalgh DJ, Williams AC, Timmins P, York P. 1999. Solubility parameters as predictors of miscibility in solid dispersions. J Pharm Sci 88(11):1182-1190.

23. DiNunzio JC, Miller DA, Yang W, McGinity JW, Williams RO, 3rd. 2008. Amorphous compositions using concentration enhancing polymers for improved bioavailability of itraconazole. Mol Pharm 5(6):968-980.

24. Mura P, Faucci MT, Manderioli A, Furlanetto S, Pinzauti S. 1998. Thermal analysis as a screening technique in preformulation studies of picotamide solid dosage forms. Drug Dev Ind Pharm 24(8):747-756.

25. Gordon M, Taylor JS. 1952. Ideal copolymers and the second order transitions of synthetic rubbers. I. Non-crystalline copolymers. J Appl Chem 2:493-500.

26. Gupta P, Bansal AK. 2005. Molecular interactions in celecoxib-PVP-meglumine amorphous system. J Pharm Pharmacol 57(3):303-310.

27. Jayachandra Babu R, Brostow W, Kalogeras IM, Sathigari S. 2009. Glass transitions in binary drug + polymer systems. Materials Letters 63(30):2666-2668.

28. Rumondor AC, Marsac PJ, Stanford LA, Taylor LS. 2009. Phase behavior of poly(vinylpyrrolidone) containing amorphous solid dispersions in the presence of moisture. Mol Pharm 6(5):1492-1505.

29. Hancock BC, Parks M. 2000. What is the true solubility advantage for amorphous pharmaceuticals? Pharm Res 17(4):397-404.

30. Shah B, Kakumanu VK, Bansal AK. 2006. Analytical techniques for quantification of amorphous/crystalline phases in pharmaceutical solids. J Pharm Sci 95(8):1641-1665.

31. Albers J, Alles R, Matthee K, Knop K, Nahrup JS, Kleinebudde P. 2009. Mechanism of drug release from polymethacrylate-based extrudates and milled strands prepared by hot-melt extrusion. Eur J Pharm Biopharm 71(2):387-394.

32. Six K, Verreck G, Peeters J, Brewster M, Van Den Mooter G. 2004. Increased physical stability and improved dissolution properties of itraconazole, a class II drug, by solid dispersions that combine fast- and slow-dissolving polymers. J Pharm Sci 93(1):124-131.

33. Craig DQ, Royall PG, Kett VL, Hopton ML. 1999. The relevance of the amorphous state to pharmaceutical dosage forms: glassy drugs and freeze dried systems. Int J Pharm 179(2):179-207.

Table 4.1 Solubility parameters for efavirenz and the polymers

Drug /Polymer	Solubility Parameter (δ) in $MPa^{1/2}$	Δδ	Miscible with EFV*	Chemical Structure
Efavirenz	24.55			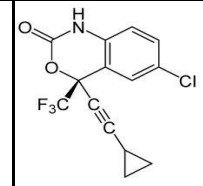
Eudragit EPO	20.55	4.0	Yes	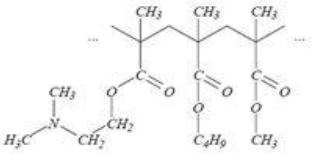
Plasdone S-630	22.94	1.61	Yes	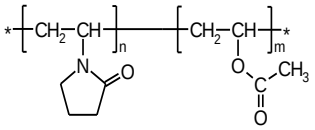

*Compounds with a 'δ' difference < 7.0 $MPa^{1/2}$ are likely to be miscible.

Table 4.2 Glass transition temperatures for the polymers and various binary mixtures

Drug : Polymer Ratio	Glass transition temperature (T_g) in ^oC	
	Eudragit EPO	Plasdone S-630
Pure polymer	45.95	94.79
PM 1:4	27.29	84.60
PM 1:1	30.27	65.93
PM 4:1	31.23	41.38

Table 4.3 Cross model parameters

Sample		η_o (Pa s)	η_∞ (Pa s)	C	M
Drug	Polymer				
0 %	100 % EPO	30867.0	0.00060	0.4081	1.0188
20 %	80 % EPO	2812.7	0.00005	0.0620	1.3243
50 %	50 % EPO	189.4	0.00001	0.0136	2.6607
80 %	20 % EPO	455.2	0.00002	0.0633	0.5649
0 %	100 % Plasdone	88401.0	0.00610	0.5577	0.8642
20 %	80 % Plasdone	4737.6	0.00009	0.0887	0.9730
50 %	50 % Plasdone	229.4	0.00001	0.0121	1.2699

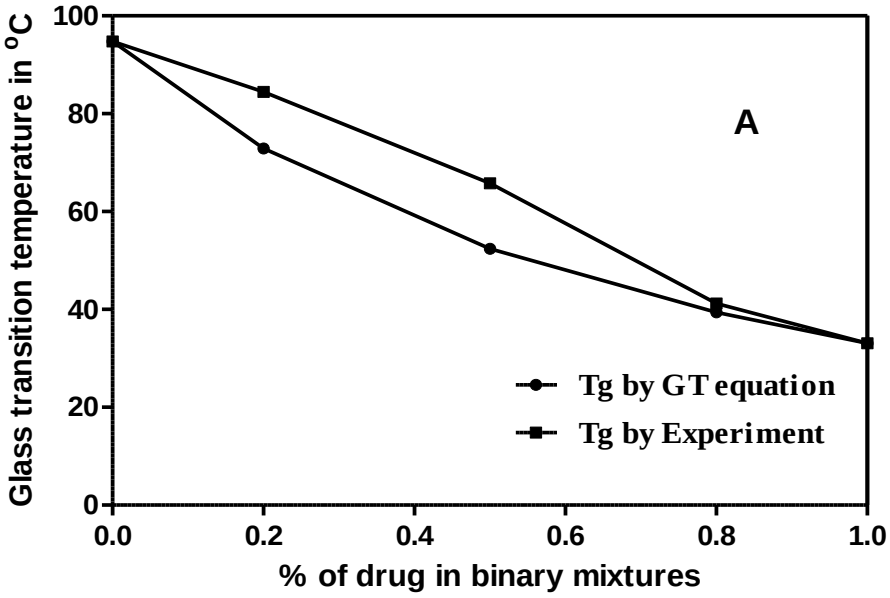

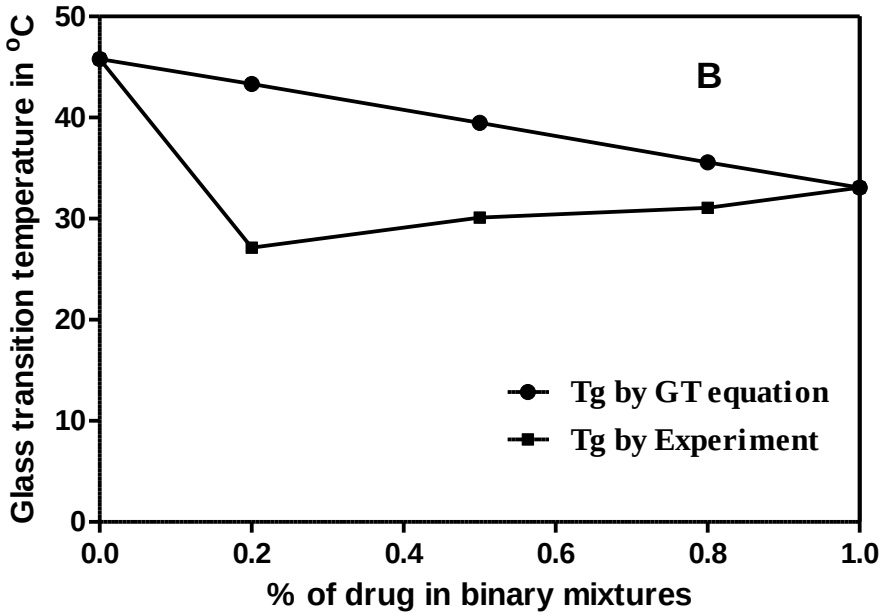

Figure 4.1 Phase diagram of efavirenz and polymer binary mixtures (a) Plasdone S-630 (b) Eudragit EPO.

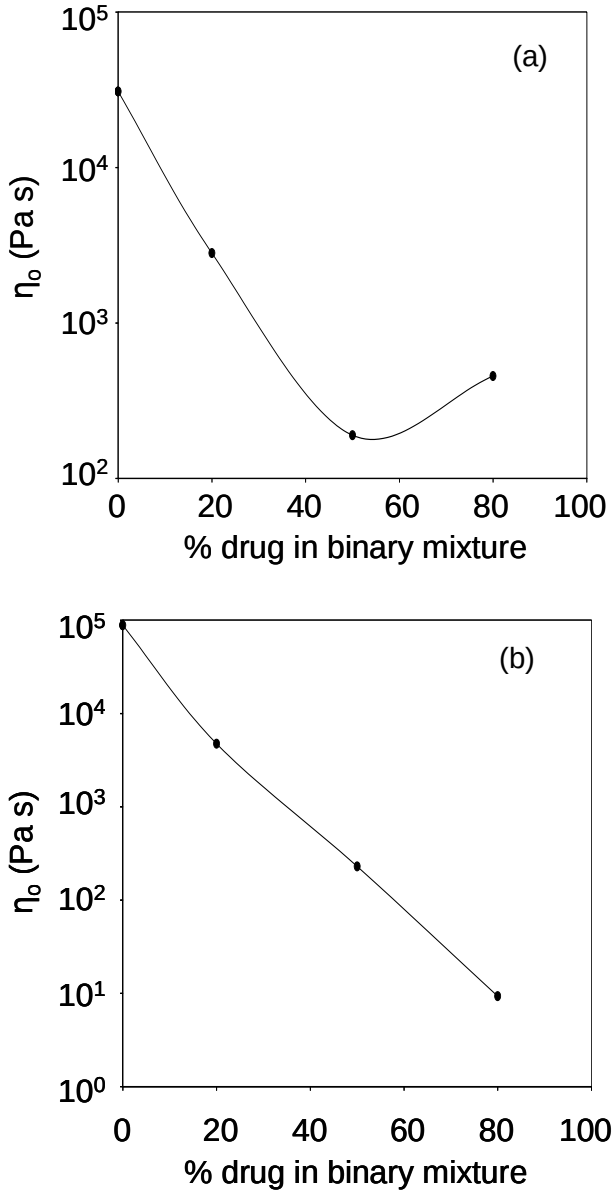

Figure 4.2 Change in zero shear viscosity with increasing concentration of EFV in polymer binary mixtures (a) Eudragit EPO (b) Plasdone S-630 (y-axis: zero shear viscosity).

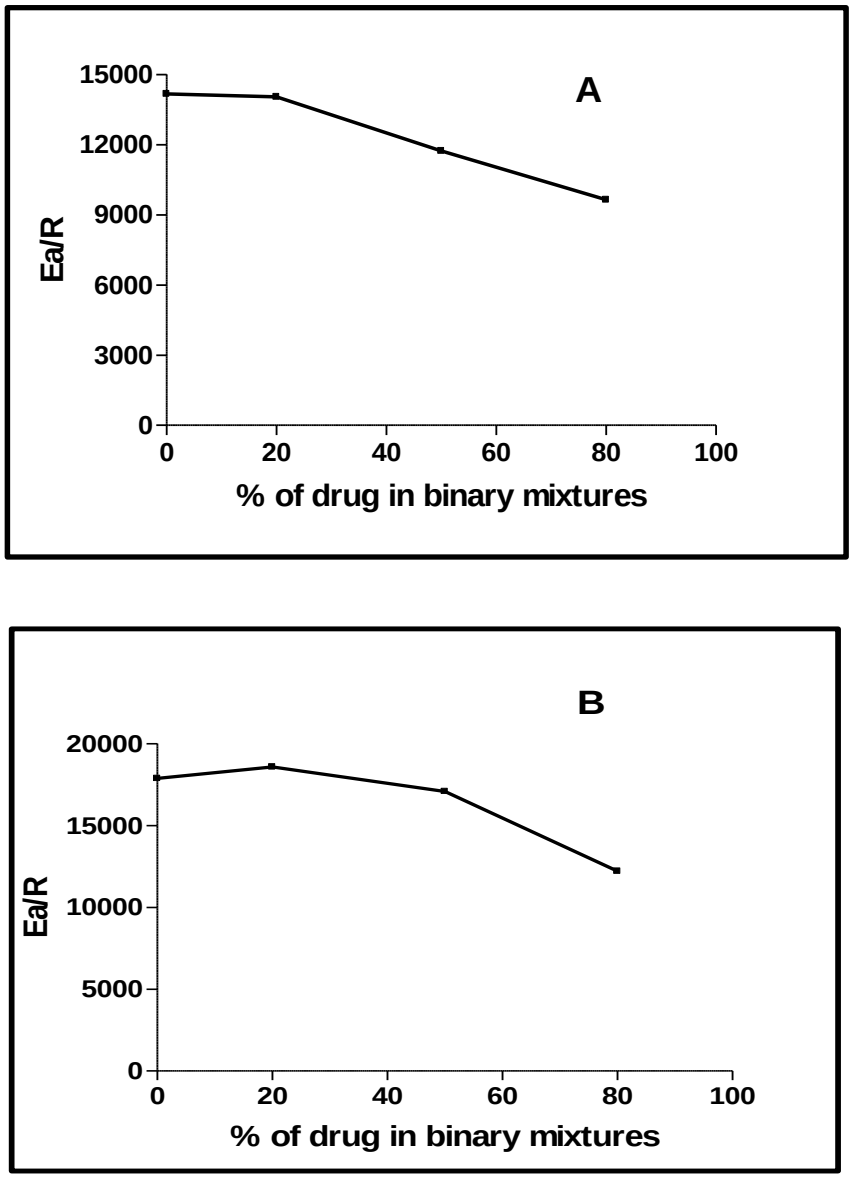

Figure 4.3 Change in activation energy with percent of EFV in polymer binary mixtures (a) Eudragit EPO (b) Plasdone S-630.

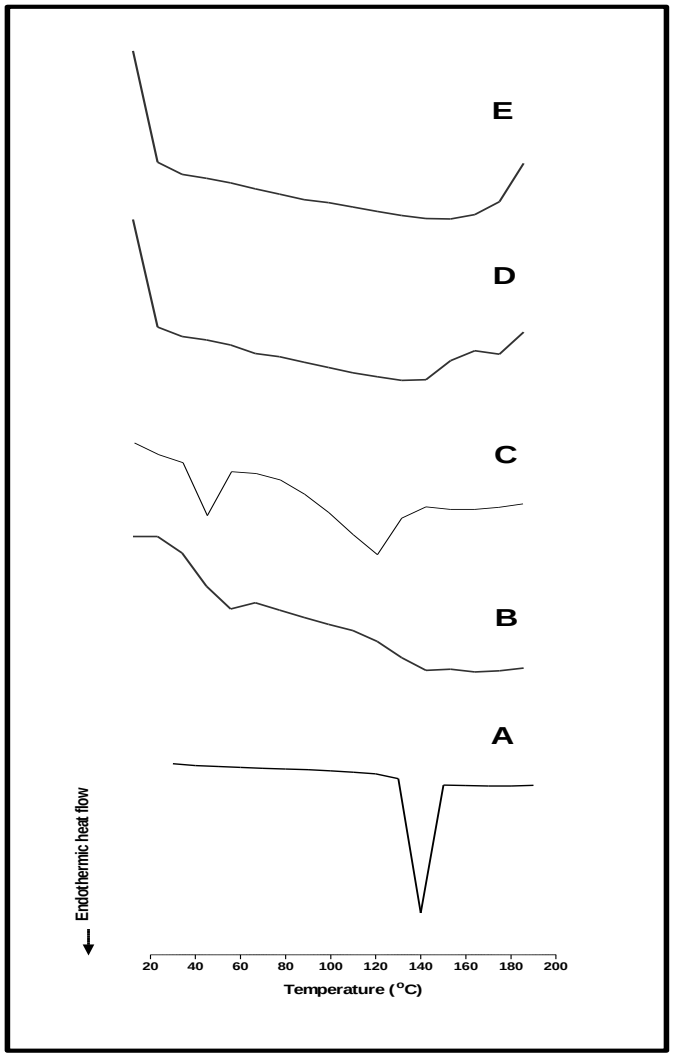

Figure 4.4 DSC thermographs of (a) EFV, (b) Eudragit EPO, (c) EFV – Eudragit EPO physical mixture, (d) EFV-Eudragit EPO HME (Initial) and (e) EFV-Eudragit EPO HME (9 months).

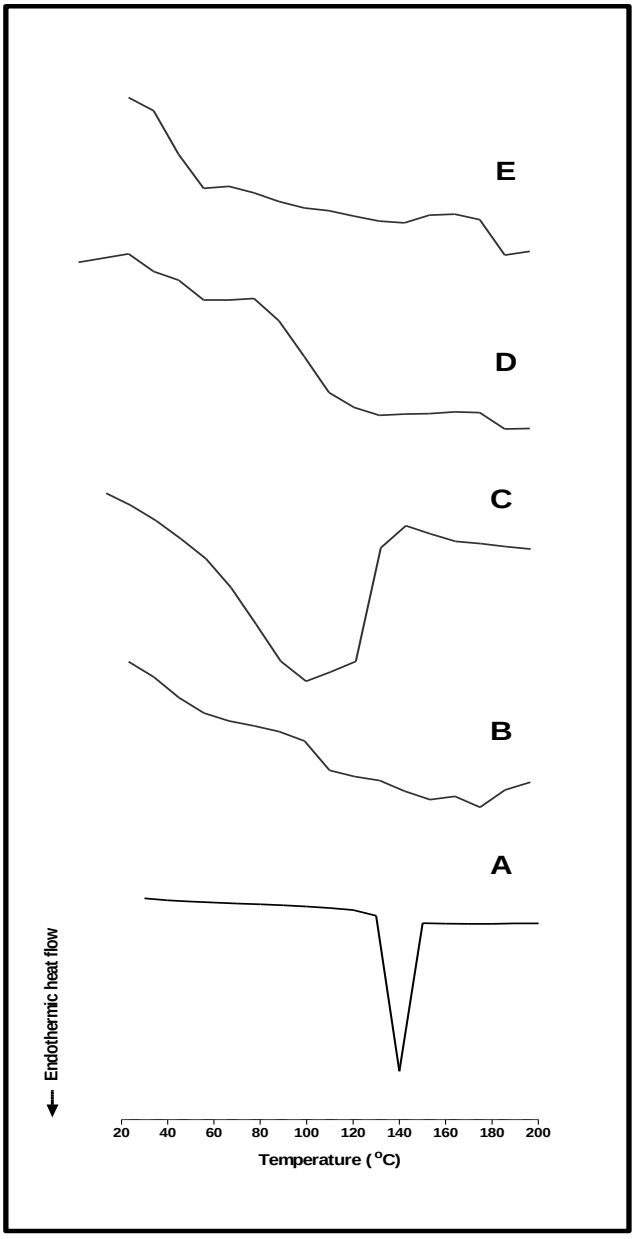

Figure 4.5 DSC thermographs of (a) EFV, (b) Plasdone S-630, (c) EFV – Plasdone S-630 physical mixture, (d) EFV – Plasdone S-630 HME (Initial) and (e) EFV-Plasdone S-630 HME (9 months).

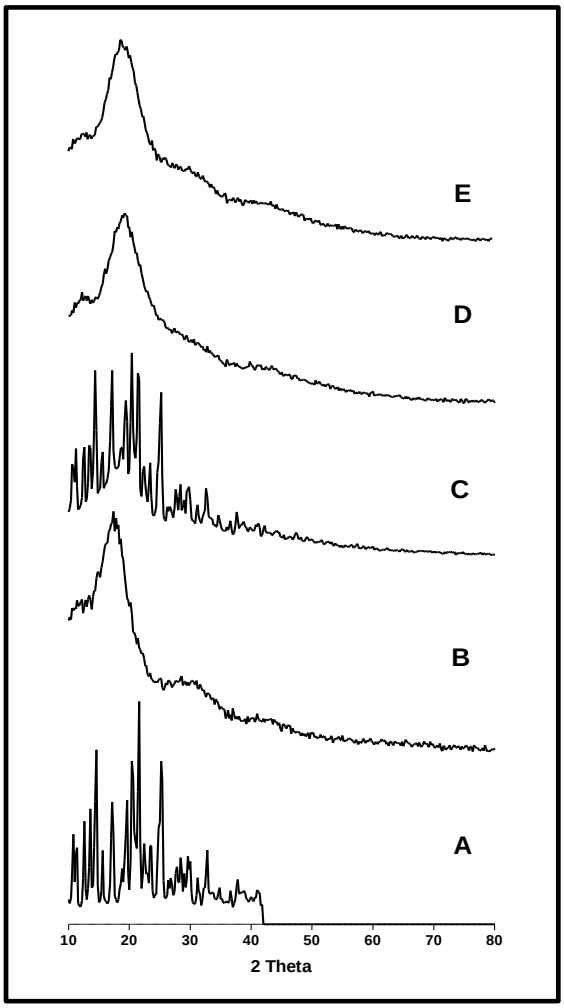

Figure 4.6 XRD profiles of (a) EFV, (b) Eudragit EPO, (c) EFV – Eudragit EPO physical mixture, (d) EFV-Eudragit EPO HME (Initial) and (e) EFV-Eudragit EPO HME (9 months).

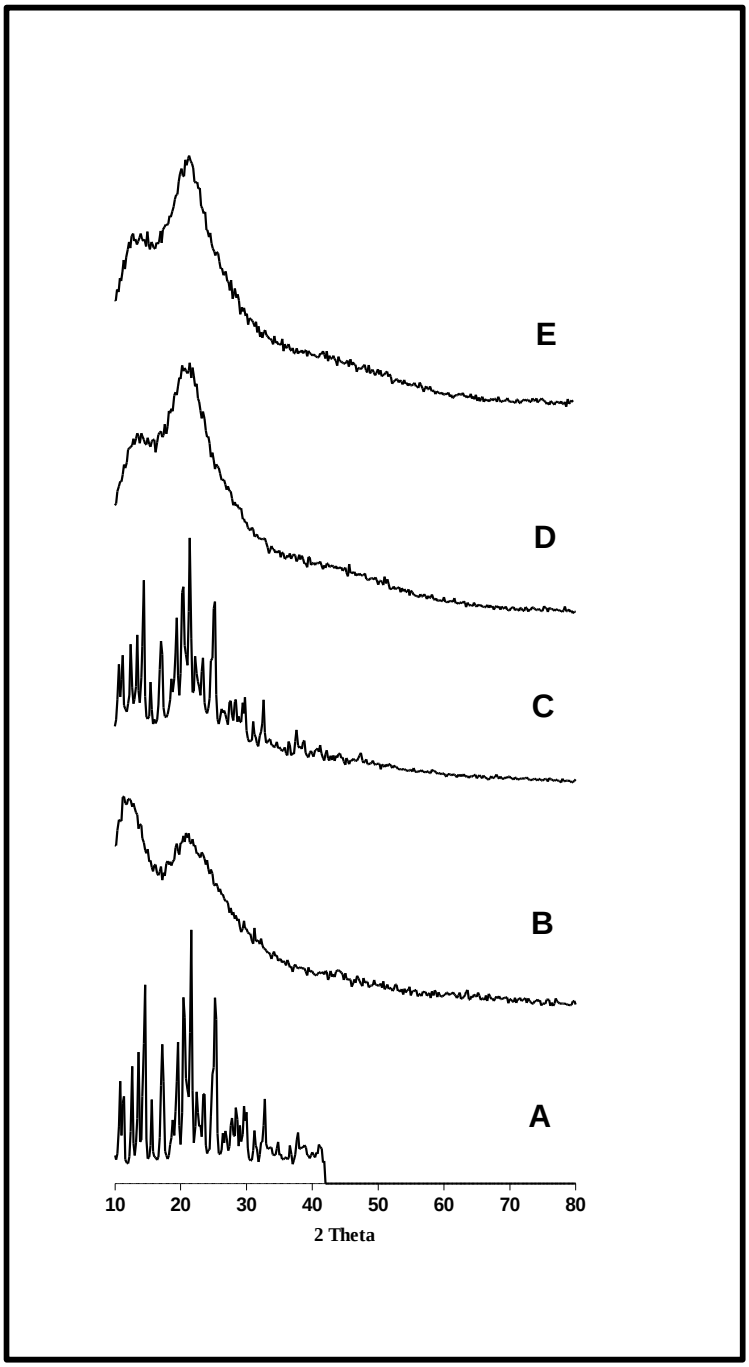

Figure 4.7 XRD profiles of (a) EFV, (b) Plasdone S-630, (c) EFV – Plasdone S-630 physical mixture, (d) EFV – Plasdone S-630 HME (Initial) and (e) EFV-Plasdone S-630 HME (9 months).

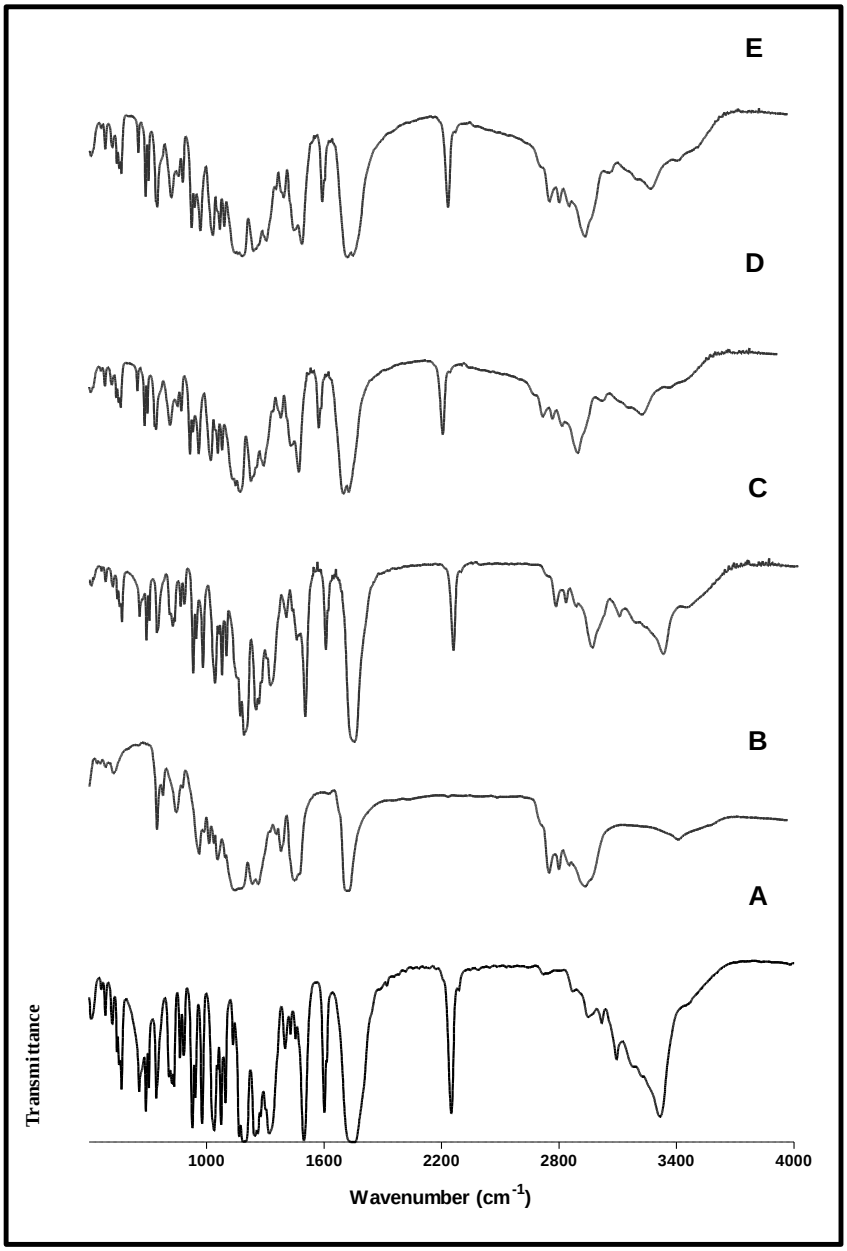

Figure 4.8 FTIR Spectra of (a) EFV, (b) Eudragit EPO, (c) EFV – Eudragit EPO physical mixture, (d) EFV-Eudragit EPO HME (Initial) and (e) EFV-Eudragit EPO HME (9 months).

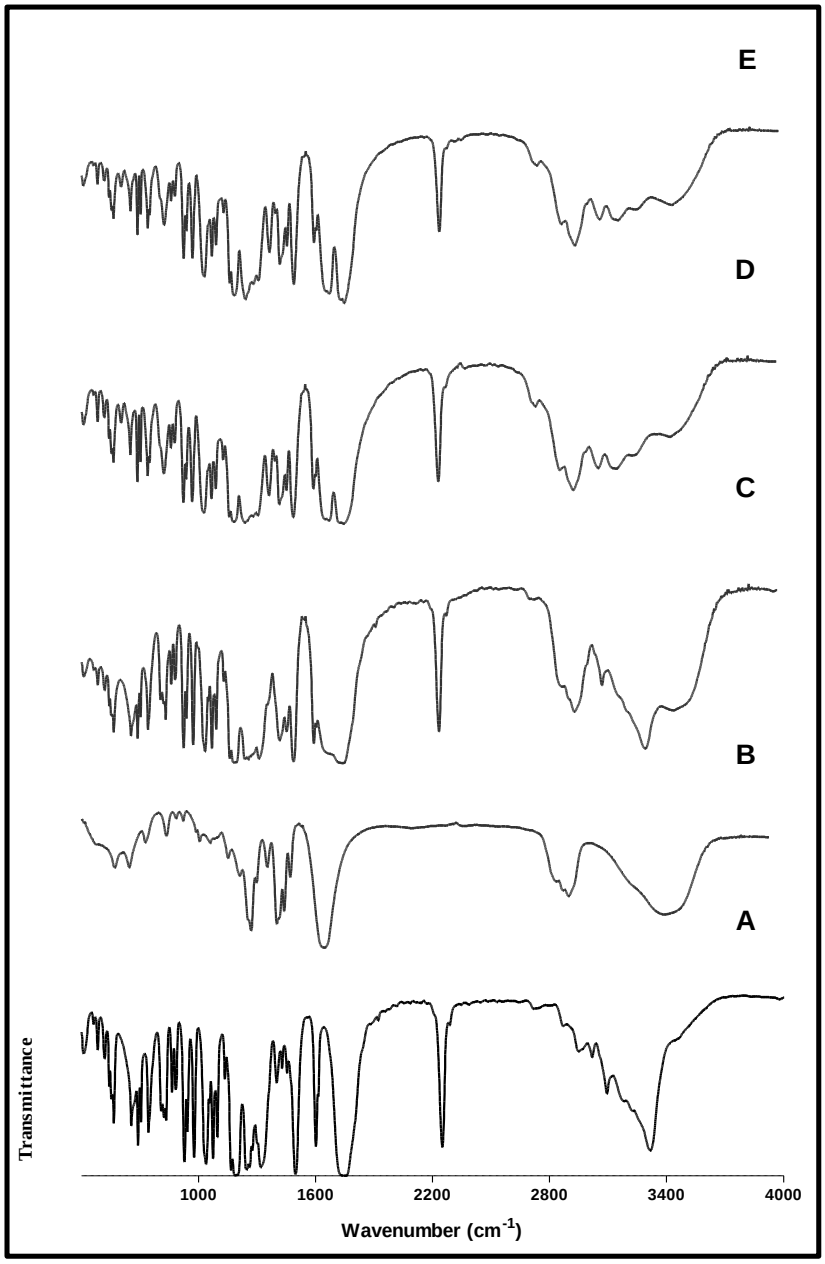

Figure 4.9 FTIR Spectra of (a) EFV, (b) Plasdone S-630, (c) EFV – Plasdone S-630 physical mixture, (d) EFV – Plasdone S-630 HME (Initial) and (e) EFV-Plasdone S-630 HME (9 months).

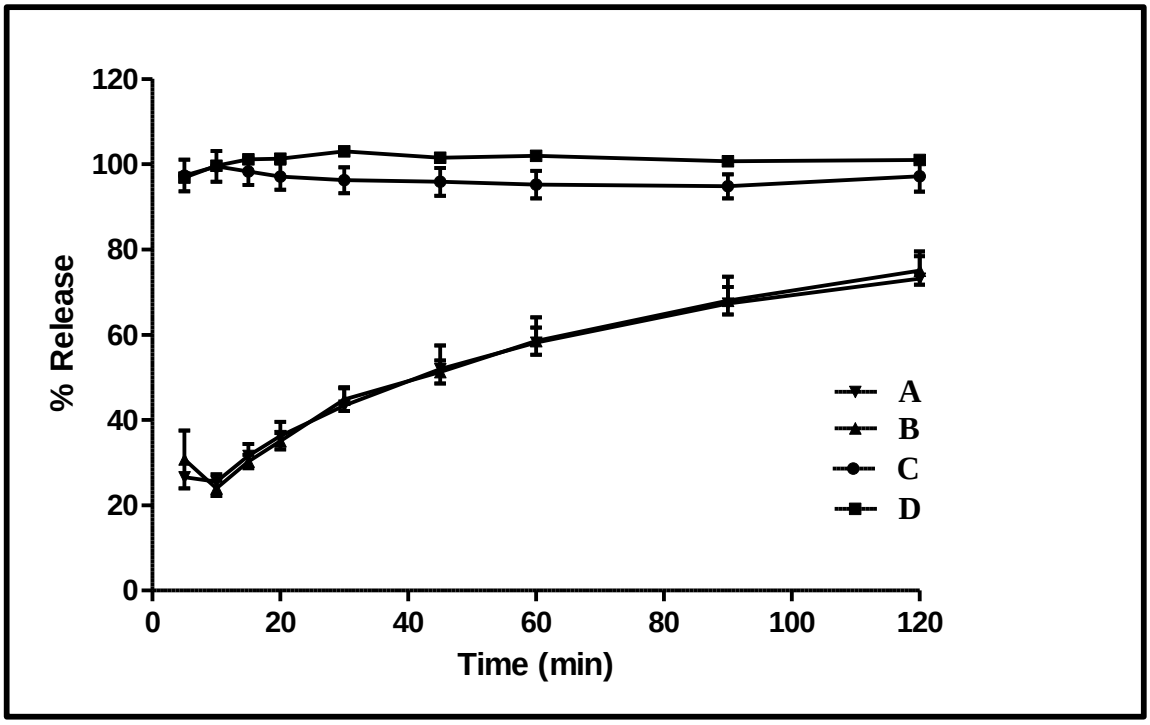

Figure 4.10 Dissolution profiles of (a) EFV, (b) EFV – Eudragit EPO physical mixture (1:1), (c) EFV-Eudragit EPO HME (Initial) and (d) EFV – Eudragit EPO HME (9 months) formulations.

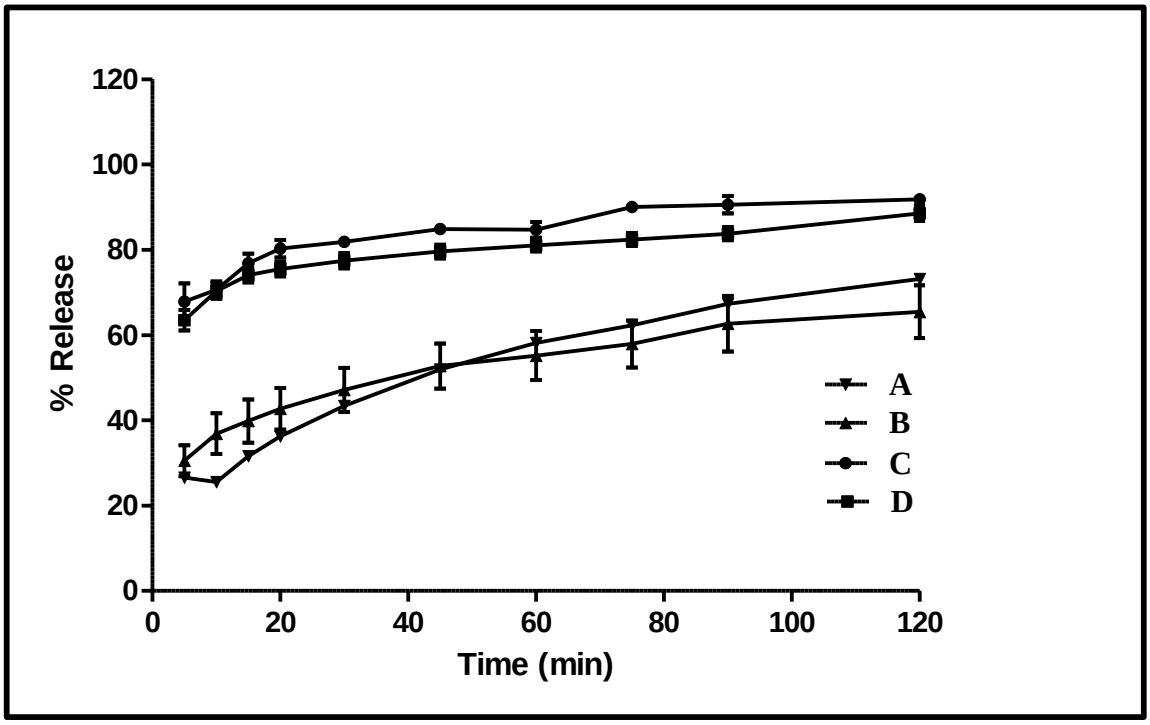

Figure 4.11 Dissolution profiles of (a) EFV, (b) EFV - Plasdone S-630 physical mixture (1:1), (c) EFV-Plasdone S-630 HME (Initial) and (d) EFV-Plasdone S-630 HME (9 months).

5. Glass Transition Behavior and Miscibility Evaluation of Hydrophobic Drugs in a Copolymer

5.1 Abstract

The knowledge of glass transition temperatures T_g in drug + polymer systems is indispensable for amorphous solid dispersions. T_g values as a function of composition make possible the determination whether a given polymer is miscible or compatible with the drug and whether the polymer will provide release of the drug at a desired rate. We have used differential scanning calorimetry and Fourier-transform infrared spectroscopy to evaluate miscibility in solid dispersions of the drugs. Carvedilol, itraconazole, nevirapine and nimodipine in the pharmaceutical grade copolymer poly(vinyl pyrrolidone-*co*-vinyl acetate) (PLS-630 Copovidone). Successful formulation of amorphous solid disperions is discussed in terms of thermophysical behavior (suppression of crystallization, negative excess volumes of mixing) and intermolecular interactions (concentrations of proton donating/accepting groups) in drug + polymer systems. Several equations were applied to the complex s-shaped $T_g(\varphi)$ patterns obtained (φ being the mass fraction of the drug). The best agreement of calculations with experiment is achieved using a recently proposed three-parameter equation, symmetric with respect to the equal concentration of both components.

5.2 Introduction

The enhancement of the bioavailability of poorly water soluble drugs is one of the main targets of drug development. Among different bioavailability enhancement approaches,[1-11] formulation of amorphous drug/polymer blends is becoming an increasingly popular strategy to enhance the absorption of active compounds with dissolution-limited oral bioavailability.[12] Amorphous drugs are advantageous over their crystalline counter parts with higher solubility, faster dissolution rate, and enhanced oral bioavailability.[13] Amorphous drug substances are physically unstable due to their higher energy state and tend to recrystallize upon storage.[14] A promising solution to this problem seems to be physical stabilization of amorphous drug phases in solid dispersions with glassy polymers.[15] Thermodynamically, the drug has a lower chemical potential when mixed with a polymer, resulting in the change of crystallization driving force. The long polymeric chain can sterically hinder the association between drug molecules and there by inhibit the recrystallization of the drug. In addition, the interaction between the drug and polymer provides an increased energy barrier for the nucleation and consequently enhancing the physical stability.[16] One thus achieves a longer time scale for drug's devitrification. The thermophysical stability is also influenced by the method of preparation,[17] and storage conditions (storing temperature and moisture levels).[18,19]

The key parameter along the route just described is the knowledge of glass transition temperatures (T_g) in binary drug + polymer systems. Since both the drug and the polymer are preferred in an amorphous (glassy) state, crystallization of either component has to be prevented. Hancock and coworkers,[20] for example, proposed that a reasonable guide to stability is to store the pharmaceutical sample at least 50 K below its

T_g, near the zero mobility, or Kauzmann, temperature. Long-term crystallization inhibition may be attained in solid dispersions of the drug in a polymer – as opposed to their physical mixtures[17,21] – where strong steric hindrances and specific intermolecular interactions take place.[22-24] For example, Konno and Taylor[25] ascribe the reduction in the nucleation rate for crystallization exhibited by felodipine (FEL) in polyvinyl pyrrolidone (PVP), hydroxypropyl methylcellulose (HPMC) and hydroxypropyl methylcellulose acetate succinate (HPMCAS), to an increase in the kinetic barrier for nucleation; the scale of the effect being related to polymer concentration. Moreover, the inhibition can be achieved via antiplasticizing effect of the polymeric component; in other words and in obvious notation, $T_{g,blend} > T_{g,drug.}$[23,26] The behavior of the ketoconazole (KET) + PVP K-25 solid dispersions studied by Van der Mooter and coworkers is a sound example.[19] The above factors determine miscibility of the components, which in turn is dictated by the thermodynamics of mixing. The entropy of mixing is always favorable (an increase on mixing) providing one driving force facilitating mixing. Another important factor that affects the miscibility is the enthalpy of mixing. The enthalpic component of the Gibbs function of mixing is controlled by the relative strength of the cohesive drug + drug, polymer + polymer and the drug + polymer intercomponent interactions. Understanding the above relationships is important for optimization of the formulation in drug-delivery systems. The glass transition temperature values tell us a difference between *high* (accelerated recrystallization, undesirable) and *low* (stabilized amorphous state) molecular mobility. Varying mass concentration φ of the drug in drug + polymer systems causes profound changes in thermophysical properties. These properties are often studied jointly with Fourier-transform infrared spectroscopy (FT-IR).

Analysis of the behavior of the glass transition temperatures of solid dispersions of pharmaceutical compounds in relation to blend composition [$T_g(\varphi)$ plots] is thus necessary for production of capsules or tablets with small size and long-term stability. In this paper, we have determined $T_g(\varphi)$ diagrams for selected drug + polymer systems to provide quantitative results characterizing drug encapsulation. The polymer was in all cases the same, the pharmaceutical grade P(VP-*co*-VA) copolymer (60 mole % vinyl pyrrolidone and 40 % vinyl acetate), known under the trade name Plasdone S-630 Copovidone or PLS-630. It was combined in turn with four poorly water soluble drugs of different properties and biomedical functions: *Carvedilol* (a non-selective adrenergic receptor blocker, indicated in the treatment of mild-to-moderate congestive heart failure), *itraconazole* (an antifungal agent that impairs ergosterol synthesis, used among others against histoplasmosis, cryptococcal meningitis and aspergillosis), *Nevirapine* (a potent, non-nucleoside reverse transcriptase inhibitor used for treatment of HIV infection and AIDS) and *nimodipine* (a calcium channel blockader with preferential cerebrovascular activity). Solid solutions of the above drugs in PLS-630 were investigated by differential scanning calorimetry (DSC) and FT-IR spectroscopy to evaluate components miscibility, crystallization inhibition and the extent of intermolecular interactions. Changes in the shape of the $T_g(\varphi)$ diagrams and the applicability of important curve-fitting equations (see following section) in their description were examined. The results are presented below, also in relation to other thermophysical characteristics.

5.2.1 *$T_g(\varphi)$ Functions*

A number of equations representing $T_g(\varphi)$ relationships for binary (1 + 2) organic

systems and copolymers, have been developed[27-35] and applied –with variable success– in drug + polymer systems. Fairly often used in binary pharmaceutical systems is the Gordon-Taylor (GT) equation.[27]

$$T_g = \frac{\varphi_1 T_{g,1} + k_{GT}(1-\varphi_1)T_{g,2}}{\varphi_1 + k_{GT}(1-\varphi_1)} \qquad (1)$$

which assumes additivity of the specific volumes of the components. φ_i, ρ_i and $T_{g,i}$ are, respectively, the weight fraction, the density, and the glass transition temperature of each component ($T_{g,1} \leq T_{g,2}$; $\varphi_1 + \varphi_2 = 1$). This equation is valid in case of volume additivity, implying that mixing of molecules of type 1 and 2 does not lead to a volume contraction or expansion. This only holds if the homomolecular interactions are of similar strength as the heteromolecular intermolecular forces. Parameter k_{GT} is claimed to represent the ratio of the free volumes of the two components[27] but is given by.[35]

$$k_{GT} = \rho_1 \Delta\alpha_1 / \rho_2 \Delta\alpha_2 \approx \rho_1 T_{g,1} / \rho_2 T_{g,2}\,. \qquad (2)$$

where $\Delta\alpha_i$ is the change in the thermal expansivities of each component at the respective T_g. Obviously the claim is unjustified since densities correspond to total specific volumes of the materials not to free volumes. It should be mentioned[36,37] that

$$1/\rho = v = v^* + v^f \qquad (3)$$

where v^* is the hard-core (incompressible) volume and v^f is the free volume. In most cases, the pretense is dropped and k_{GT} is used as a free fitting parameter.

There is also the Fox equation,[28]

$$\frac{1}{T_g} = \frac{\varphi_1}{T_{g,1}} + \frac{1-\varphi_1}{T_{g,2}} \qquad (4)$$

and the so-called simple rule of mixtures

$$T_g = \varphi_1 T_{g,1} + (1 - \varphi_1) T_{g,2} \quad (5)$$

both possessing the advantage that only T_g values for pure components are needed in the calculations. Theoretical predictions of the $T_g(\varphi)$ pattern are also possible through the Couchman-Karasz equation,[29]

$$lnT_g = \frac{x_1 \Delta C_{p,1} lnT_{g,1} + \Delta C_{p,2}(1-x_1) lnT_{g,2}}{x_1 \Delta C_{p,1} + (1-x_1)\Delta C_{p,2}} \quad (6)$$

in which, x_i and $\Delta C_{p,i}$ are, respectively, the molar fraction and the difference in the heat capacity of the liquid and the heat capacity of the glass forms. Unfortunately, the application of the above mentioned functions in binary pharmaceutical compound + polymer systems lead to smooth, monotonous $T_g(\varphi)$ dependences, that as a rule, either substantially overestimate[18,23,38-43] or underestimate[24,44-46] the experimental ones.

Better in terms of representing strong or asymmetric shapes of $T_g(\varphi)$ diagrams, including a few types of S-shaped dependencies, appears to be the Kwei equation,[30]

$$T_g = \frac{\varphi_1 T_{g,1} + k_{Kw}(1-\varphi_1) T_{g,2}}{\varphi_1 + k_{Kw}(1-\varphi_1)} + q\varphi_1(1-\varphi_1) \quad (7)$$

This contains beyond Eq. (1) a quadratic term after rearrangement, and an empirical interaction-dependent parameter (q). Conformational entropy changes upon mixing are believed to be accounted for by addition of higher-order terms such as those appearing in the Brekner-Schneider-Cantow (BSC) equation,[31,33]

$$T_g = T_{g,1} + (T_{g,2} - T_{g,1})[(1+K_1)\varphi_{2c} - (K_1 + K_2)\varphi_{2c}^2 + K_2 \varphi_{2c}^3] \quad (8)$$

with

$$\varphi_{2c} = k\varphi_2 / (\varphi_1 + k\varphi_2); \; k \approx T_{g,1} / T_{g,2} \quad (9)$$

Parameter K_1 mainly accounts for the differences between the interaction energies of the binary heteromolecular and homomolecular interactions, while parameter K_2 is considered to comprise energetic effects induced by conformational changes (i.e., contributions from conformational entropy changes due to hetero-contact formation). Both parameters contain different amounts of both enthalpic and entropic contributions rendering difficult a straightforward interpretation of their values.

In spite of this, poor representation of experimental patterns is regularly reported in cases of non-random mixing; specific interactions leading to both composition-dependent enthalpic and entropic changes are the source of highly irregular $T_g(\varphi)$ patterns.[25,47-49] The above problems led us to development of the simpler formula

$$T_g = \varphi_1 T_{g,1} + (1 - \varphi_1) T_{g,2} + \varphi_1(1 - \varphi_1)[a_0 + a_1(2\varphi_1 - 1) + a_2(2\varphi_1 - 1)^2] \qquad (10)$$

hereafter denoted as BCKV equation.[34] The quadratic polynomial on its right side, centered around $2\varphi_1 - 1 = 0$, is defined to represent deviations from linearity; i.e., with $a_0 = a_1 = a_2 = 0$, the equation leads to the simple rule of mixtures. Equation (10) transforms to the Jenckel-Heusch equation[50] when only $a_0 \neq 0$. The type and level of the observed deviation is primarily described by parameter a_0, while parameters a_1 and a_2 reflect the strength of asymmetric contributions. Based on comparisons among the fitting results obtained for numerous binary polymer systems,[35,47] , using equation (10) and previous $T_g(\varphi)$ functions, the empirical parameter a_0 and its normalized form, $a_0/\Delta T_g$ ($\Delta T_g = \Delta T_{g,2} - T_{g,1}$), mainly reflects differences between the interaction energies of the hetero- (intercomponent) and homo- (intracomponent) interactions. In proof of that,

dependencies have been established among a_0 and the prime parameters of the most common fitting functions (e.g., K_{GT} or q)[47]. The magnitude and sign of the higher-order fitting parameters of equation (10) is in part related to the system- and composition-dependent energetic contribution of hetero-contacts, entropic effects and structural nanoheterogeneities (e.g., nanocrystalline phases) observed in some blend compositions .[35,47] Therefore, the number and magnitude of the adjustable parameters required to represent an experimental $T_g(\varphi)$ pattern provide quantitative measures of system's complexity.

5.3 Materials and methods

5.3.1 *Materials*

Carvedilol and nevirapine were provided by Aurobindo Pharma (Hyderabad, India) as gift samples (Table 5.1). Nimodipine was obtained as a gift sample from Sun Pharmaceuticals (Vadodara, India). Itraconazole was procured from Letco Medical (Decatur, AL, USA). Plasdone S-630 copovidone was provided as a research sample by ISP technologies (Wayne, NJ, USA).

5.3.2 *Sample Preparation*

Drug and polymer physical mixtures were prepared in 1.0 g quantities by geometrical mixing in various ratios and further vortex mixed for 2 - 3 minutes. Prior to measurements, the samples were stored at room temperature in glass vials placed in desiccators, containing silica gel or P_2O_5. Solid dispersions of the different samples were prepared within the differential scanning calorimeter, by melting the physical mixtures in

the course of the first heating scan, performed from room temperature to 200 – 270 ^{o}C (heating rate 10 ^{o}C/min), and subsequently cooling the melt to -20 ^{o}C at a rate 5 ^{o}C/min.

5.3.3 Density Measurements

The true density of the samples was determined (in duplicate) using a gas displacement pycnometer (model no. Accupyc 1330, Micromeritics, Norcross, GA).

5.3.4 Fourier-Transform Infrared Spectroscopy

Infrared spectra of selected dried samples were obtained using an FT-IR apparatus (Nicolet IR 100, Thermo Scientific, USA). The formulation sample was mixed with 100 fold KBr for preparing the pellets. The final spectra were composed of 128 scans performed in range 400 - 4000 cm^{-1} with 2 cm^{-1} resolution.

5.3.5 *Differential Scanning Calorimetry*

Thermal events were studied using a Q200 differential scanning calorimeter (TA Instruments, New Castle, DE, USA) with a refrigeration cooling system (RCS) in a standard mode. Nitrogen was the purge gas at a flow rate of 50 ml/min. The samples (6 - 10 mg) were weighed in aluminum pans and subjected to heat-cool-heat cycle for the T_g determination. The single T_g values reported here correspond to the midpoint temperature of the heat capacity change recorded during the 2nd heat cycle (averages of at least 2 measurements). The scanning rate employed was 10 ^{o}C/min for heating and 5^{o}C/min for cooling. Scanning temperature range was from 25 ^{o}C to 200 ^{o}C and then from 200 ^{o}C to -20 ^{o}C, and finally from -20 ^{o}C to 200 ^{o}C. In the case of Nevirapine the samples were

heated up to 270 ^{o}C because the drug melting point is near 240 ^{o}C.

5.4 Results and Discussion

5.4.1 *Excess volumes*

Figure 5.1a shows the results of the true density measurements performed for the pure drugs, the amorphous polymer, and their mixtures. The data reveal a drastic positive deviation of the experimental densities from the expected mass-averaged linear density variation. A more meaningful representation of the data emerges by plotting the excess volume of mixing per g of the sample mass (Figure 5.1b),

$$V^{E} = V_{exp} - V_{lin} \qquad (11)$$

where the experimental and linear specific volumes were obtained using the relations $V_{exp} = 1/\rho$ and $V_{lin} = \varphi_1/\rho_1 + (1 - \varphi_1)/\rho_2$, respectively (subscripts: 1 for drug, 2 for PLS-630).

A persistently negative excess mixing volume is seen throughout the entire range of blend compositions. With the exception of the NEV + PLS-630 system, the maximal *structural contraction* is attained at early stages of drug's addition (φ_{drug} up to 0.2). Two effects are presumed to act here. The first is penetration of the drug into structural microscopic voids in the structure of the neat polymer; $V^{E} < 0$ is the result, apparently a dominating effect. Partial amorphization of initially crystalline drug should result in $V^{E} > 0$, apparently a minor effect here.

5.4.2 *FT-IR analysis*

Components miscibility and thermal stability in binary polymer-containing systems are usually related to strong specific interactions, namely hydrogen-bonding (δH)

and ionic ones. Molecular structures of our chemicals suggest the formation of δH interactions between some of our drug molecules (acidic N-H and O-H groups in CVD; N-H groups in NEV and NMP; no H^+ donor groups in ITZ) and the polymeric component (basic C=O groups in PLS-630 copovidone).

In Figure 5.2 we show FT-IR spectra of pure CVD, PLS-630, and their 1:1 *physical mixture* (PM) and *solid dispersion* (SD). We note the carbonyl stretching region (1500 – 1800 cm^{-1}) and the OH and NH stretching region (3150 – 3450 cm^{-1}). Carvedilol has three H^+ donor groups per molecule (as contrasted to nought or one acidic group in the other compounds), which can interassociate with either the cyclic amide C=O groups of vinyl pyrrolidone or the C=O groups of vinyl acetate monomers in Copovidone. Irrespective of the type of mixing (PM or SD), the spectral position of the skeleton stretching vibrations of the C=C bonds [ν(C=C) at 1504, 1591 and 1608 cm^{-1}] in the aromatic ring of Carvedilol (1502 – 1608 cm^{-1} region), as well as the C-H stretching vibrations (3000 – 3100 cm^{-1}) and the out-of-plane or in-plane aromatic bending vibrations (at lower wavenumbers,[51] not shown here for brevity) remain unaffected by polymer addition. More importantly, in the physical mixtures, no changes in the NH [ν(NH) at 3308 cm^{-1}] and OH [ν(OH) at 3346 cm^{-1}] stretching vibration frequencies of CVD appear in the 3150 – 3450 cm^{-1} region. These bands are relatively weak, suggesting a limited degree of interactions of the proton donating groups of carvedilol (>NH and -OH) and the proton accepting carbonyls in PLS-630. We note, however, a clear split of the dual C=O stretching vibration signal of Copovidone - apparent only in the physical mixture. In the solid dispersion, the 3308 cm^{-1} and 3346 cm^{-1} bands of the drug complex disappear completely, apparently reflecting strong intercomponent interactions.

The vibrational spectra of Nevirapine (Fig. 5.3) are also of interest. One expects a competition of the C=O groups present both in copovidone and NEV for hydrogen bonding interaction with proton accepting NH groups in the drug. Thus, a drastic weakening of the broad NH stretching mode of NEV, ν(NH) observed at 3190 cm^{-1}, is seen in the solid dispersion environment. An analogous conclusion can be extracted from spectral shifts of characteristic deformation signals. Ayala et al.[52] report that a band ascribed to out-of-plane deformation of the NH and the C=O bonds, calculated using density functional theory methods to appear at 726 cm^{-1}, shifts to 804 cm^{-1} as a result of hydrogen bonding and the formation of centrosymmetric molecular dimers. The 804 cm^{-1} band is present in pure NEV and its 1:1 physical mixture, but disappears in the solid dispersion (the diagram not shown here for brevity). The NEV band placed around 3300 cm^{-1} (previously assigned to the first overtone of the ν(C=O) band at 1650 cm^{-1}) completely vanishes in the solid dispersion while there is a strong overlap of the C=O bands in the 1500 – 1800 cm^{-1} region. The hydroxyl band, with ν(OH) at 3503 cm^{-1}, characteristic of the pseudo-polymorphic (hemihydrate) crystalline form of NEV,[52] is absent in our spectra. Therefore, the crystalline fraction of the drug in both the physical mixes and the solid dispersions is most likely organized in the anhydrous (Type I) crystalline form.

5.4.3 DSC results

A general feature of the second heating DSC traces for our blends is the presence of a single glass transition signal at each blend composition; in immiscible systems one would detect two glass transitions. We recall that a T_g value is merely a convenient

representation of a temperature range, and that the glass transition is not a first order transition (Paul Ehrenfest terminology). The above observation suggests *nonequilibrium* miscibility in all systems and compositions under study. The term "nonequilibrium" underlines the fact that below T_g the stability of such solid dispersions relies heavily on the kinetics of phase separation and/or crystallization instead of thermodynamics.[53] In the glassy state ($T \leq T_g$), molecular mobilities are drastically suppressed; polymer chain conformations are practically frozen to a nonequilibrium "high energy" state and drug's (re)crystallization proceeds slowly.[53,54]

Compositional variation of the respective glass transition temperatures is displayed in Figure 5.4. The curves have been obtained using Eqs. (1), (7), (8) and (10); given complex shapes of $T_g(\varphi)$ diagrams, other equations were not usable. The respective parameters and the coefficients of determination (R-square) are listed in Table 5.2. These were obtained by applying a Levenberg-Marquardt least-square minimization routine to the experimental data. The GT equation falls short in describing the strongly s-shaped diagrams for solid dispersions of ITZ, NEV and CVD in PLS-630. The situation slightly improves in the case of the NMP + PLS-630 blend, where the fitting estimate of k_{GT} = 0.74 is (within the limits of error) close to its 'theoretical' value k_{GT} (and k_{kw}) $\approx \rho_1 T_{g,1}/\rho_2 T_{g,2}$ = 0.78. Similar arguments apply also in the case of the Kwei equation. Somewhat better results are obtained using the BSC formula, with the BCKV function providing the highest accuracy in all systems.

The parameters k_{GT}, q (Kwei equation) and a_0 (BCKV equation) progressively decrease in the order: ITZ > NMP > NEV ≥ CVD. These parameters are considered semi-quantitative measures of the strength of intercomponent interactions,[35] without excluding

possible contributions of entropic factors (e.g., the presence of heterogeneities in chains' packing and conformations, and in large local-density fluctuations).[47] Given the differences in ΔT_g (= $T_{g,2} - T_{g,1}$), a more representative indicator of the degree of deviation from linearity is obtained comparing the (dimensionless) reduced $a_0/\Delta T_g$ estimates (Table 5.2). The maximal positive deviation from the rule of mixtures is observed in the ITZ + PLS-630 system (a_0, $a_0/\Delta T_g > 0$), at a very low drug loading (denoted by the $a_1 << 0$ estimate); this is consonant with the highly negative excess mixing volume (V^E) observed in the same compositional region (Fig. 5.1b). In other words, improved packing hinders movements of polymeric chains and pushes glass transition temperatures upwards. In the other systems with $a_0 < 0$, the maximal negative deviation is observed at high drug loading (again $a_1 \neq 0$). Maximal negative deviation is observed in the dispersions of nevirapine, while the nimodipine solid dispersions demonstrate a behavior very close to the simple rule of mixtures (i.e., $a_0/\Delta T_g$ approaches zero). In general at high drug loadings, blend's T_g remains close to $T_{g,drug}$ (= $T_{g,1}$). This is a rather common and not clearly understood behavior encountered in drug + polymer molecular dispersions[23,24,38,39] and is in part reflected also in large values of our a_2 parameter.

In miscible binary blends the melting point T_m of the crystalline component is usually lower than in pure phase. This is expected due to both morphological and thermodynamic reasons. The former class of reasons comprises changes in the crystal lamella thickness caused by blending, changes in the degree of crystallinity and in physical nature of the amorphous phase surrounding the lamellae. The latter relates to the strength of interactions among blend components. Melting point depression in our

systems is clearly demonstrated in Figure 5.5a; it is fairly strong in the mixtures comprising ITZ and NEV and weaker in the CVD or NMP containing mixtures. This suggests a satisfactory degree of mixing among blend components and probably sufficient short-term inhibition of crystallization. The results shown in this figure pertain to physical mixtures, since our solid dispersions are formed by powder's consolidation during the subsequent first cooling scan. The importance of the latter observation lays in our ability to accomplish even more effective long-term crystallization inhibition by using more elaborate mixing techniques (such as spin casting or hot-melt extrusion). There are methods of calculation of equilibrium melting diagrams in terms of the Flory-Huggins-Staverman interaction parameter χ_{12}, but these methods are not very accurate[53,55] Flory himself proposed a better model of thermodynamic behavior of mixtures taking into account equation of state contributions[36] – a model which provides results of better accuracy, but requires more data[56] Our melting point depression results suggest $\chi_{12} \leq 0$ (i.e. appreciable attraction between the components) - in agreement with the composition-dependent single-T_g diagrams in our systems.

Amorphous solid dispersions should be prepared preferably at a drug concentration below the solid solubility of its crystalline form, so as to achieve a homogeneous dispersion. If that solubility limit is exceeded, the drug may undergo crystal growth upon storage leading to physical instability of the amorphous solid dispersions[57]A first indication of polymer's influence on drug crystallization can be extracted by considering the compositional variation of the apparent melting enthalpies ΔH_m per g of sample obtained from the first heating DSC scans. The percentage of drug that remains crystalline in each mixture, $w_{c,drug}$, can be calculated as

$$w_{c,drug} = \frac{\Delta H_m}{\Delta H_m^0} \frac{100}{\varphi_{drug}} (\%) \qquad (12)$$

Where $\Delta H_m{}^0$ is the apparent (extrapolated) melting enthalpy per 1 g of fully crystalline pure drug. The results obtained using Eq. (12) are presented in Figure 5.5b. As expected, the degree of crystallinity of the drug in the freshly prepared drug + polymer physical mixes goes down with increasing concentration of the polymer.

For majority of our blends studied by DSC, no exothermic or endothermic peaks are seen during cooling or the second heating cycle. Thus, the cooling rate of 5 ^{o}C/min is in most cases sufficiently high to prevent drug recrystallization on the timescale of the DSC experiment. An exception is pure nevirapine and some of its blends, which demonstrate a series of rather complex and strongly composition-dependent thermal events. These include a cold crystallization exothermic peak in the 1:1 mixture, broad melting peaks during the first heating scan (particularly for 1:4 and 4:1 drug-to-polymer weight ratios), and crystallization exotherms and melting endotherms during the second heating scan (in pure NEV and in the 1:1 blend only). Evidently, the low rigidity provided by the polymeric component in its blends with nevirapine (in this case ΔT_g = $T_{g(PLS\text{-}630)} - T_{g(NEV)} \approx +9$ K only) allows for an enhanced drug molecule mobility and easier organization into crystalline phases at low cooling rates. The latter adversely affects drug's solubility; thus, PLS-630 is not a good encapsulant in this case in pharmaceutical oral drug-delivery systems, whether tablets or granules.

The glass transition temperature *vs*. composition dependencies determined here for materials prepared by the fusion method can be combined with previously published results for molecular dispersions prepared by other techniques.[23,24,38,46,48] In Figure 5.6

we show $T_g(\varphi)$ relations for solid dispersions of a model drug MK-0591, Sucrose, indomethacin, itraconazole, efavirenz and loperamide drugs in various grades of P(VP-*co*-VA) copolymers, and results of the use of the BCKV Eq. (10). The first three blends were prepared using the solvent evaporation technique, the following two using the hot-melt extrusion method and the latter by spray drying of appropriate solutions. The parameters obtained using equations (8) and (10) are provided in Table 5.3. The issue of drug + polymer interactions has been considered by various research groups (e.g. Nair and coworkers[42] and McGinity and collaborators).[41,43] . The present results indicate that the occurrence of a high number of proton donor sites in the drug molecule is not mandatory for achieving miscibility and crystallization inhibition. For example, $a_0 > 0$ and miscibility is verified in the case of the MK-0591, EFV and ITZ solid dispersions with P(VP-*co*-VA) copolymers – in which no (or only one per drug molecule) intermolecular hydrogen bonds are possible. From the fitting data included in tables 5.2 and 5.3, it appears that for the dispersions obtained with EFV and ITZ entropic effects supply the major contribution to the observed miscibility; both $a_1/\Delta T_g$ and K_2 are negative, while the parameters conveying the strength/influence of enthalpic factors are near zero ($a_0/\Delta T_g$) or even negative (K_1). In the other system, the ion-dipole interaction between the COO^-Na^+ group of MK-0591 and the cyclic amide group of vinyl pyrrolidone monomer promotes miscibility and drug crystallization inhibition; K_1, K_2, and $a_0/\Delta T_g > 0$, in agreement with the above explanation. On the other hand, in the case of the sucrose mixtures hydrogen bonding interactions have been verified by FT-IR spectroscopy studies, while we have a strongly negative $a_0/\Delta T_g$. In this case the magnitude of negative deviation is apparently determined by entropic effects, which

counterbalance components' interassociation. In proof of that, Shamblin et al.[38] report $V^E > 0$, of the order of 0.1 – 1 %. The antiplasticizing effect of the polymer matrix has been reported to account for the achieved miscibility and crystallization inhibition in the completely amorphous loperamide + P(VP-*co*-VA) solid dispersions, in which δH bonds are absent.[26] As seen above, our approach relies particularly on the dependence of glass transition temperatures on composition. The knowledge of $T_g(\varphi)$ relations as embodied by parameters of Eq. (10), their signs and magnitudes, allows quantification of usability of a given polymer as an encapsulant for a given drug.

5.5 References

1. Rasenack N, Mueller BW. 2002. Dissolution Rate Enhancement by in Situ Micronization of Poorly Water-Soluble Drugs. Pharm Res 19(12):1894-1900.
2. Liversidge GG, Cundy KC. 1995. Particle size reduction for improvement of oral bioavailability of hydrophobic drugs: I. Absolute oral bioavailability of nanocrystalline danazol in beagle dogs. Int J Pharm 125(1):91-97.
3. Brewster ME, Loftsson T, Estes KS, Lin JL, Fridriksdottir H, Bodor N. 1992. Effect of various cyclodextrins on solution stability and dissolution rate of doxorubicin hydrochloride. Int J Pharm 79(2-3):289-299.
4. Sathigari S, Chadha G, Phillip LYH, Wright N, Parsons DL, Rangari VK, Fasina O, Babu RJ. 2009. Physicochemical characterization of efavirenz-cyclodextrin inclusion complexes. AAPS PharmSciTech 10(1):81-87.
5. Kennedy M, Hu J, Gao P, Li L, Ali-Reynolds A, Chal B, Gupta V, Ma C, Mahajan N, Akrami A, Surapaneni S. 2008. Enhanced Bioavailability of a Poorly

Soluble VR1 Antagonist Using an Amorphous Solid Dispersion Approach: A Case Study. Mol Pharm 5(6):981-993.

6. Joshi HN, Tejwani RW, Davidovich M, Sahasrabudhe VP, Jemal M, Bathala MS, Varia SA, Serajuddin ATM. 2004. Bioavailability enhancement of a poorly water-soluble drug by solid dispersion in polyethylene glycol-polysorbate 80 mixture. Int J Pharm 269(1):251-258.
7. Han HK, Choi HK. 2007. Improved absorption of meloxicam via salt formation with ethanolamines. Eur J Pharm Biopharm 65(1):99-103.
8. Gwak HS, Choi JS, Choi HK. 2005. Enhanced bioavailability of piroxicam via salt formation with ethanolamines. Int J Pharm 297(1-2):156-161.
9. Balakrishnan A, Rege BD, Amidon GL, Polli JE. 2004. Surfactant-mediated dissolution: Contributions of solubility enhancement and relatively low micelle diffusivity. J Pharm Sci 93(8):2064-2075.
10. Viernstein H, Weiss-Greiler P, Wolschann P. 2003. Solubility enhancement of low soluble biologically active compounds-temperature and cosolvent dependent inclusion complexation. Int J Pharm 256(1-2):85-94.
11. Blagden N, de Matas M, Gavan PT, York P. 2007. Crystal engineering of active pharmaceutical ingredients to improve solubility and dissolution rates. Adv Drug Deliv Rev 59(7):617-630.
12. Janssens S, De Zeure A, Paudel A, Van Humbeeck J, Rombaut P, Van den Mooter G. Influence of preparation methods on solid state supersaturation of amorphous solid dispersions: a case study with itraconazole and eudragit e100. Pharm Res 27(5):775-785.

13. Qian F, Huang J, Hussain MA. Drug-polymer solubility and miscibility: Stability consideration and practical challenges in amorphous solid dispersion development. J Pharm Sci 99(7):2941-2947.
14. Hancock BC, Zografi G. 1997. Characteristics and significance of the amorphous state in pharmaceutical systems. J Pharm Sci 86:1-12.
15. Craig DQ. 2002. The mechanisms of drug release from solid dispersions in water-soluble polymers. Int J Pharm 231(2):131-144.
16. Yang J, Grey K, Doney J. 2010. An improved kinetics approach to describe the physical stability of amorphous solid dispersions. Int J Pharm 384(1-2):24-31.
17. Sinha S, Baboota S, Ali M, Kumar A, Ali J. 2009. Solid dispersion: An alternative technique for bioavailability enhancement of poorly soluble drugs. J Dispersion Sci Technol 30:1458-1473.
18. Marsac PJ, Rumondor AC, Nivens DE, Kestur US, Stanciu L, Taylor LS.2010. Effect of temperature and moisture on the miscibility of amorphous dispersions of felodipine and poly(vinyl pyrrolidone). J Pharm Sci 99(1):169-185.
19. Van den Mooter G, Wuyts M, Blaton N, Busson R, Grobet P, Augustijns P, Kinget R. 2001. Physical stabilisation of amorphous ketoconazole in solid dispersions with polyvinylpyrrolidone K25. Eur J Pharm Sci 12(3):261-269.
20. Hancock BC, Shamblin SL, Zografi G. 1995. Molecular mobility of amorphous pharmaceutical solids below their glass transition temperatures. Pharm Res 12(6):799-806.

21. Di Martino P, Joiris E, Gobetto R, Masic A, Palmieri GF, Martelli S. 2004. Ketoprofen-poly(vinylpyrrolidone) physical interaction. J Cryst Growth 265:302-308.

22. Taylor LS, Zografi G. 1997. Spectroscopic characterization of interactions between PVP and indomethacin in amorphous molecular dispersions. Pharm Res 14(12):1691-1698.

23. Matsumoto T, Zografi G. 1999. Physical properties of solid molecular dispersions of indomethacin with poly(vinylpyrrolidone) and poly(vinylpyrrolidone-co-vinyl-acetate) in relation to indomethacin crystallization. Pharm Res 16(11):1722-1728.

24. Khougaz K, Clas SD. 2000. Crystallization inhibition in solid dispersions of MK-0591 and poly(vinylpyrrolidone) polymers. J Pharm Sci 89(10):1325-1334.

25. Konno H, Taylor LS. 2006. Influence of different polymers on the crystallization tendency of molecularly dispersed amorphous felodipine. J Pharm Sci 95(12):2692-2705.

26. Weuts I, Kempen D, Decorte A, Verreck G, Peeters J, Brewster M, Van den Mooter G. 2004. Phase behaviour analysis of solid dispersions of loperamide and two structurally related compounds with the polymers PVP-K30 and PVP-VA64. Eur J Pharm Sci 22(5):375-385.

27. Gordon M, Taylor JS. 1952. Ideal copolymers and the second-order transitions of synthetic rubbers I. Noncrystalline copolymers. J Appl Chem 2:493-500.

28. Fox GT. 1956. Influence of diluent and of copolymer composition on the glass temperature of a polymer system. Bull Am Phys Soc 1:123.

29. Couchman PR, Karasz FE. 1978. Classical thermodynamic discussion of effect of composition on glass transition temperatures. Macromolecules 11(1):117-119.
30. Kwei TK. 1984. The effect of hydrogen bonding on the glass transition temperatures of polymer mixtures. J Polym Sci Lett 22:307-313.
31. Brekner MJ, Schneider HA, Cantow HJ. 1988. Approach to the composition dependence of the glass transition temperature of compatible polymer blends 2: The effect of local chain orientation. Makromol Chem 189:2085-2097.
32. Kovacs AJ. 1963. Adv. Polym. Sci 3:394-507.
33. Schneider HA. 1997. Conformational entropy contributions to the glass temperature of blends of miscible polymers. J Res Natl Inst Stand Technol 102(2):229-248.
34. Brostow W, Chiu R, Kalogeras IM, Vassilikou-Dova A. 2008. Prediction of glass transition temperatures: binary blends and copolymers. Mater Lett 62:3152-3155.
35. Kalogeras IM, Brostow W. 2009. Glass transition temperatures in binary polymer blends. J Polym Sci Phys 47:80-95.
36. Flory PJ. 1985. Selected Works, Vol. 3, Stanford University Press.
37. Brostow W. 2009. Reliability and prediction of long-term performance of polymer blend materials. Pure & Appl Chem 81(3):417-432.
38. Shamblin SL, Taylor LS, Zografi G. 1998. Mixing behavior of colyophilized binary systems. J Pharm Sci 87(6):694-701.
39. Shamblin SL, Huang EY, Zografi G. 1996. The effects of co-lyophilized polymer additives on the glass transition temperature and crystallization of amorphous sucrose. J Thermal Anal 47:1567-1579.

40. Berggren J, Alderborn G. 2003. Effect of polymer content and molecular weight on the morphology and heat- and moisture-induced transformations of spray-dried composite particles of amorphous lactose and poly(vinylpyrrolidone). Pharm Res 20(7):1039-1046.

41. Wu C, McGinity JW. 2001. Influence of ibuprofen as a solid-state plasticizer in Eudragit RS 30 D on the physicochemical properties of coated beads. AAPS PharmSciTech 2(4):24.

42. Nair R, Nyamweya N, Gonen S, Martinez-Miranda LJ, Hoag SW. 2001. Influence of various drugs on the glass transition temperature of poly(vinylpyrrolidone): a thermodynamic and spectroscopic investigation. Int J Pharm 225(1-2):83-96.

43. Omelczuk MO, McGinity JW. 1992. The influence of polymer glass transition temperature and molecular weight on drug release from tablets containing poly(DL-lactic acid). Pharm Res 9(1):26-32.

44. Marsac PJ, Konno H, Taylor LS. 2006. A comparison of the physical stability of amorphous felodipine and nifedipine systems. Pharm Res 23(10):2306-2316.

45. Andrews GP, AbuDiak OA, Jones DS.2010. Physicochemical characterization of hot melt extruded bicalutamide-polyvinylpyrrolidone solid dispersions. J Pharm Sci 99(3):1322-1335.

46. Six K, Verreck G, Peeters J, Brewster M, Van Den Mooter G. 2004. Increased physical stability and improved dissolution properties of itraconazole, a class II drug, by solid dispersions that combine fast- and slow-dissolving polymers. J Pharm Sci 93(1):124-131.

47. Kalogeras IM. 2010. Description and molecular interpretation of anomalous compositional dependence of the glass transition temperatures in binary organic mixtures. Thermochim Acta 509:135-146.

48. Babu RJ, Brostow W, Kalogeras IM, Sathigari S. 2009. Glass transition in binary drug + polymer systems. Mater Lett 63:2666-2668.

49. Albers J, Alles R, Matthee K, Knop K, Nahrup JS, Kleinebudde P. 2009. Mechanism of drug release from polymethacrylate-based extrudates and milled strands prepared by hot-melt extrusion. Eur J Pharm Biopharm 71(2):387-394.

50. Jenckel E, Heusch R. 1953. Lowering the freezing temperature of organic glasses with solvents. Kolloid-Z 130:89-105.

51. Jagannathan L, Meenakshi R, Gunasekaran S, Srinivasan S. 2010. FTIR-FT-Raman and UB-vis spectra and quantum chemical investigation of carvedilol. Molec Simulat 36(4):283-290.

52. Ayala AP, Siesler HW, Wardell SMSV, Boechat N, Dabbene V, Cuffini SL. 2007. Vibrational spectra of antiretroviral drugs: nevirapine. Mol struct 828(1-3):201-210.

53. Qian F, Huang J, Hussain MA. 2010. Drug-polymer solubility and miscibility: Stability consideration and practical challenges in amorphous solid dispersion development. J Pharm Sci 99(7):2941-2947.

54. Tao J, Sun Y, Zhang GG, Yu L. 2009. Solubility of small-molecule crystals in polymers: D-mannitol in PVP, indomethacin in PVP/VA, and nifedipine in PVP/VA. Pharm Res 26(4):855-864.

55. Cheung W, Stein RS. 1994. Critical analysis of the phase behavior of poly (.epsilon-capralactone) (PCL) 1 polycarbonate (PC) blends. Macromolecules 27(9):2512-2519.

56. Brostow W. 1971. Macromolecules 4:742.

57. Huang J, Wigent RJ. 2009. Determination of drug and polymer miscibility and solid solubility for design of stable amorphous solid dispersion. Am Pharm Rev 12:18-26.

Table 5.1 Densities ρ, molecular masses M_w, glass transition temperatures T_g, changes ΔC_p in heat capacities at T_g, melting temperatures T_m and enthalpies ΔH_m, and molecular structures of the chemicals.

Chemical	**ρ (g/cm^3)**	**H$^+$ donor Sites**	**H$^+$ acceptor sites [(a)]**	***M*$_w$ (g/mol)**	***T*$_g$ (K) [(b)]**	**Δ*C*$_p$ (J/g ^{o}C)**	***T*$_m$ (K) [(b)]**	**Δ*H*$_m$ (J/g)**	**Molecular structure**
Plasdone S-630 copovidone (PLS-630)	1.162	0	2	24,000 – 30,000	371.2	2.52	-	-	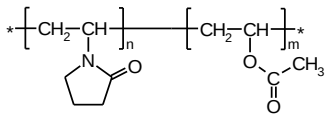
Nevirapine (NEV)	1.387	1	5	266.3	362.3	5.01	518.5	1388	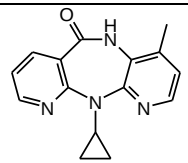
Itraconazole (ITZ)	1.352	0	14	705.6	331.5	3.77	440.4	819	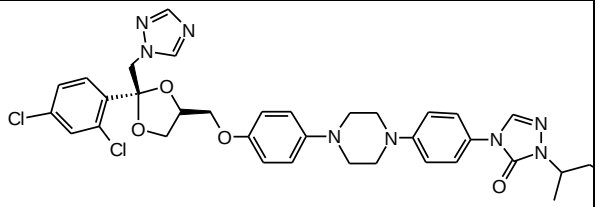
Carvedilol (CVD)	1.275	3	6	406.5	313.9	9.31	388.6	1148	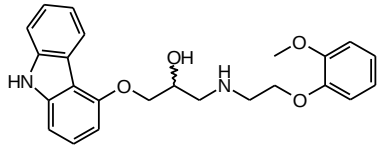
Nimodipine (NMP)	1.275	1	9	418.4	288.3	4.78	397.7	916	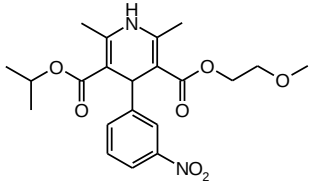

(a) For PLS-630 the number refers to H$^+$ acceptor sites per VP and VA monomer (see following discussion).

(b) The standard deviation in the measurement of T_g or T_m is within ± 0.5 K.

Table 5.2 Parameters of the $T_g(\varphi)$ equations and coefficient of determination (R-square) values.

Equation	**Drug molecule**			
	ITZ	**NMP**	**NEV**	**CVD**
GT				
k_{GT}	1.6 ± 0.8	0.74 ± 0.07	0.10 ± 0.12	0.56 ± 0.12
R^2	0.9042	0.9914	0.6921	0.9588
Kwei				
k_{kw}	0.89	0.78	0.98	0.85
q	30.9 ± 17.7	-6.5 ± 7.8	-23.4 ± 1.9	-31.0 ± 10.0
R^2	0.9140	0.9937	0.9634	0.9699
BSC				
K_1	-1.51 ± 0.24	-0.43 ± 0.17	-3.4 ± 0.5	-1.54 ± 0.15
K_2	-4.52 ± 0.42	-0.73 ± 0.31	-1.9 ± 1.1	-2.26 ± 0.30
K_1 - K_2	3.01	0.30	-1.50	0.72
R^2	0.9967	0.9968	0.9758	0.9968
BCKV				
a_0	14.4 ± 4.2	-18.3 ± 4.2	-25.6 ± 1.2	-44.7 ± 3.2
a_1	-89.7 ± 6.9	-30.2 ± 6.5	-7.3 ± 2.6	-56.0 ± 5.5
a_2	42.0 ± 14.0	-40.8 ± 13.2	23.8 ± 6.1	51.0 ± 11.0
$a_0/\Delta T_g$	+0.363	-0.221	-2.876	-0.780
$a_1/\Delta T_g$	-2.259	-0.364	-0.820	-0.977
R^2	0.9982	0.9994	0.9949	0.9989

Table 5.3 Mixture information and curve-fitting results for the parameters incorporated in the BCKV equation for literature data on *solid dispersions* of pharmaceutical compounds in P(VP-*co*-VA) copolymers (with T_gs in the range 368 – 384 K).

Drug	$T_{g,drug}$ **(K)**	**Functional groups**		**BSC parameters**			**BCKV parameters**					
		H^+ donor sites	**H^+ acceptor Sites**	K_1	K_2	R^2	a_0	a_1	a_2	$a_0/\Delta T_g$	$a_1/\Delta T_g$	R^2
MK-0591 [11]	401.8	0	5	1.07 ± 0.25	0.43 ± 0.41	0.9902	19.0 ± 1.8	0	-15.3 ± 8.5	0.873	0	0.9927
Efavirenz (EFV) [34]	306.1	1	3	-0.4 ± 0.2	-0.9 ± 0.1	0.9971	8 ± 1	-32 ± 3	-39 ± 7	0.129	-0.516	1
Itraconazole (ITZ) [32]	332.4	0	12	-0.13 ± 0.06	-0.65 ± 0.11	0.9952	5.6 ± 0.8	-16.6 ± 2.1	0	0.114	-0.339	0.9997
Indomethacin (IND) [4]	315	1	5	0.07 ± 0.05	0	0.9961	-6.4 ± 3.0	0	0	-0.107	0	0.9961
Loperamide (LOP) [13]	342	1	4	-0.28 ± 0.05	0	0.9932	-19.1 ± 2.7	0	18.6 ± 12.4	-0.455	0	0.9947
Sucrose (SUC) [25]	348	8	11	-1.66 ± 0.24	-1.38 ± 0.46	0.9831	-35.1 ± 2.4	-15.3 ± 4.8	39.3 ± 10.7	-1.210	-0.531	0.9921

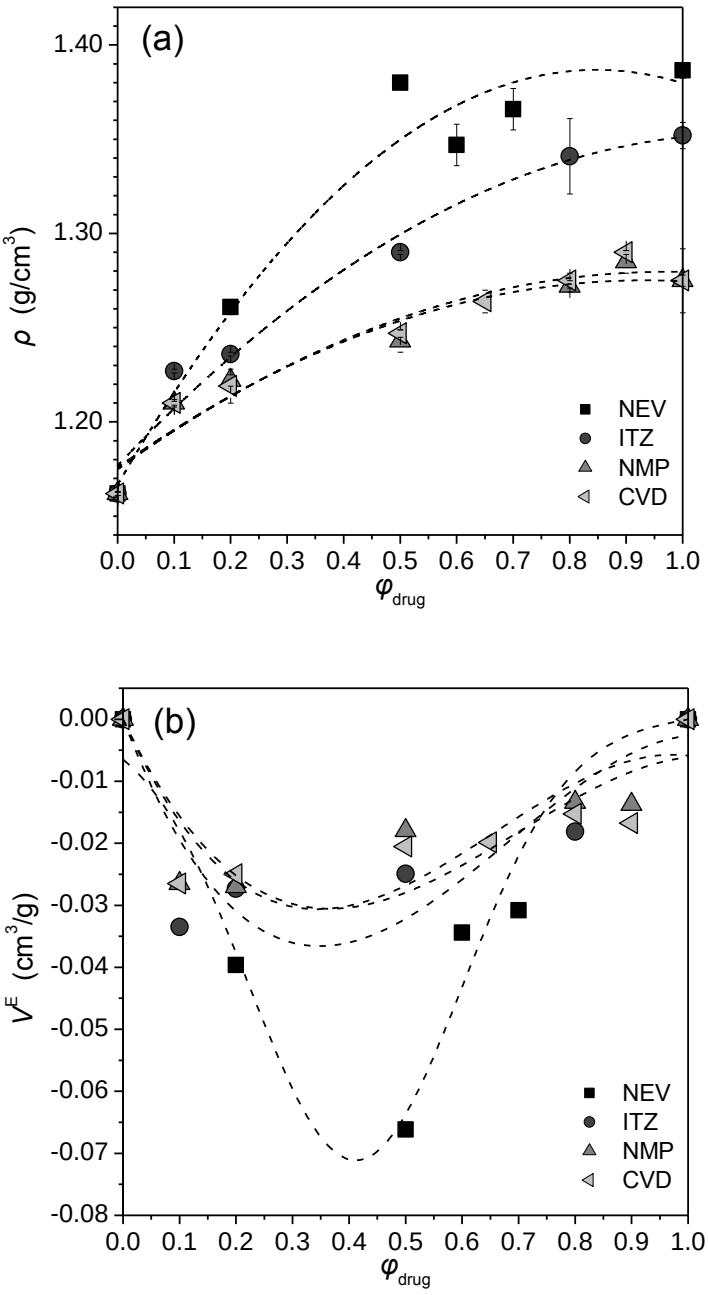

Figure 5.1 Compositional variation of: (a) mixtures density, and (b) the excess mixing volume per gram of sample's mass. The bars account for the standard deviation of the data.

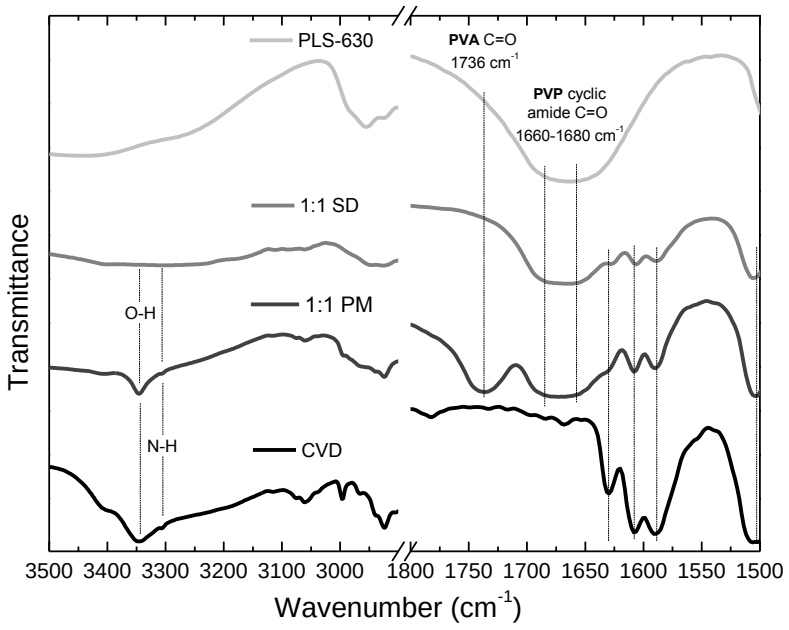

Figure 5.2 Part of the FT-IR spectra recorded for CVD, PLS-630, and the physical mixture (PM) and solid dispersion (SD) of the 1:1 CVD + PLS-630 composition.

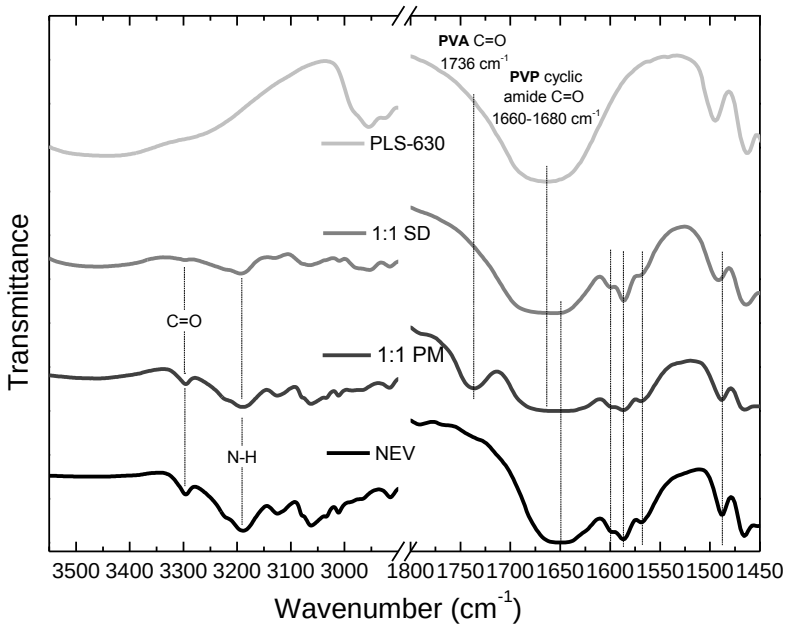

Figure 5.3 Part of the FT-IR spectra recorded for NEV, PLS-630, and the physical mixture (PM) and solid dispersion (SD) of the 1:1 NEV + PLS-630 composition.

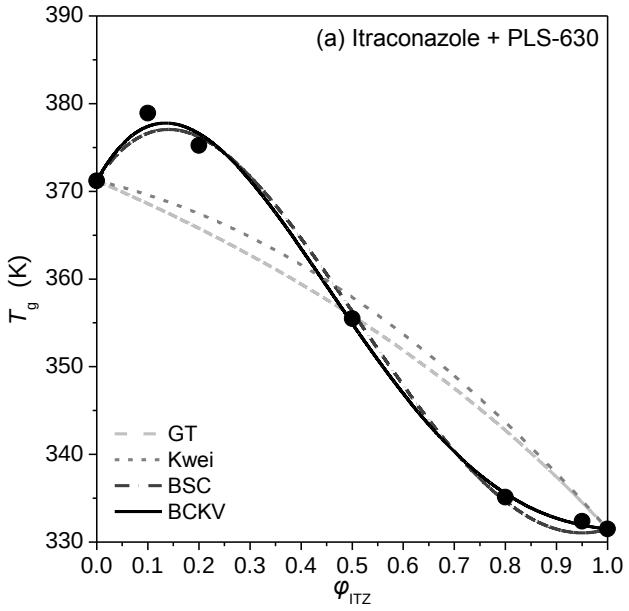
(a) Itraconazole + PLS-630
T_g (K)
φ_{ITZ}
GT
Kwei
BSC
BCKV

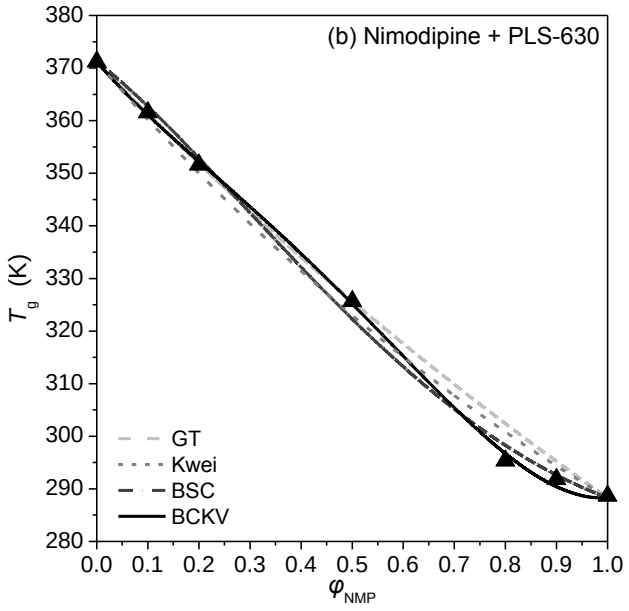
(b) Nimodipine + PLS-630
T_g (K)
φ_{NMP}
GT
Kwei
BSC
BCKV

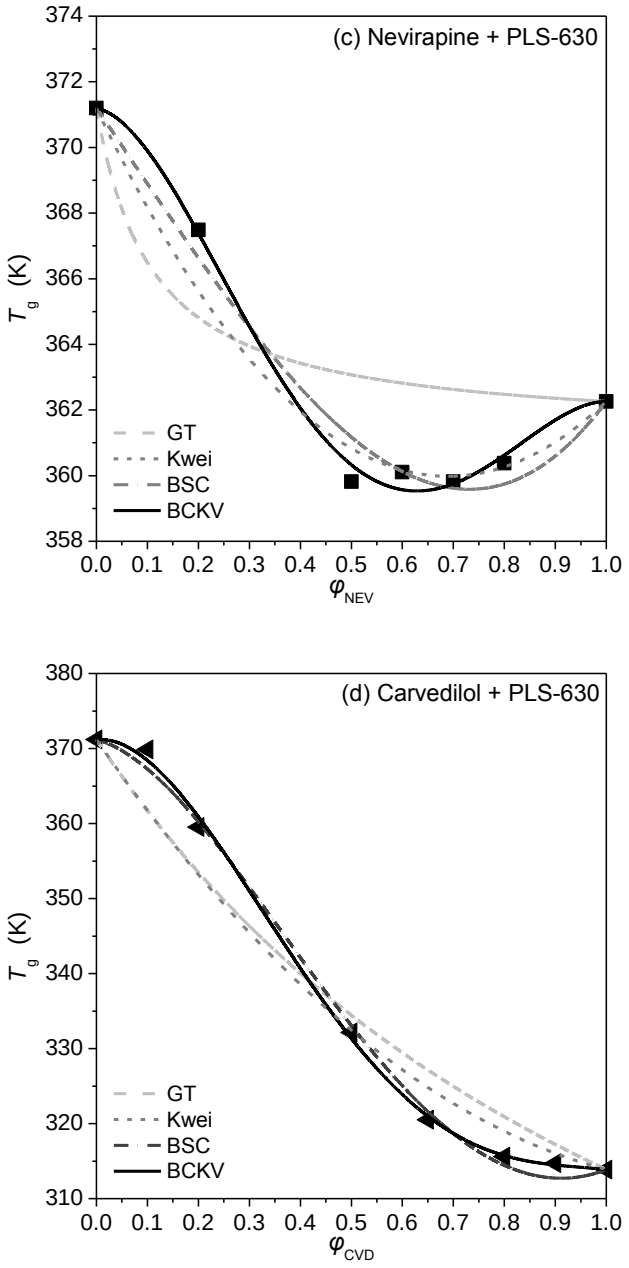

Figure 5.4 Compositional variation of blend T_g for the *solid dispersions* of (a) ITZ, (b) NMP, (c) NEV and (d) CVD with PLS-630.

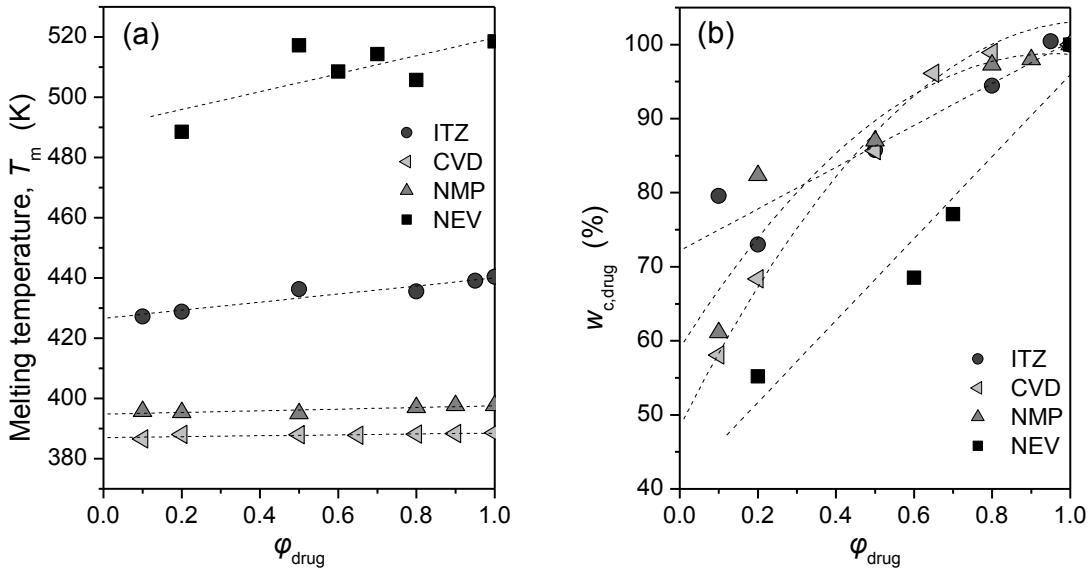

Figure 5.5 Compositional variation of (a) the melting temperatures (T_m) and (b) the percentage of drug that exists in a crystalline phase ($w_{c,drug}$), obtained from the first heating DSC scans of the pure drugs and their physical mixtures with amorphous Plasdone S-630 copolymer. Averages of two measurements are reported.

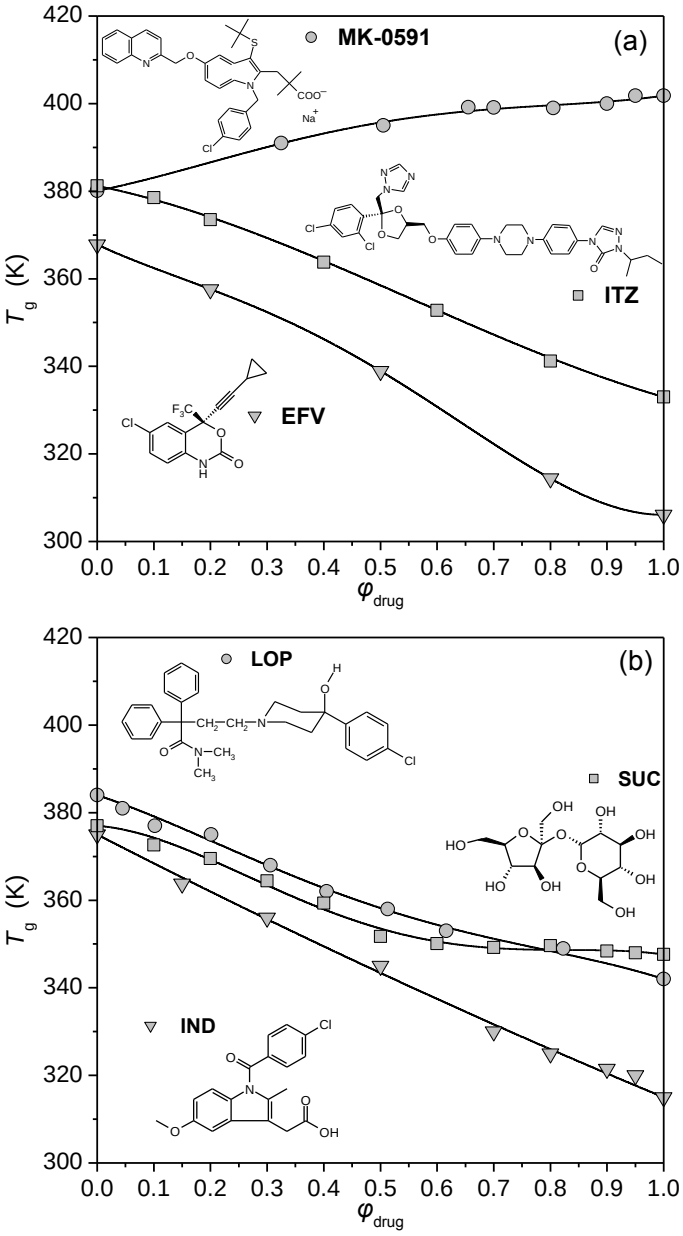

Figure 5.6 Compositional variations of blend T_g for *solid dispersions* of (a) MK-0591, EFV, ITZ, and (b) SUC, IND and LOP drugs in various grades of P(VP-*co*-VA) copolymers, and their description using the BCKV equation. Drugs' chemical structures are also inserted.

6. Complexation with Cyclodextrins for Dissolution Enhancement

6.1 Abstract

Efavirenz (EFV) is an oral anti-human immunodeficiency virus type 1(HIV-1) drug with extremely poor aqueous solubility. Thus, its gastro-intestinal absorption is limited by the dissolution rate of the drug. The objective of this study was to characterize the inclusion complexes of EFV with β-cyclodextrin (β-CD), hydroxypropyl β-CD (HPβCD) and randomly methylated β-CD (RMβCD) to improve the solubility and dissolution of EFV. The inclusion complexation of EFV with cyclodextrins (CDs) in the liquid state was characterized by phase solubility studies. The solid state characterization of various EFV and CD systems was performed by X-ray diffraction (XRD), differential scanning calorimetry (DSC), and scanning electron microscopy (SEM) analyses. Dissolution studies were carried out in distilled water using USP dissolution rate testing equipment. Phase solubility studies provided an A_L type solubility diagram for β-CD and A_P type solubility diagram for HPβCD and RMβCD. The phase solubility data enabled calculating stability constants (Ks) for EFV-βCD, EFV-HPβCD and EFV-RMβCD systems, 288, 469 and 1073 M^{-1}, respectively. The physical and kneaded mixtures of EFV with CDs generally provided higher dissolution of EFV as expected. The dissolution of EFV was substantially higher with HPβCD and RMβCD inclusion complexes prepared by the freeze drying method. Thus, complexation with (HPβCD and RMβCD could possibly improve the dissolution rate limited absorption of EFV.

6.2 Introduction

Efavirenz (EFV) [(S)-6-chloro-4-(cyclopropylethynyl)-1, 4-dihydro-4-(trifluoromethyl)-2H-3, 1-benzoxazin-2-one] is a non nucleoside reverse transcriptase inhibitor (NNRTI) approved for the treatment of human immunodeficiency virus type 1(HIV-1) infection (Fig. 6.1)**.** It is a crystalline lipophilic solid (log octanol water partition coefficient of 5.4) with a molecular mass of 315.68 and an aqueous solubility of 9.0 μg/ml.[1,2] This is a class II drug (low solubility, high permeability) according to the biopharmaceutical classification system (BCS) guidance by the Food and Drug Administration (FDA).[3,4] Highly permeable, poorly soluble drugs often demonstrate poor gastrointestinal (GI) absorption due to inadequate drug solubility in GI fluids.[5] Furthermore, Efavirenz has a considerably low intrinsic dissolution rate of 0.037 mg/cm^2/min (unpublished findings), which suggests dissolution rate limited absorption problems for this drug. The intrinsic dissolution rate less than 0.1 mg/min/cm^2 could be a rate limiting factor for oral absorption of the given drug.[6] EFV is currently marketed as tablets and capsules containing the drug in the crystalline form with controlled particle size. For poorly water soluble drugs, the solid state properties of the drug such as particle size, crystal structure and physical form greatly influence their dissolution properties, and also directly influence their bulk powder properties such as density and flowability.[7,8] EFV is a hydrophobic drug with low density and high flow resistance.[9] Since the particle size and morphology are the critical parameters in the development of formulations for effective GI drug delivery there is a need to develop the amorphous state of EFV with enhanced solubility related oral bioavailability.[10]

Cyclodextrins (CDs) are cyclic (α-1,4)-linked oligosaccharides of α-D-glucopyranose containing a relatively hydrophobic central cavity and hydrophilic outer surface. Complexation with CDs enhances the solubility, dissolution rate, and bioavailability of poorly soluble drugs.[11] In addition to solid dosage forms, the pharmaceutical development of oral liquid dosage forms of EFV for use in pediatrics or in adults with difficulty in swallowing is challenging. Not only is the solubility of EFV very low, but it imparts a strong and prolonged burning sensation to the mouth and throat when incorporated in water containing liquid formulations.[2] CDs can be used to reduce the GI irritation and unpleasant taste of drugs.[12] CDs possess a special ability to complex drugs to increase solubility, reduce bitterness, enhance stability and decrease tissue irritation upon dosing.[13] The objective of this study was to characterize the inclusion complexes of EFV with β-cyclodextrin (β-CD), hydroxypropyl-β-CD (HPβCD) and randomly methylated-β-CD (RMβCD) to improve solubility and dissolution. It is also expected that the burning sensation of oral liquid based EFV formulations could be minimized by inclusion complexation with CDs.

6.3 Materials and methods

6.3.1 *Materials*

Efavirenz was a generous gift from Aurobindo Pharma Co. (Hyderabad, India). β-cyclodextrin was kindly provided by ISP technologies (Wayne, NJ). Hydroxypropyl-βCD and Randomly methylated-βCD were procured from Cyclodex Technologies Inc (High Springs FL). All reagents and solvents used were of analytical grade.

6.3.2 *Phase solubility studies*

Phase solubility diagrams of EFV with various CDs in water at 25^{o} C were obtained according to Higuchi and Connors.[14] An excess of drug was added to 5 ml of water or CD aqueous solutions (0.002 - 0.3 M) in 20 ml glass vials and sonicated for 30 min. 5 times a day for 2 days. After equilibration for 24 h, aliquots of the supernatant were withdrawn, filtered through 0.22 μm nylon membranes and the EFV content, after suitable dilution, was determined spectrophotometrically at 246 nm (Shimadzu UV-VIS spectrophotometer, Norcross, GA). Each experiment was conducted in triplicate. The apparent 1:1 stability constants of the EFV-CD complexes were calculated from the linear portion of the phase solubility diagrams.[15]

6.3.3 *Preparation of CD formulations*

Various EFV-CD formulations were prepared in a 1:1 molar ratio by the following methods:

a) Physical mixing: Efavirenz and CD were mixed intimately in a screw cap glass vial. To ensure uniform mixing the vial was subjected to vortex mixing for 5 min.

b) Kneading: CD and EFV were blended together in a mortar with 1 ml of 50% ethanol, kneaded for 15 minutes and dried at 50^{o}C for 24 h. The resultant dry solid mass was powdered well, passed through a 60 mesh sieve and stored in a sealed glass vial.

c) Freeze-drying: The required 1:1 stoichiometric quantity of EFV (1M) was dissolved in 50% ethanol and added to an aqueous solution of HPβCD or RMβCD (1M). In the case of βCD, an isopropyl alcohol:water (3:4) mixture was used. The resulting solutions were frozen at -70^{o}C and lyophilized in a freeze-dryer (Labconco, FreezeZone, Kansas City,

MO). The lyophilized powder was passed through a 60 mesh sieve and stored in a sealed glass vial.

6.3.4 *Differential scanning calorimetry (DSC) studies*

DSC analysis was performed using a Q200 DSC apparatus (New Castle, DE). The samples were sealed in aluminum pans and the DSC thermograms were recorded at a heating rate of 10^{o} C/min from 30^{o}C to 180^{o}C.

6.3.5 *X-ray diffraction (XRD) studies*

X-ray powder diffraction patterns were obtained at room temperature with a Rigaku XRD analyzer (Rigaku Americas, The Woodlands, TX) using Cu Kα radiation. The scanning speed employed was 2^{o} /min.

6.3.6 *Scanning electron microscopy (SEM) studies*

The surface morphology of EFV and its binary systems with various CDs was analyzed by a scanning electron microscope (JEOL-JSM-5800, Tokyo, Japan). The powdered samples were uniformly spread on double-sided carbon tape, fixed on a stainless steel stub, and coated with gold /palladium to prevent charge build-up by the electrons absorbed by the specimen. The micrographs were obtained at an excitation voltage of 12 kV and magnification factors of 1000.

6.3.7 *Dissolution rate studies*

The dissolution rate studies of the formulations were performed in 500 ml distilled water using USP-II dissolution apparatus (Hansen Research, Chatsworth, CA) at a temperature of 37^{o}C and a stirring rate of 50 rpm. The sink conditions were maintained throughout the period of dissolution study**.** Efavirenz and binary mixtures of EFV with various CDs, each containing 10 mg of EFV were subjected to dissolution testing. The drug and various drug – CD mixtures (physical, kneaded and freeze dried) were passed through an 80 mesh sieve prior to conducting the dissolution studies**.** At fixed time intervals, 10 ml samples were withdrawn through a filter and the drug content was assayed spectrophotometrically at 246 nm. The dissolution profiles were evaluated on the basis of the dissolution efficiency parameter at 30 min (DE_{30}, %) and at 180 min. (DE_{180}, %). The dissolution efficiency parameters were calculated from the area under the dissolution curves and expressed as a percent of the area of the rectangle described by 100 % dissolution in the same time period.[15]

6.3.8 *Statistical analysis*

The differences between multiple groups of dissolution efficiency data (DE_{30min} and DE_{180min}) were assessed by analysis of variance (ANOVA) followed by Turkey's post test to determine the level of significance between different groups. Mean differences with $P < 0.05$ were considered to be significant.

6.4 Results and discussion

6.4.1 *Phase solubility studies*

Traditional phase solubility analysis of the effect of complexing agent on the drug compound can provide not only the stability constant of the complex but also to gives insight into the stoichiometry of the complex at equilibrium.[10] The phase solubility diagrams were obtained by plotting the apparent equilibrium concentration of the drug against CD concentrations and are shown in Figure 6.2. For βCD, the apparent solubility of EFV increased linearly as a function of βCD concentration over the entire concentration range studied. This linearity was characteristic of an A_L-type system[10] and suggested the formation of inclusion complexes in a 1:1 EFV:CD molar ratio. For HPβCD and RMβCD, the apparent solubility of EFV increased linearly as a function of the corresponding CD to approximately 80mM indicating the formation of inclusion complexes in a 1:1 molar ratio. At higher CD concentrations, the slope of the plot increased rapidly indicating the formation of 1:2 or higher complexes. The apparent stability constants (Ks) of the 1:1 complexes were calculated from the initial linear slopes of the phase solubility diagrams and the intrinsic solubility (S_o) of EFV.[14] The Ks values of the EFV-βCD, EFV-HPβCD and EFV-RMβCD complexes were 288, 469 and 1073 M^{-1}, respectively.

6.4.2 *X-ray diffraction studies*

Figure 6.3 shows the X-ray diffraction patterns of EFV, βCD, HPβCD and RMβCD and the binary systems of EFV with various CDs. The XRD pattern of EFV presented multiple peaks indicating the crystalline nature of the drug. Among the CDs,

the βCD exhibited a typical crystalline diffraction pattern and diffraction peaks relevant to crystalline EFV were detectable in all the binary systems with βCD. Both HPβCD and RMβCD exhibited an amorphous diffraction pattern (Fig. 6.3). The diffraction patterns of physical mixtures of EFV with HPβCD and RMβCD revealed the presence of free crystalline drug. The diffraction peak intensity in the kneaded mixture of HPβCD was similar to the physical mixture. However, an amorphous structure was observed for the kneaded mixture with RMβCD, indicating complex formation. Complete drug amorphization was observed in the freeze dried products of EFV with each amorphous βCD derivative (HPβCD and RMβCD). Similar results were reported for other drugs with amorphous βCD, derivatives.[16, 17]

6.4.3 *Differential scanning calorimetry*

For drugs that form inclusion complexes with CDs, DSC is a fast and relatively inexpensive technique to examine the absence of the drug melting endotherm in order to verify that the drug was successfully complexed.[18] The DSC thermograms of EFV, βCD, HPβCD, RMβCD and the binary systems of CDs with EFV are shown in Figure 6.4. Efavirenz showed the typical behavior of an anhydrous crystalline drug with a well defined melting peak at 137.2^{o} C (ΔH = 49.10 J/g).The DSC curve of βCD exhibited a very broad endothermal phenomenon between 60 and 120^{o}C due to the loss of water.[19] The DSC thermograms for EFV-βCD complexes have a small endothermic peak for the physical and kneaded mixtures, and the freeze dried formulation, suggesting that each had a free EFV component. It appears that the freeze drying method did not produce a complete inclusion complex. In the case of EFV-HPβCD formulations, the DSC

thermograms have a small endothermic peak for the physical and kneaded mixtures corresponding to the melting point of EFV. However, in the freeze dried mixture the endothermic peak was absent suggesting the formation of an inclusion complex without any free EFV. Similar results were observed for EFV-RMβCD complexes, but in contrast to HPβCD, the endothermic peak was also completely absent for the kneaded mixture. This suggested a solid state interaction of RMβCD and EFV by the kneading method as well as the freeze dried method. All of the DSC results were in good agreement with those obtained by XRD to prove the complexation of EFV with CDs in the solid state.

6.4.4 *Scanning Electron Microscopy*

The scanning electron microphotographs of EFV and its binary systems with various CDs are presented in Figure 6.5. Efavirenz was in the form of distinct regularly sized crystals. In the physical mixtures, the typical EFV crystals, which were mixed between the CD particles or coated to their surface, were clearly detectable, thus confirming the presence of crystalline drug. It was also evident that βCD is a crystalline solid while HPβCD and RMβCD are homogeneous spherical shaped spray dried particles in the micron size range.[20] In the kneaded mixtures of CD and EFV, it is still possible to distinguish EFV crystals associated with the CDs which had lost their original shape due to the kneading process. In the freeze dried products the original morphology of EFV and CD have disappeared and it was not possible to differentiate the two components. Generally, all freeze dried products appeared to have less crystalline structure with a uniform appearance. Again, crystals of EFV were not distinguishable, indicative of the presence of a new solid phase. While the SEM technique is inadequate to conclude in the

formation of a genuine complex, the microphotographs support the consecution of a new single component.[20, 21]

6.4.5 *Dissolution rate studies*

Dissolution profiles for the drug, physical mixture of the drug and CD, and/or complex of drug and CD are often presented to demonstrate the influence of a CD on dissolution kinetics and the total amount of drug in solution.[22] Rapid dissolution as compared with the pure drug is the characteristic behavior of inclusion complexes.[23] The dissolution profiles of EFV and various binary systems are presented in Figure 6.6. It was observed during these studies that the hydrophobic property of the drug prevented its contact with the dissolution medium causing it to float on the surface. Thus, only ~10% (1 mg) of the EFV dissolved even after 180 min. Physical mixtures prepared with various CDs yielded a dissolution profile that was slightly higher than that of EFV. The improvement in dissolution rate with the physical mixtures can be attributed to both improved drug wettability due to the presence of the hydrophilic CD which can reduce the interfacial tension between poorly soluble drug and dissolution medium, and the formation of readily soluble complexes in the dissolution medium.[24] The kneaded mixture and freeze dried mixture of βCD, HPβCD and RMβCD showed a significant increase in EFV dissolution compared to their corresponding physical mixture. This suggested a better interaction of the drug with CD by these processes, as expected from the physicochemical characterization.

The dissolution efficiency data calculated based on 30 minutes (DE_{30}) and 180 min (DE_{180}) are presented in Table 6.1. The DE_{30min} of the HPβCD kneaded mixtures

and freeze dried complexes were both about 20 fold higher than EFV ($P < 0.001$). The DE_{180min} of the HPβCD kneaded mixtures and freeze dried complexes were about 10 fold higher than EFV ($P < 0.001$). The DE_{30min} of the RMβCD kneaded mixtures and freeze dried complexes were about 6 and 8 fold, respectively, higher than EFV ($P < 0.001$). The DE_{180min} of the RMβCD kneaded mixtures and inclusion complexes were about 4 and 8 fold higher, respectively, than EFV ($P < 0.001$). The freeze dried product showed much better dissolution than the kneaded product with RMβCD. This suggested better complexation by the freeze-drying technique, as might be expected. However, the dissolution profiles for the kneaded and freeze dried mixtures were very similar for βCD as well as for HPβCD. This suggests that complex formation can occur efficiently through simple kneading for these compounds, though not for RMβCD.

Among all the complexes the EFV-HPβCD kneaded and freeze-dried mixtures exhibited the best dissolution by far based on DE_{30min} values. Based on the physico-chemical data presented one would not expect such a large difference in the dissolution rates of the HPβCD and RMβCD freeze dried formulations. Based on the phase solubility diagram (Fig. 6.2) and resulting Ks values, one would actually predict better dissolution with RMβCD. It is clear from the dissolution profiles (Fig. 6.6) for HPβCD that there is rapid dissolution of the EFV as a complex, reaching the maximum concentration (~55%) within approximately 30min. In contrast, the dissolution profile for freeze dried RMβCD shows a relatively slow and continuous increase in the % EFV dissolved that reaches ~55% dissolved after 180 min. There is no clear explanation for this phenomenon. Dollo et al,[25] studied the effect of HPβCD and Sulfobutyl Ether-7-βCD (SBE7βCD) on the solubility and dissolution rate improvement of anetholetrithione.

The K_s values of HPβCD and SBE7βCD complexes were 6227 and 12834, respectively, indicating much better solubility by the SBEβCD complex. The dissolution studies in contrast demonstrated initial slow dissolution by the SBEβCD complex as compared to HPβCD. In an earlier study,[26] we found and initial slow dissolution by the RMβCD complex of gefitinib as compared to HPβCD, though the former complex had a much higher solubility and Ks value.

6.5 Conclusions

Phase solubility studies demonstrated an A_L type solubility diagram for β-CD indicating the formation of inclusion complexes in a EFV: CD 1:1 stoichiometric ratio. An A_P type solubility diagram for HPβCD and RMβCD indicated a 1:1 stoichiometry complex in the initial linear portion, and 1:2 or greater stoichiometry complexes at higher CD concentrations. The inclusion complex formation of EFV with different CDs in the solid state was confirmed by DSC, X-RD and SEM studies. The dissolution of EFV was substantially higher for HPβCD and RMβCD inclusion complexes prepared by the freeze drying method. Thus, complexation with HPβCD and RMβCD could possibly help improve the dissolution rate limited absorption problems for EFV.

6.6 Acknowledgement

The authors are thankful to Aurobindo Pharma (Hyderabad, India) and International Specialty Products Inc (Wayne NJ) for their generosity.

6.7 References

1. Maurin MB, Rowe SM, Blom K, Pierce ME. 2002. Kinetics and mechanism of hydrolysis of efavirenz. Pharm Res 19:517-522.
2. Bahal SM, Romansky JM, Alvarez FJ. 2003. Medium chain triglycerides as vehicle for palatable oral liquids. Pharm Dev Technol 8:111-115.
3. Kasim NA, Whitehouse M, Ramachandran C, Bermejo M, Lennernaes H, Hussain AS, Junginger HE, Stavchansky SA, Midha KK, Shah VP, Amidon GL. 2004. Molecular properties of WHO essential drugs and provisional biopharmaceutical classification. Mol Pharm 1:85-96.
4. Takano R, Sugano K, Higashida A, Hayashi Y, Machida M, Aso Y, Yamashita S. 2006. Oral absorption of poorly water-soluble drugs: Computer simulation of fraction absorbed in humans from a miniscale dissolution test. Pharm Res 23:1144-1156.
5. Aungst BJ, Nguyen NH, Taylor NJ, Bindra DS. 2002. Formulation and food effects on the oral absorption of a poorly water soluble, highly permeable antiretroviral agent. J Pharm Sci 91:1390-1395.
6. Kaplan SA. 1972. Biopharmaceutical considerations in drug formulation design and evaluation. Drug Metab Rev 1:15-34.
7. Shah VP. 2005. The role of dissolution testing in the regulation of pharmaceuticals: The FDA perspective. Pharm Dissolution Test. 81-96.
8. Walton DE, Mumford CJ. 1999. Spray dried products - characterization of particle morphology. Chem Eng Res Des 77:21-38.

9. Viana ODS, Benigno JJ, Silva RMF, Morais de Medeiros FP, Grangeiro SJ, de Albuquerque MM, Neto PJR. Development of formulations and technology for obtaining of efavirenz coated tablets - anti-HIV therapy. Rev Bras Cienc Farm 42:505-511 (2006).

10. Gao JZ, Hussain MA, Motheram R, Gray DAB, Benedek IH, Fiske WD, Doll WJ, Sandefer E, Page RC, Digenis GA. 2007. Investigation of human pharmacoscintigraphic behavior of two tablets and a capsule formulation of a high dose, poorly water soluble/highly permeable drug (efavirenz). J Pharm Sci 96:2970-2977.

11. Brewster ME, Loftsson T. 2007. Cyclodextrins as pharmaceutical solubilizers. Adv Drug Deliv Rev 59:645-666.

12. Szejtli J, Szente L. 2005. Elimination of bitter, disgusting tastes of drugs and foods by cyclodextrins. Eur J Pharm Biopharm. 61:115-125.

13. Challa R, Ahuja A, Ali J, Khar RK. 2005. Cyclodextrins in drug delivery: An updated review. AAPS PharmSciTech. 6:E329-357.

14. Higuchi T, Connors KA. 1965. Phase-solubility techniques. Adv. Anal. Chem. Instr. 4:117-212.

15. Khan KA, Rhodes CT. 1974. Effect of compaction pressure on the dissolution efficiency of direct compression systems. Pharm Acta Helv 49:258-261.

16. Rajendrakumar K, Madhusudan S, Pralhad T. 2005. Cyclodextrin complexes of valdecoxib: Properties and anti-inflammatory activity in rat. Eur J Pharm Biopharm 60:39-46.

17. Mura P, Zerrouk N, Faucci MT, Maestrelli F, Chemtob C. 2002. Comparative study of ibuproxam complexation with amorphous beta-cyclodextrin derivatives in solution and in the solid state. Eur J Pharm Biopharm 54:181-191.

18. Miller LA, Carrier RL, Ahmed I. 2007. Practical considerations in development of solid dosage forms that contain cyclodextrin. J Pharm Sci 96:1691-1707.

19. Zingone G, Rubessa F. 2005. Preformulation study of the inclusion complex warfarin-beta -cyclodextrin. Int J Pharm 291:3-10.

20. Figueiras A, Carvalho RA, Ribeiro L, Torres-Labandeira JJ, Veiga FJB. 2007. Solid-state characterization and dissolution profiles of the inclusion complexes of omeprazole with native and chemically modified beta-cyclodextrin. Eur J Pharm Biopharm 67:531-539.

21. Sinha VR, Anitha R, Ghosh S, Nanda A, Kumria R. 2005. Complexation of celecoxib with beta-cyclodextrin: Characterization of the interaction in solution and in solid state. J Pharm Sci 94:676-687.

22. Carrier RL, Miller LA, Ahmed I. 2007. The utility of cyclodextrins for enhancing oral bioavailability. J Control Release 123:78-99.

23. Baboota S, Dhaliwal M, Kohli K. 2005. Physicochemical characterization, in vitro dissolution behavior, and pharmacodynamic studies of rofecoxib-cyclodextrin inclusion compounds. Preparation and properties of rofecoxib hydroxypropyl beta-cyclodextrin inclusion complex: A technical note. AAPS PharmSciTech. 6:E83-90.

24. Corrigan OI, Stanley CT. 1982. Mechanism of drug dissolution rate enhancement from beta-cyclodextrin-drug systems. J Pharm Pharmacol 34:621-626.

25. Dollo G, Corre PL, Chollet M, Chevanne F, Bertault M, Burgot JL, Le Verge R. 1999. Improvement in solubility and dissolution rate of 1, 2-dithiole-3-thiones upon complexation with beta-cyclodextrin and its hydroxypropyl and sulfobutyl ether-7 derivatives. J Pharm Sci. 88:889-895.

26. Lee YH, Babu RJ. Enhancement of solubility and dissolution rate of Gefitinib by complexation with cyclodextrins. Contributed poster; 28th Annual meeting of the Graduate Research Association of Students in Pharmacy, Tallahassee, FL, USA; 6/6-8/08.

Table 6.1 Effect of CDs on the Dissolution efficiency of Efavirenz

Product	Dissolution Efficiency 0-30 min	Dissolution Efficiency 0-180 min
Efavirenz	1.51 ± 0.645	5.64 ± 1.149
Effect of βCD Efavirenz		
Physical mixture	6.78 ± 0.170*	18.74 ± 2.100**
Kneaded mixture	9.34 ± 1.364**	30.95 ± 0.058***
Freeze Dried mixture	11.26 ± 1.304***	31.16 ± 2.189***
Effect of HPβCD Efavirenz		
Physical mixture	9.74 ± 1.177**	21.08 ± 1.900***
Kneaded mixture	33.04 ± 0.625***	49.98 ± 1.053***
Freeze Dried mixture	29.87 ± 1.805***	54.25 ± 1.031***
Effect of RMβCD		
Efavirenz	7.47 ± 0.573**	19.84 ± 1.425**
Physical mixture	8.60 ± 1.552**	24.58 ± 2.684***
Kneaded mixture	12.78 ± 0.317***	43.13 ± 0.331***
Freeze Dried mixture		

* $P < 0.05$, ** $P < 0.01$, *** $P < 0.001$ versus Efavirenz

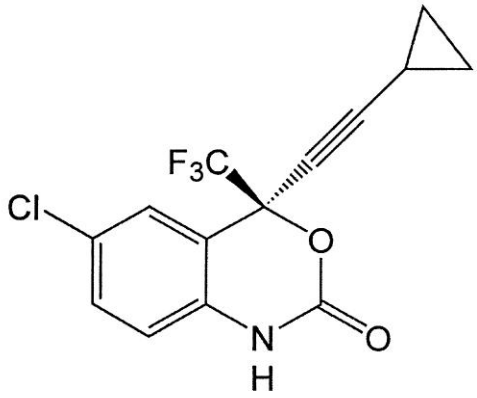

Figure 6.1 Structure of Efavirenz

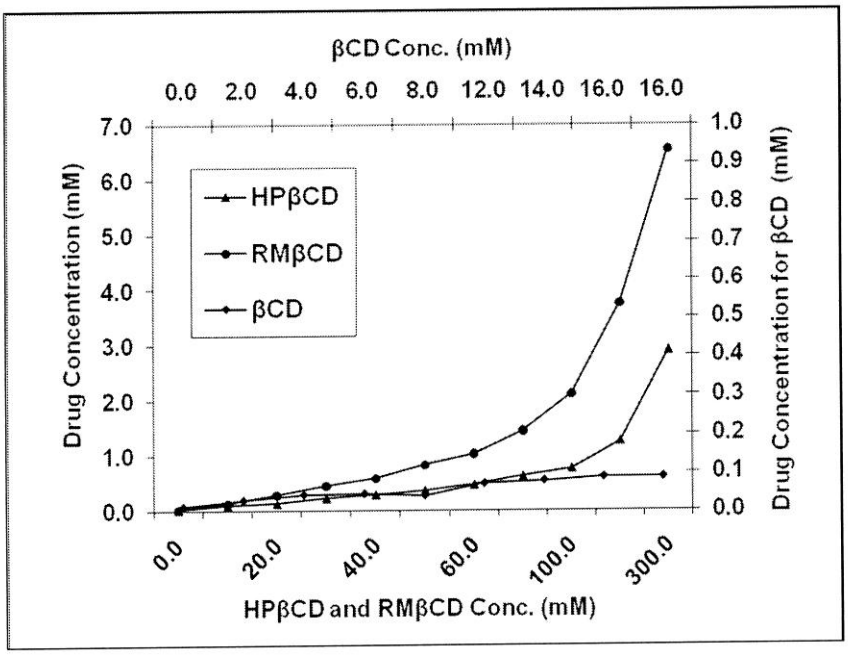

Figure 6.2 Phase solubility diagram of Efavirenz with βCD, HPβCD and RMβCD in water at room temperature (~25^{o}C).

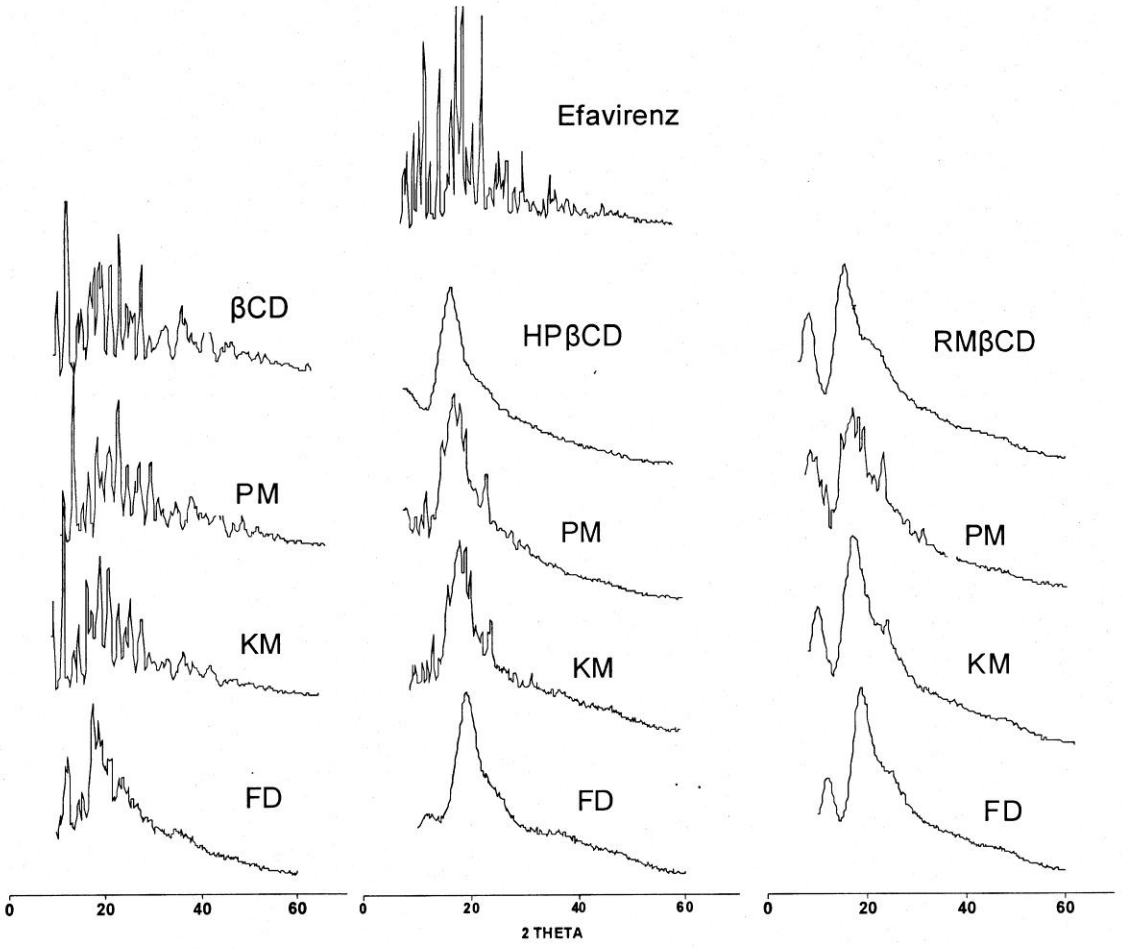

Figure 6.3 X-ray diffraction analysis of Efavirenz, βCD, HPβCD, RMβCD, and their physical mixtures (PM), kneaded mixtures (KM) and freeze dried complexes (FD).

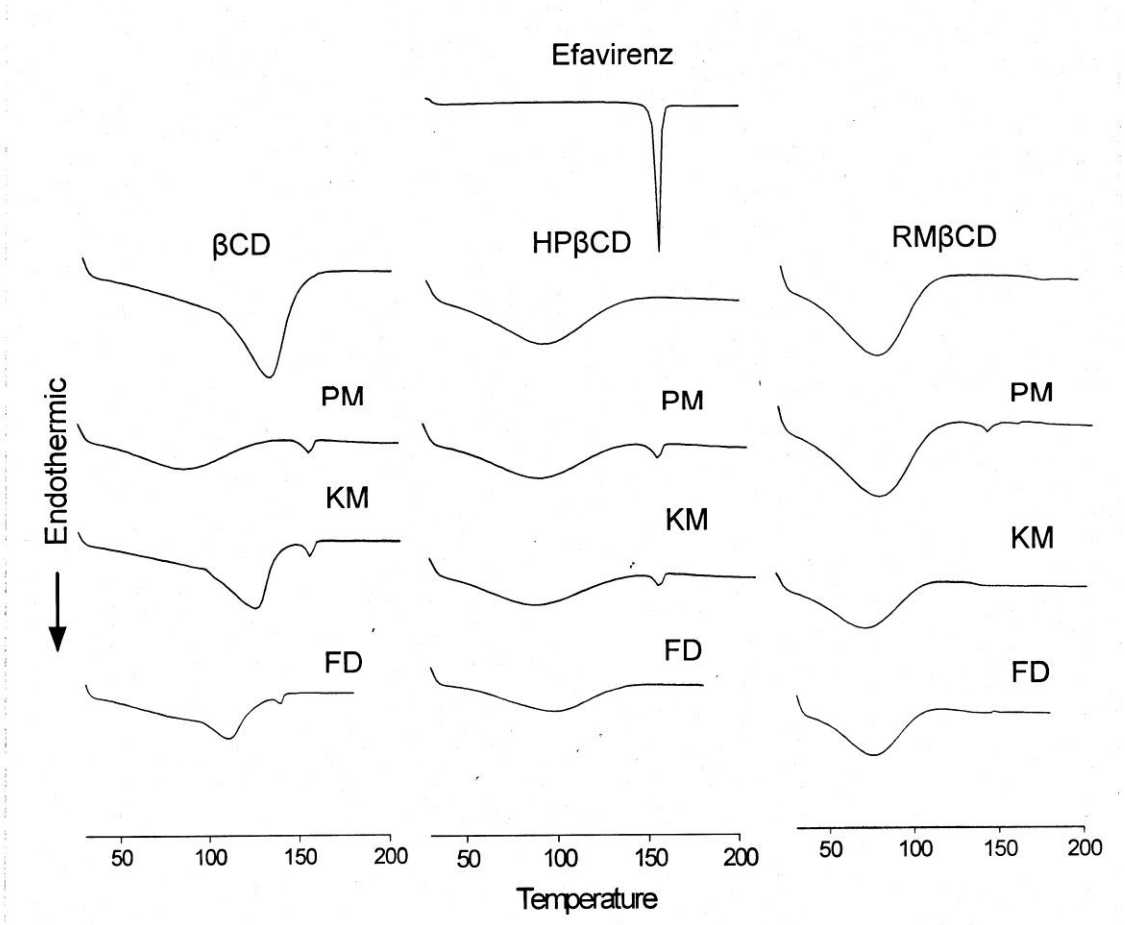

Figure 6.4 Differential scanning calorimetry thermograms of Efavirenz, βCD, HPβCD, RMβCD, and their physical mixtures (PM), kneaded mixtures (KM) and freeze dried complexes (FD).

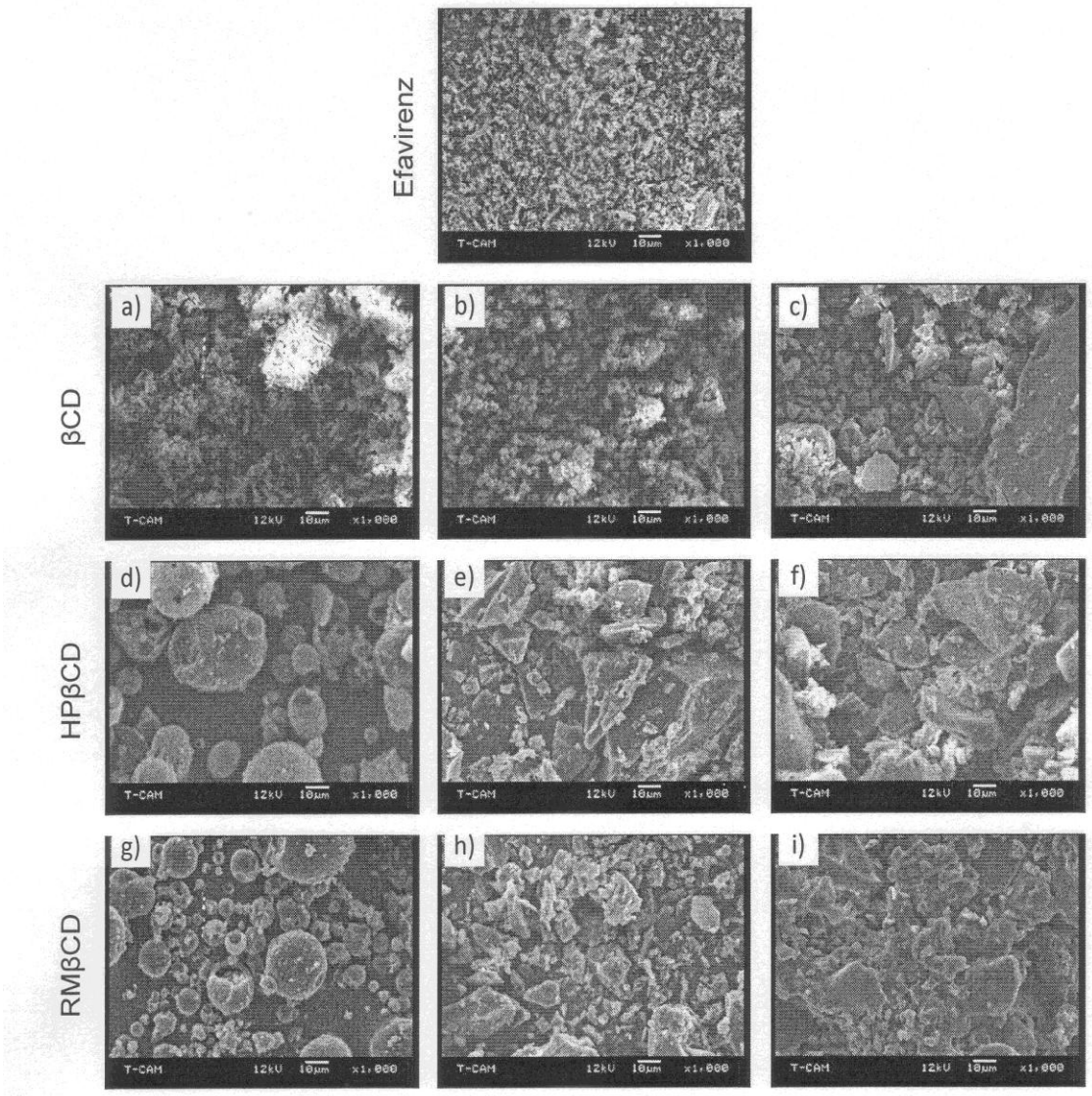

Figure 6.5 Scanning electron microphotographs of Efavirenz, physical mixture of EFV with βCD (a), kneaded mixture of EFV with βCD (b), inclusion complex of EFV with βCD (c), physical mixture of EFV with HPβCD (d), kneaded mixture of EFV with HPβCD (e), inclusion complex of EFV with HPβCD (f), physical mixture of EFV with RMβCD (g), kneaded mixture of EFV with RMβCD (h), and inclusion complex of EFV with RMβCD (i).

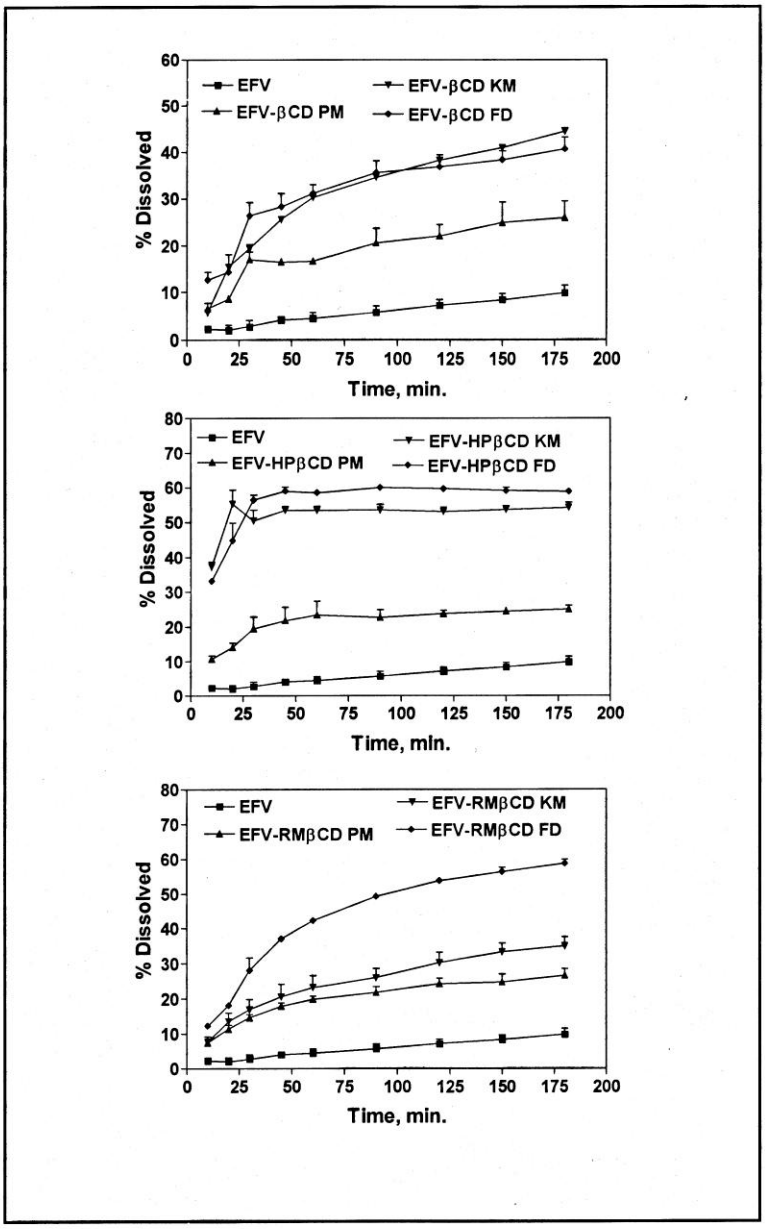

Figure 6.6 Dissolution profiles of various Efavirenz-CD formulations. PM, Physical mixture; KM, kneaded mixture; FD, Freeze dried complex.

7. Summary and Future Works

The poor aqueous solubility of drugs remains one of the most challenging aspects for the formulation scientist during drug development. Aqueous solubility of the drug is the most critical property affecting the oral bioavailability of class-II (poorly soluble and highly permeable) drugs according to the biopharmaceutical classification system (BCS). If the dissolution rate of these compounds is enhanced, then the bioavailability following oral administration may be significantly improved. Correlation of *in-vivo* results with dissolution tests is likely to be best for BCS class-II drugs because the dissolution rate is the primary limiting aspect to absorption.

Various approaches have been used to improve the dissolution rate, and hence the oral bioavailability, of poorly aqueous soluble compounds. Micronization, the most commonly used industrial approach for dissolution enhancement suffers from drug agglomeration problems. Deagglomeration of the micron-sized particles is usually carried out by subsequent mixing of cohesive drug particles with pharmaceutical excipients. Currently available mixers are not effective in deagglomeration of highly cohesive drug particles or they require very high shear or impaction acting as particle size reduction devices rather than conventional mixers. The use of high energy mixers may affect the crystal lattice of the particles, influencing the physicochemical stability of the drug. The

tumbler mixer, which is the most commonly used blender in the pharmaceutical industry, is not effective for deagglomeration of micron/nano-sized particles.

Amorphous drug-polymer systems is one of the most frequently reported strategies in the pharmaceutical literature. However, despite the extensive research efforts, only a few products utilizing an amorphous system are commercially available. The reason is that the amorphous systems are thermodynamically unstable and can cause product stability issues during storage. Although a large number of studies have been published on the subject, the mechanism of stabilization of amorphous systems in polymer mixtures is still not well established.

This dissertation has successfully addressed the drug agglomeration issue in micronization and also the drug polymer miscibility, one of the critical attributes that affects the stability of the amorphous systems. A novel method of simultaneous particle formation by the supercritical anti solvent method and co-mixing with pharmaceutical excipients has been developed. This method was used for preventing the agglomeration of micronized particles. Itraconazole microflakes were deposited on the surface of fast flo-lactose and this system was stabilized with poloxamer 407. These systems demonstrated superior dissolution profiles as compared to the microflakes of itraconazole without the excipients or stabilizers. The importance of drug polymer miscibility in the development of amorphous systems has been also addressed. The physically stable efavirenz (EFV) drug-polymer (Eudragit EPO and Plasdone S-630) amorphous systems were successfully prepared by the hot melt extrusion method by understanding thermal and rheological properties of the drug-polymer blends. Successful formation of amorphous drug-polymer systems is also discussed in terms of thermophysical behavior

(suppression of crystallization, negative excess volume of mixing) and intermolecular interactions (concentrations of proton donating/accepting groups) in different drug-polymer systems. Carvedilol, itraconazole, nevirapine and nimodipine are used as model drugs with Plasdone S-630. Several equations were used to represent the glass transition (T_g) of blends with different drug loadings, and the best agreement of the calculations with the experimental values is achieved by a newly proposed three parameter equation. The research also successfully demonstrated the dissolution enhancement of EFV by complexation with cyclodextrins (CDs) The inclusion complexes of EFV with β-CD and its derivatives were prepared and characterized both in liquid and solid states. The inclusion complexation of EFV with CDs in the liquid state was characterized by phase solubility studies. The solid state characterization of various EFV and CD systems was performed by X-ray diffraction, differential scanning calorimetry, and scanning electron microscopy analyses. The dissolution of EFV was substantially higher with hydroxypropyl βCD and randomly methylated βCD inclusion complexes prepared by the freeze drying method.

The future work is directed to demonstrate the applicability of SAS-DEM method for deagglomeration of drug particles and for understanding miscibility of drug - polymer systems in the melt extrusion for enhancement of bioavailability of the poorly soluble drugs.

i. SAS-DEM method has been successfully utilized for the drug dissolution enhancement of Itraconazole by preventing the agglomeration of flaky drug particles. The PLX produced loose agglomerates with superior dissolution

properties even at higher drug loadings upto 50% w/w. Further studies are directed to understand various forces involved in the agglomeration of drug particles, drug deposition on the excipient and agglomeration of drug particles in the presence of PLX.

ii. For melt extrusion systems of Efavirenz, *in-vivo* bioavailability studies are suggested, so that *in vitro – in vivo* correlations of the dissolution and drug bioavailability can be performed.

iii. For the drug-polymer miscibility studies, further solid state characterizations should performed using thermally stimulated depolarization current and dielectric relaxation studies. Due to the complexities of the drug-polymer systems and due to sensitivity limits of the conventional analytical techniques like DSC and XRD have some limitations.

Appendix: Journal Publications and Conference Presentations

Journal Publications

1. Single-Step Preparation and Deagglomeration of Itraconazole Nanoflakes by the supercritical antisolvent method for dissolution enhancement. 2010. (Accepted 01/27/2011, – *Journal of Pharmaceutical Sciences*).
2. Glass transitions in binary drug+polymer systems. 2010. *Materials Letters* 63(30):2666-2668.
3. Amorphous State Characterization of Efavirenz-Polymer Hot Melt Extrusion Systems for Dissolution Enhancement. (Submitted for publication – *European Journal of Pharmacaceutical Sciences*).
4. Encapsulation of Hydrophobic Drugs in a Copolymer: Glass Transition Behaviour and Miscibility Evaluation. (Accepted for publication – *Journal of Polymer Engineering Sciences*).
5. Physicochemical characterization of efavirenz-cyclodextrin inclusion complexes. 2009. *AAPS PharmSciTech* 10(1):81-87.

Other Co-Authored Publications

1. Sanganwar GP, **Sathigari S**, Babu RJ, Gupta RB. 2010. Simultaneous production and co-mixing of microparticles of nevirapine with excipients by supercritical

antisolvent method for dissolution enhancement. *European Journal of Pharmaceutical Sciences* 39(1-3):164-174.

2. Phillip Lee YH, **Sathigari S**, Jean Lin YJ, Ravis WR, Chadha G, Parsons DL, Rangari VK, Wright N, Babu RJ 2009. Gefitinib-cyclodextrin inclusion complexes: physico-chemical characterization and dissolution studies. *Drug Development and Industrial Pharmacy* 35(9):1113-1120.
3. Chadha G, **Sathigari S,** Parsons DL, Babu RJ. 2010. In-vitro percutaneous absorption of genistein from topical gels through human skin. *Drug Development and Industrial Pharmacy* (Accepted).
4. Babu RJ, **Sathigari S,** Kumar MT, Pandit JK. 2009. Formulation of controlled release gellan gum macro beads of amoxicillin. *Current Drug Delivery* 7(1):36-43.

Conference Presentations

1. **Sathigari S**, Parsons DL, Fasina O and Babu RJ. Improving the Dissolution of Efavirenz by Complexation with Cyclodextrins - *AAPS 2007 Annual meeting & Exposition*, Nov 10-15, San Diego, CA.
2. **Sathigari S**, Uthayathas S, Dhanasekaran M, Chadha G, Parsons DL, Babu RJ, Shenoy D, Cox C, Lee R. Micellar Nanoparticle Based Topical Formulations of Alprostadil: In vitro & In vivo – *AAPS 2008 Annual meeting & Exposition*, Nov 16-20, Atlanta, GA.

3. Chadha G, **Sathigari S**, Parsons DL, Babu RJ, Palakurthi S. In-vitro percutaneous absorption of genistein from topical gel vehicles through human skin - *AAPS 2008 Annual meeting & Exposition*, Nov 16-20, Atlanta, GA.
4. **Sathigari S**, Radhakrishna VK, Parsons DL, Davis VA, Babu RJ. Enhancemnet of Dissolution of Efavirenz by Hot melt extrusion technology – *GRASP 2009 Annual meeting*, June 5-7, Atlanta, GA
5. **Sathigari S**, Sanganwar GP, Gupta RB, Parsons DL, and Babu RJ. Enhancemnet of Dissolution by Simultaneous crystallization of poorly soluble drug and mixing with pharmaceutical carrier(s) using supercritical fluid anti-solvent process – *AAPS 2009 Annual meeting & Exposition*, Nov 8-12, Los Angeles, CA.
6. **Sathigari S**, Wilson S, Scoggins M, Melendez A, Vera H, Clark B, Shah U. Fluid Bed Granulation: Identifying Critical Process Parameters and Developing Design Space - *AAPS 2009 Annual meeting & Exposition*, Nov 8-12, Los Angeles, CA.
7. Babu RJ, Brostow W, Kalogeras IM, **Sathigari S.** Encapsulation of hydrophobic drugs in PPV-VA copolymer – *Polychar 18 World forum on advanced materials*, April 7-10, Siegen, Germany.
8. **Sathigari S**, Ober C, Gupta RB, Parsons DL, and Babu RJ. Simultaneous production and co-mixing of Itraconazole micro.nanoflakes with stabilizers and pharmaceutical carriers by a supercritical antisolvent method for dissolution enhancement - *AAPS 2010 Annual meeting & Exposition*, Nov 14-18, New Orleans, LA.